UPGRADING HEAVY OIL/BITUMEN EMULSIONS VIA IN SITU HYDROGEN GENERATION

Flora T.T. Ng
Department of Chemical Engineering
University of Waterloo
Waterloo, Ontario
Canada, N2L 3G1
email: fttng@cape.uwaterloo.ca

Keywords: upgrading, heavy oil/bitumen emulsions, in situ hydrogen

Abstract

Canada has large reserves of heavy oils and tarsand bitumen. These heavy oils are recovered as emulsions via steam injection techniques.Current technologies for emulsion treatment and upgrading require multistage processing. Recently, we have developed a novel process for upgrading heavy oil emulsions in a single stage process where emulsion breaking and upgrading occurred in the same reactor. This process is based on the activation of water in an emulsion via the water gas shift reaction to generate hydrogen for in situ upgrading. This paper is focussed on the catalytic desulphurization in an emulsion using dispersed catalysts. The activity of in situ hydrogen will be compared with that of molecular hydrogen. Synthesis gas was found to be effective for upgrading emulsions. The emulsion upgrading technology could also be used to process emulsions derived from hot water extraction of tarsands bitumen.

Introduction

Canada has large reserves of high sulphur heavy oils and oil sand bitumen. As conventional oil reserves continue to decrease, it will become necessary to utilize more of the high sulphur heavy oil and oil sand bitumen in the future. Technologies for the recovery of heavy oils include steam flooding, cyclic steam injection or fire flooding of reservoirs while hot water was used to extract bitumen from tarsands. These methods of recovery of heavy oil and bitumen produce emulsions. In order to utilize the heavy oils and bitumen, the emulsions have to be broken and separated into water and oil phases in emulsion treatment plants. Subsequently, the bitumen or heavy oils are upgraded where sulphur removal and hydrocracking occurred before being utilized in conventional refineries. In summary, current technologies for emulsion treatment and upgrading require multistage processing and are costly. Thus alternative technologies for processing heavy oil/bitumen emulsions would be attractive.

We have developed in our laboratory a novel single stage process for upgrading emulsions via activation of water in the emulsion through the water gas shift reaction (WGSR) to provide hydrogen in situ for catalytic desulphurization and hydrocracking (1).This process could potentially reduce the environmental impact derived from the discharge of emulsions into tailings ponds. It is clear that in order to further develop the heavy oil/bitumen resources, new processes should be economically viable, flexible while assuring the quality of the environment. Our novel emulsion upgrading process could potentially achieve the above goals. It is envisaged that a single stage emulsion upgrading will minimize waste streams, lower the cost for hydrogen production and potentially break very stable emulsions which cause environmental hazards as in tailings pond.

In addition to our patents on emulsion upgrading, there are other patents related to the use of CO and synthesis gas for upgrading emulsions or heavy oils, including down hole upgrading (2). Aquathermolysis which utilizes water at 280 °C for hydrolysis of hydrocarbons in heavy oil, resulting in viscosity reduction and sulphur removal has been reported (3) . There are also reports of the aqueous high temperature chemistry of hydrocarbons and heterocylces (4) with a view to elucidate the chemistry involved in the steam stimulation of heavy oil reservoirs (~ 200-300 °C).

Experimental

All experiments were performed either in a 300 mL or a 1000 mL stainless steel batch autoclave (Autoclave Engineers). The synthetic emulsions were prepared by using toluene, water and an emulsifier (BASF P105). Dispsersed catalysts such as molybdic acid, phosphomolybdic acid, ammonium molybdate and ammonium tetrathiomolybdate were used. Model compounds such as benzothiophene (BTH) , dibenzothiophene were used to obtain kinetics of desulphurization (HDS) in an emulsion. HDS of a diesel fraction from Cold Lake bitumen was also studied.

The experiments were carried out over a temperature range of 320- 380 °C. The reactor was heated up at a rate of 2 °C per minute as recommended by Autoclave Engineers. The initial loading presssure of CO, synthesis gas (a 1:1 mol ratio of CO: H_2) or H_2 was between 300- 600 psig. For some of the experiments , samples of gas or liquid were taken for analysis. At the end of the reaction , the reactor was allowed to cool down overnight to room temperature. Gas, liquid and solids were then collected and analyzed. The gaseous product was collected in a gas bag and analyzed using gas chromatography (Perkin Elmer Model 8500) equipped with a thermal conductivity detector. The inlet system composed of a 1.5 m Hayesep C column in series with a 2 m molecular sieve column. Liquid analysis was carried out in the same GC using a 30 m DB-1701 fused silica capillary column and a flame ionization detector. X-ray fluorescence (Oxford Model Lab X-1000) was used to determine the sulphur content of the diesel fraction. X-ray diffraction, X-ray photoelectron spectroscopy and thermoanalysis techniques were used to characterize the spent catalysts.

Results and Discussion

Our initial research was based on the desulphurization of a synthetic emulsion (toluene/water) containing benzothiophene, a model compound for sulphur species in heavy oil. Simulated emulsions were used to provide a better understanding of the chemical and physical processes involved in upgrading heavy oil emulsions. Such information serves to provide a basis for the interpretation of data from experiments involving heavy oil emulsions.

Under the reaction conditions of 320 -380 °C and 300 -600 psig initial loading pressure of CO, the dispersed Mo catalysts were found to be effective catalysts for the HDS of BTH in an emulsion. The emulsion was found to be broken completely into 2 separate oil and water phases, with some black solids identified to be some form of MoS_x accumulated at the bottom of the reactor. Essentially complete sulphur removal could be achieved. Gas samples taken during the reaction showed that CO decreases as a function of time, while that CO_2 and H_2 increases as a function of time. In the absence of sulphur compounds ,the amount of CO_2 and H_2 were found to be equimolar as expected according to the stoichiometery of the water gas shift reaction shown in equation 1 (Fig 1). However, in the presence of sulphur compounds, the amount of H_2 was found to be less than CO_2 which was attributed to the consumption of H_2 during the reaction (Fig. 2).

A kinetic study was carried out for the production of hydrogen from the water gas shift reaction. In the absence of benzothiophene, the reaction followed a reversible pseudo first order kinetics. In the presence of benzothiophene, an irreversible first order reaction was observed (5). Similar behaviour was observed for molybdic acid and phosphomolybdic acid. The rate constants obtained for both catalysts were very similar suggesting that probably the same catalytic species was involved in the reaction (Table 1). It is interesting to note that the rate constant obtained in the presence of benzothiophene is higher than in the absence of benzothiophene. This could be attributed at least partly to the formation of a MoS_x species when benzothiophene was present and it has been reported that MoS_x is more active for the water gas shift reaction than Mo oxides (6). Indeed we found that the WGSR reaction proceeded at a faster rate when ammonium tetrathiomolybdate was used. Variation of the initial CO loading pressure from 300 - 600 psig also indicated a first order dependence on CO.

The kinetics of the HDS of BTH was obtained by analysis of liquid samples taken from the reactor. GC analysis indicated that dibenzothiophene was the intermediate of the reaction and that ethylbenzene was the final product (Fig 3). Therefore the reaction pathway for the desulphurization of benzothiophene could be represented by equations 1-3.

$$H_2O\text{ (emulsion)} + CO \underset{k_{-1}}{\overset{k_1}{\rightleftharpoons}} H_2 + CO_2 \qquad (1)$$

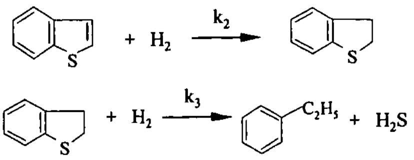

(2)

(3)

Mechanisms for the desulphurization of benzothiophene have been reviewed by a number of researchers (7). Two reaction schemes have been proposed. One involves the initial hydrogenation of benzothiophene to dihydrobenzothiophene, followed by sulphur removal to give ethylbenzene and H_2S. The second scheme is the direct desulphurization via C-S bond cleavage resulting in H_2S and styrene which is then hydrogenated to give ethylbenzene. Since dihydrobenzothiophene was detected as an intermediate in our reaction, the predominant pathway for desulphurization is hydrogenation of benzothiophene to give dihydrobenzothiophene which then undergoes hydrogenolysis to give ethylbenzene.

The desulphurization of benzothiophene in an emulsion with externally supplied molecular hydrogen was carried out .The reactivity of in situ hydrogen was found to be about 7 times that of supplied molecular hydrogen. This may be attributed to the fact that the in situ hydrogen may be more like atomic hydrogen and hence has a higher reactivity than molecular hydrogen. A higher reactivity of in situ hydrogen for HDS reactions has also been reported (8).

Results of HDS of dibenozthiophene in an emulsion indicated the rate constant for water gas shift reaction is essentially the same as that obtained with benzothiophene(10). The rate constant for sulphur removal is about a factor of 5 smaller than that of benzothiophene. This result is in accordance with the data by Ma et al (10). The activity of in situ hydrogen was found to be higher than that of molecular hydrogen. Product analysis revealed that the major pathway for desulphurization is via the hydrogenation of the aromatic ring to give tetrahydrodibenzothiophene. Since hydrogenation rather than hydrogenolysis apparently is the main pathway for the desulphurization of benzothiophene and dibenzothiophene , it may account for the higher activity of in situ hydrogen compared with molecular hydrogen.

Recently we examined the desulphurization of a diesel fraction from Cold Lake(11). Water was added to the diesel to simulate an emulsion.The reaction was carried out under the same reaction conditions as the model compounds benzothiophene and dibenzothiophene. The rate constant for the water gas shift reaction was found to be similar to that obtained in the presence of model compounds. However, the rate constant for desulphurization with in situ hydrogen was found to be similar to that of molecular hydrogen. It has been reported that diesel contains a mixture of sulphur compounds including substituted dibenzothiophenes which are very resistant to desulphurization. The difference between the reactivity of in situ hydrogen and molecular hydrogen towards model compounds and diesel may be due to the presence of highly substituted dibenzothiophene type compounds. Due to the steric hindrances of the substitued alkyl groups, the in situ hydrogen that was produced from the water gas shift reaction will decompose to give molecular hydrogen before it could be utilized for the desulphurization process.

Similar rate constants for desulphurization were observed when synthesis gas (1:1 mol ratio of CO: H_2) was used for the upgrading of diesel . This is an important result since this implies that CO is not an inhibitor for HDS. Since the cost of hydrogen for upgrading is high, the use of a cheaper source of hydrogen for upgrading will be attractive for the process economics

Conclusions

Dispersed molybdenum catalysts are effective for catalyzing the water gas shift reaction to generate hydrogen in situ for the desulphurization and upgrading of heavy oil/bitumen emulsions. The in situ hydrogen was found to be more active for the desulphurization of model compounds such as benzothiophene and dibenzothiophene. However, the reactivity of in situ hydrogen and molecular hydrogen was found to be about the same for the desulphurization of diesel. Synthesis gas could be utilized for the upgrading of heavy oil/bitumen emulsions.

Acknowledgement

Financial support from the Natural Sciences and Engineering Research Council of Canada (Strategic Grant Research Program, Industrially Oriented Research Program) and the Imperial Oil Research Grant Program are gratefully acknowledged.

References

1. Ng, F.T.T. and Tsakiri, S.K., US Patent, 5,055,175,199, 1991; Canadian Patent, 1317150, 1993; Ng, F.T.T. and Tsakiri, S.K., Fuel, 71, 1309 (1992); ibid , 72, 211 (1993)
2. Weissman, J.G., Kessler, R.V., Sawicki, R.A.,Belgrave, J.D.M, Laureshen, C.J., Mehta, S.A., Moore, R.G. and Ursenbach, M.G., Energy and Fuels, 10, 883, (1996).
3. Clarke, P.D., Clarke, R.A., Hyne, J.B., and Lesage, AOSTRA J. Res., 6, 29 (1990)

4.Katritzky, A.R. Lapucha, A.R., Luxem, F.J. Greenhill and Siskin, M., Energy and Fuels, 4, 572 (1990).

5. Milad, I.K., Hajek, P., Rintjema, R. J. and Ng, F.T.T. , unpublished data.

6. Hou, P., Mecker, D., Wise, H., J. Catal., 80, 280 (1983).

7. Daly, F.T., J. Catal., 51, 221 (1978).

8.Kumer, M., Akgerman A., and Anthony R.G., Ind. Eng. Chem. Process Dev., 23, 88 (1984) : Hook, B.D. and Akgerman, A., ibid, 25, 278 (1986).

9. Liu, C., Guruparanathan, S., Ganeshalingham, S. and Ng, F.T.T., unpublished data.

10. Ma, X., Sakanishi, K., Isoda, T. and Mochida, I., Ind. Eng. Chem. Res. 34, 748, (1995)

11. Siewe, C.N., and Ng, F.T.T., Energy and Fuels, (1998), in press.

Table I. Rate Constants for WGSR and HDS of BTH at 340 °C (4775 ppm Mo, 600 psig CO loading pressure, 49 mL toluene, 9.8 mL BTH, 21 mL water, stirring speed = 500 rpm)

Catalyst	Pseudo First Order Rate Constant[a]		
	$k_1' \times 10^4 (s^{-1})$	$k_2' \times 10^4 (s^{-1})$	$k_3' \times 10^4 (s^{-1})$
MA	2.3 1.4[b]	2.0	4.1
PMA	2.2 1.1[b]	2.3	3.8

[a] $k_1' = k_1[H_2O]$, $k_2' = k_2[H_2]$, $k_3' = k_3[H_2]$

[b] WGSR runs, no BTH added

MA = molybdic acid

PMA = phosphomolybdic acid

Figure 1. Product Distribution with time for the WGSR

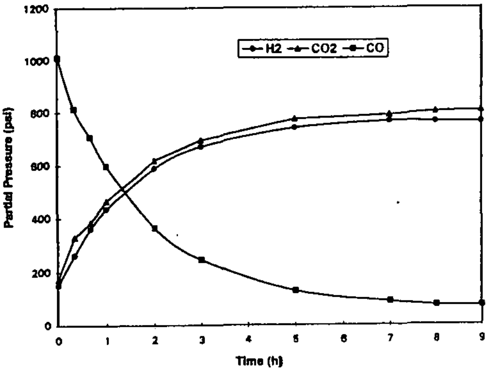

REACTION PROFILE FOR WGSR @ 380 °C.

(Pco_0 = 600 psig ; 70 ml H_2O/196 ml TOLUENE; 1.78 g MoO_3; 1300 rpm).

Figure 2. Product distribution of the WGSR with time in the presence of BTH

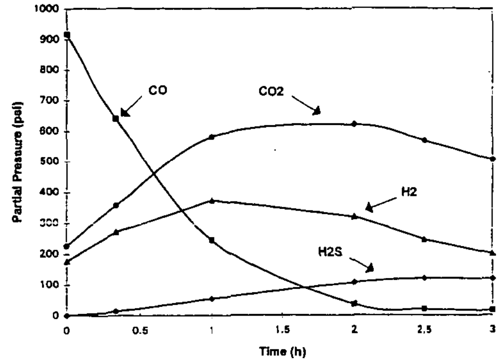

REACTION PROFILE FOR WGSR @ 380 °C.

(P_{CO_0} = 600 psig ; BTH_0 = 267 mmol; 70 ml H_2O/163 ml TOLUENE; 1.78 g MoO_3; 1300 rpm).

Figure 3. Product distribution for the HDS of BTH with *in situ* H_2

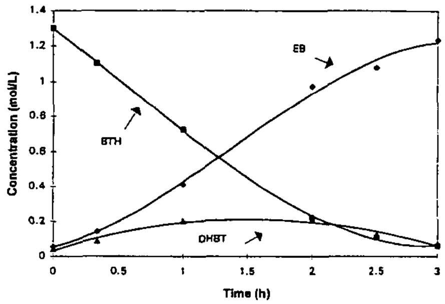

REACTION PROFILE FOR HDS @ 380 °C.

(P_{CO_0} = 600 psig ; BTH_0 = 267 mmol; 70 ml H_2O/163 ml TOLUENE; 1.78 g MoO_3; 1300 rpm).

Viscosity Reduction in Extra Heavy Crude Oils

Mark W. Badger and Harold H. Schobert
The Laboratory for Hydrocarbon Process Chemistry
The Energy Institute. 209 Academic Projects Building
The Pennsylvania State University
University Park. Pennsylvania. 16802-2303

Introduction

The next few years will see a change in the sources of crude oil in the global market. Advances in exploration and production technologies in the petroleum industry are creating new major sources in areas that were previously off limits for reasons of geography, politics and technology. Some of the new areas at exploitation will have a major significance on the US markets, namely, Latin America, especially Venezuela, and Canadian heavy oil and synthetic crude oil projects (1).

Latin American sources are expected to increase production to around 4.2 million bbl/day by 2005. Of this 1 million bbl/day is expected to be extra-heavy Orinoco oil from Venezuela. It has been projected that imports to the US from Latin America will increase by around 2.7 million bbl/day during the same period. As well as this, a big increase in crude oil production will come heavy crude oil reserves in Western Canada. These reserves are intended to be produced a diluted heavy crudes and as synthetic oils, with varying degrees of upgrading. It is expected that by 2005 another 700,00 bbl/day will be coming from Canadian heavy oil fields. Most of this will end up in the US Mid-West Market. This supply will replace the US supplies at lighter crude.

With such increases of heavy crude oil sources making there way into the US market in the near future now seems a good time to exploit new avenues of research into the reduction at their viscosity. Some of these crude oils can have viscosities in excess of 15,000 centistokes at 100°F (2). In order for these crude oils to be transported via pipeline from the source, the viscosity must be lower than 150 centistokes at 100°F. The crude oils being very viscous on extraction have to go through some processing e.g. gas plasticization, thermal cracking or blending with lighter distillate fractions, to enable them to be transported by pipeline.

Taking blending for an example, typically the crude oils are blended with a kerosene distillate fraction. This process has its disadvantages. In some cases up to 30 wt.% of kerosene must be added to sufficiently reduce the viscosity, this uses up a great quantity of a valuable commercial product. Also the added kerosene must be processed again through the refinery along with heavy crude oil.

It is widely assumed that the asphaltene molecules in oils agglomerate to form micelle-like clusters. Interactions between these clusters contribute towards the viscosity of the oils. By breaking these agglomerates apart viscosity will be reduced. The kerosene used to cut the oils and reduce viscosity only does so by being an effective diluent. It does not break down the agglomerates by any significant amount. The following work is from a scoping study, the objective of which was to see whether the viscosity of extra heavy crude oils could be reduced by the addition of other chemical compounds and/or distillate fractions, which may break down the asphaltene agglomerates, and thus achieve greater viscosity reductions, when compared with kerosene. The intention is to then augment the better of these additive compounds with kerosene, thus initiating viscosity reduction for less volume of diluent.

In this period of initial investigation several dispersants with differing physical and chemical properties have been assessed for their effect on viscosity reduction. Figure 1 shows the chemical structure and the polarity of the compounds, in Debye units (DU). The compounds were chosen for their ring type structures. The presence of π electrons in the ring may play a role in the interaction between the compounds added and the π electrons in the polyaromatic systems of the asphaltene agglomerates. The compounds were kept to one ring to keep the size of the molecules small and allow for a greater diffusion through the crude oil matrix, and penetration into the asphaltene agglomerates.

Experimental

All of the compounds used in this study were purchased from the Aldrich Chemical company, except for the xylenes mix which came from Marathon Oil's Texas City refinery. The sample characteristics of the extra heavy crude oil are shown in Table 1.

The experiments were performed using 70ml tubing bomb reactors, into which was placed a known weight of extra heavy crude oil. To this 2.4, 4.8 or 8.3 wt.% of additive compound was added, the reactor was sealed and purged with nitrogen gas. The reactors were placed into a heated sandbath and shaken for 2 hours at 200 °C. The resulting mixtures were then removed from the reactors and stored in sealed containers under nitrogen.

The viscosity measurements were carried out using a Brookfield DV-III programmable viscometer, fitted with Thermosel system for viscosity measurements at elevated temperatures. The viscosities were measured at 140 °F. The measurements were taken when the sample was at equilibrium. That is at the point when increases in the shear rate (related to spindle rotation) resulted in no or little (<1%) change in the viscosity measured. In other words the mixture exhibited signs of a Newtonian fluid.

Table 1. Sample characteristics of the extra heavy crude oil used in this study.

SAMPLE CHARACTERISTICS	
Carbon	76.6%
Hydrogen	10.5%
Nitrogen	0.7%
Sulfur	-
Average Molecular Weight	548
Liquid Density (g/ml)	1.013
API Gravity	8
Boiling Point/Wt%	>200 °C/99.8%
Viscosity (cP@140 °F)	7800

Results and Discussion

Figure 2 shows the raw viscosity/dispersant data to date. In the plot it can be seen that the additive compounds used have a diverse effect on viscosity. The major general trend to note is that with the increasing polarity of the dispersant there is an increase in the measured viscosity. The higher the polarity of an additive compound the stronger the dipole-dipole interactions are between them (3,4). Therefore they can break down the asphaltene agglomerates, but still have an attractive binding force throughout the mixture which in turn binds the molecules together and hence increases viscosity. The viscosity reduction however may not just be related to the break down of the asphaltene agglomerates. A more simple answer may be related to Eyring's theory of liquid viscosity (5). Although we have not looked in depth into using Eyring's theory, a relationship between dilution effects and viscosity can be deduced from it. More accurate calculations must be conducted including the relative densities, heats of vaporization, molar volumes and molecular weight of the as received compounds and the mixtures. However these calculations do not take into account the full effect of the dipole interactions, which are significant.

These are not the only factors worth noting. Solubility of the dispersant in the heavy crude will play a major role in viscosity reduction. If partial solubility or phase separation is occurring, then a lower than expected viscosity measurement will be recorded. This is because when phase separation occurs then the more fluid phase, i.e. the additive compound, may tend to concentrate around the spindle of the viscometer, and thus lower apparent viscosity. This would then explain why the viscosity measurements seems to be low for acetophenone and cyclohexanone (see Figure 3). We know that the crude oil sample is soluble in toluene, xylenes and the N-methyl pyrrolidinone. The curve in the line is too low where the cyclohexanone and acetophenone are. It is not likely that viscosity would level off when using miscible additive compounds with polarities between 1 and 3 DU. Therefore, partial solubility must be the cause for the lower measurements. However, solubility experiments should be conducted to prove this hypothesis

Assuming that the heavy crude oils are soluble in the dispersants, then molecular size of the additive compound may have an important role in viscosity reduction. Smaller molecules or molecules with the correct physical and chemical characteristics to fit into the gaps between the asphaltene agglomerates can reduce the viscosity to a greater extent. This is caused by deeper penetration, which induces greater break up of the asphaltene agglomerates.

One of the goals of this work is to determine whether an additive compound could be added to the kerosene diluent and enhance viscosity reduction. This theory assumes that the additive can break down the asphaltene agglomerates. For this to take effect only a small quantity of additive compound may be needed. For example, if 1 wt.% is sufficient to initiate the breakdown of the asphaltene agglomerates, then less kerosene would be needed to cut the viscosity to a level required for pipeline transportation.

Figure 4 shows a plot of log log viscosity against weight percent of additive compound in the crude oil. From this we took the y axis intercept for each additive compound and plotted it against its polarity. The resulting plot (Figure 5) was produced. From this we can assume that at low concentrations of additive compound in the crude oil, a compound with a polarity of around 0.6-0.7 Debye units and the right structural and chemical characteristics could lower viscosity more than other additive compounds, due to its greater dispersive qualities. This conclusion however needs verification through a detailed study of additive compounds with polarities in this area, as well as studies using mixtures of kerosene and additive compounds.

It can be seen from the data in Figure 2 that when toluene or xylenes mix is used then the measured viscosities are up to 50% lower than the equivalent weight percent for kerosene. In areas of heavy oil extraction where a supply of these lighter distillates is available, then using toluene or a xylenes mix from the BTX fraction may be a viable alternative to kerosene. Also a lower volume of distillate would be used. An extra advantage is that toluene and xylenes have a low enough boiling point that they could be removed, at nearly a 100% yield, from the crude oil prior to processing. By setting up a recycle stream costs of the operation would be lowered considerably. Plus if the feed for the recycle stream needs to be topped up, toluene and xylenes are made from the heavy crude oils during the refining process.

Conclusions

In this period of initial investigation it has been shown that the viscosity of extra heavy crude oils can be reduced to a greater extent using some additive compounds, when compared to using the conventional diluent kerosene. Interesting interactions, related to polarity, have been observed between the additive compounds and the crude oil matrix. There may be some scope to initiate a computer simulation of these interactions, as well as studying the mechanism through which asphaltene agglomerates are broken apart. Further work must include the study of additive compounds with polarities between 0.5 and 2.5 Debye units. Also reduction in the quantity of additive compound to 1 wt.% and lower must be studied, to evaluate whether there is still a linear relationship to the viscosity reduction at low concentrations.

References

1. Hermes, R.A., Oil and Gas Journal 96, 3, 16, (Jan. 19th 1998)
2. Butler, R.M., in "Thermal Recovery of Oil and Bitumen" Prentice-Hall, New Jersey. 1991.
3. Temperley, H.N.V, Trevena, D.H., in "Liquids and Their Properties - A Molecular and Macroscopic Treatise with Applications" Wiley, New York. 1978.
4. Reichardt, C., in " Solvent Effects in Organic Chemistry" Verlag Chemie-Weinheim, New York. 1979.
5. Glasstone, S., Laidler, K.J., Eyring, H., in "The Theory of Rate Processes - The Kinetics of Chemical Reactions, Viscosity, Diffusion and Electrochemical Phenomena" McGraw-Hill, New York. 1941.
6. Riddick, J.A., Bunger, W.B., in "Techniques of Chemistry. Volume II - Organic Solvents" Third Edition. Wiley-Interscience, New York.

Acknowledgments

The authors would like to thank the Marathon Oil Company for its financial support of this project. Also to Dr. Mark Plummer (Marathon Oil) and Professor Paul Painter (Penn State University) for their help, and Mihai Marasteanu, Steve Krumm and Craig Brickley of the Pennsylvania Transport Institute, at Penn State University, for their help with the viscometry measurements.

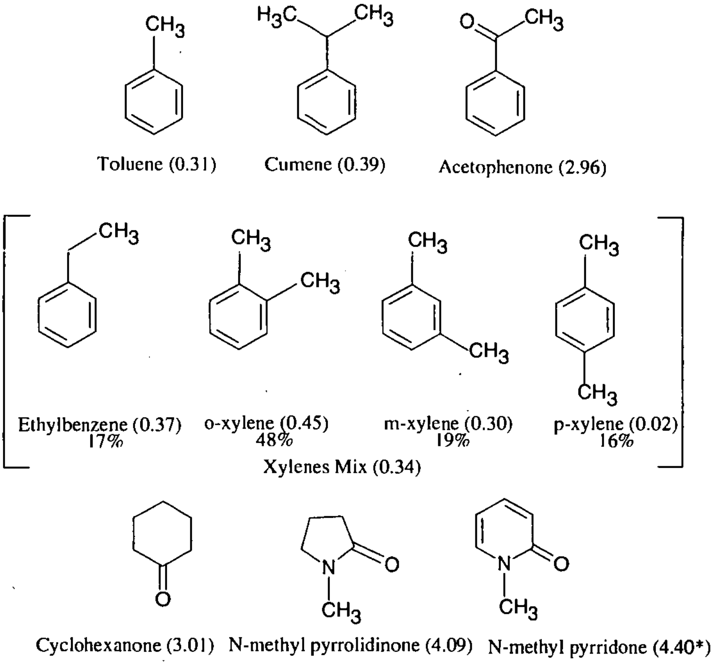
CH3
Toluene (0.31)
H3C CH3
Cumene (0.39)
O CH3
Acetophenone (2.96)
CH3
Ethylbenzene (0.37)
17%
CH3 CH3
o-xylene (0.45)
48%
CH3 CH3
m-xylene (0.30)
19%
CH3 CH3
p-xylene (0.02)
16%
Xylenes Mix (0.34)
O
Cyclohexanone (3.01)
N O CH3
N-methyl pyrrolidinone (4.09)
N O CH3
N-methyl pyrridone (4.40*)

Figure 1. Chemical structures and polarities (in Debye units) of the additives used.
* This value was calculated. The rest were taken from known data (6).

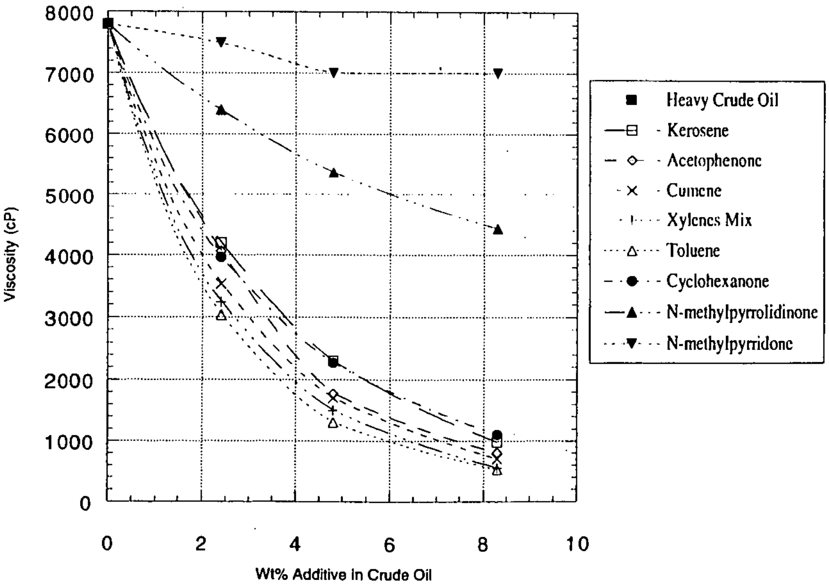

Figure 2. Plot of viscosity against wt.% of additive compound in the crude oil.

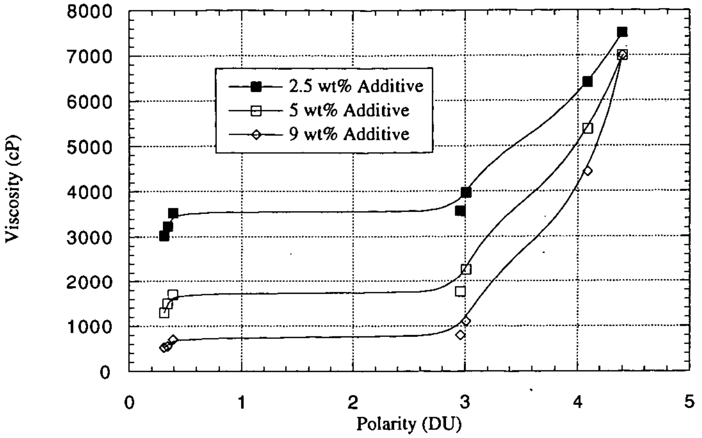

Figure 3. Plot of polarity of additives against measured viscosity

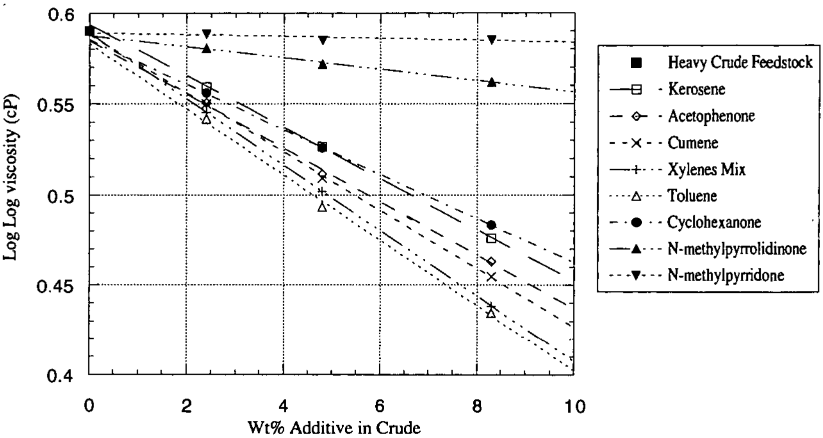

Figure 4. Log log viscosity vs. wt.% of additive in crude oil

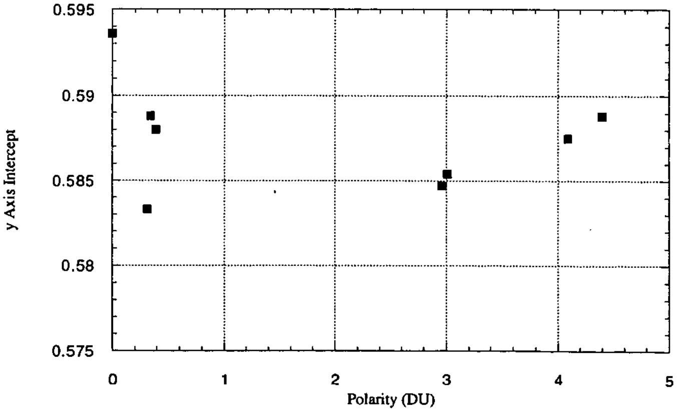

Figure 5. Plot of polarity of additive compounds against y axis intercepts from Figure 4.

RESID CONVERSIONS WITH CATALYSTS DERIVED FROM PHOSPHOMOLYBDATES

Belma Demirel, Ann Thomas and Edwin N. Givens

University of Kentucky Center for Applied Energy Research, 2540 Research Park Drive,
Lexington, KY 40511-8410

ABSTRACT

Hydroconversion of coal and petroleum derived heavy resids have been studied using both dispersed and impregnated Mo catalysts derived from phosphomolybdic acid (PMA). The dispersed catalysts were generated in situ by introducing the PMA supported on coal. During reaction the support essentially disappears producing a highly dispersed Mo catalyst, which is as active as the catalysts produced from common organic-soluble Mo precursors. The activity of PMA impregnated high-surface area aluminas has been compared with commercially available Mo catalysts. The resid conversion activities of catalysts prepared from both Ni and Co phosphomolybdates have also been determined. The activities of the alumina supported salts will be compared with the corresponding commercially-available alumina-supported bimetallic catalysts.

INTRODUCTION

Resid is defined as the fraction of petroleum, bitumen or coal liquids that does not distill under vacuum at atmospheric equivalent boiling points over 500°C. Resids are typically coked, hydroprocessed or used in manufacturing asphalts [1-5]. Coprocessing of coals with petroleum resid has been the subject of a number of studies in recent years with the intention of integrating coal into conventional petroleum refining operations [2, 3, 6-10]. Studies have suggested that combining coal liquefaction and heavy residue upgrading is economically feasible. It has been claimed that the presence of coal will reduce the deposition of coke and metals on the catalyst. In addition, heavy resids will also act as hydrogen transfer agents for coal conversion [2-4, 11-12].

In the near future, the resid content is expected to increase as price increases. Therefore, it becomes necessary to upgrade these fractions into distillable fractions. Hydrogenation is required in order to convert resids into more valuable products. Molybdenum based catalysts are generated *in-situ* from inorganic or organometallic compounds as precursors [13]. The metal precursors typically decompose thermally transforming into highly dispersed metal sulfides [14]. Although the exact form of the catalyst is not known, it appears to be some form of molybdenum sulfide, although apparently not MoS_2. Lopez et al. reported that the atomic ratio of molybdenum was less than two in the active catalysts isolated from processing heavy petroleum fractions with ammonium molybdate and thiomolybdate precursors [15]. Polyoxomolybdates have been known to create active, well-dispersed catalysts for converting both coal and resids. Bearden and Aldridge [16, 17] and Gatsis and Plaines [18] have reported hydroconversion processes for converting oil, coal or mixtures utilizing a catalyst prepared by first forming an aqueous solution of PMA and phosphoric acid. Our studies showed that phosphomolybdic acid (PMA) is readily transformed in the reaction media to produce an active form of catalyst for liquefaction of Wyodak coal [5, 19].

We have further expanded our work on PMA derived catalysts to investigate various methods of dispersing the molybdenum in the reaction mixture. The use of coal as a carrier is intriguing since it is inexpensive and largely converts to liquid product during the reaction thereby eliminating the necessity of recovering and disposing of a solid byproduct. Unfortunately, coal does not possess the unique activating effect that alumina imparts to molybdenum catalysts. This work reported here compares the activities of precursors when dispersed on coal and supported on Al_2O_3. The objective of this work is to convert both coal and petroleum derived resids to distillates boiling below 525°C using PMA and Ni and Co phosphomolybdate precursors.

EXPERIMENTAL

Wyodak coal from the Black Thunder Mine in Wright, Wyoming was supplied by Hydrocarbon Technologies, Inc. Proximate and ultimate analysis of the coal are given in Table 1. The solvents combined a 343-524°C distillate (Wilsonville Run 258 period B) and 524°C$^+$ deashed resid (Wilsonville Run 258 period A) that were obtained from the Advanced Coal Liquefaction R&D

Facility at Wilsonville, Alabama. Alumina was obtained from AKZO (AO-60; surface area, 180 m^2/g). Phosphomolybdic acid (PMA) was supplied by Aldrich Chemicals Inc. $Co_3(PMo_{12}O_{40})_2$ (CoPM), $Ni_3(PMo_{12}O_{40})_2$ (NiPM) and $K_3PMo_{12}O_{40}$ (KPM) were synthesized in our laboratory.

The Ni, Co and K salts of PMA were impregnated onto either coal or Al_2O_3 by adding aqueous solutions that contained the appropriate concentration of the individual metal salts to provide a final loading of 15 mg or 1000 mg of Mo per kg feed. During addition, the powdered coal or the Al_2O_3 support was continually stirred to assure even dispersion. The potassium salt was soluble only after adding a few drops of KOH to the water.

Activity tests were carried out in a 50-cc micro autoclave at 440°C and 1350 psig (cold) for 30 minutes. The reactor was equipped with a thermocouple, and connected to a pressure transducer for monitoring temperature and pressure during the reaction. Experiments were repeated at least once to confirm the reproducibility. In a typical experiment, 2.5 g of $524°C^-$ distillate, 4.0 g of deashed resid and 0.35 g of metal impregnated coal (on dry basis) or Al_2O_3. The reactor was loaded, pressurized with H_2S/H_2 (3 wt% H_2S in H_2), submerged in a fluidized sand bath and agitated continuously at the rate of 400 cycles per minute at the specified temperature. After quenching, solid and liquid products were removed from the reactor using tetrahydrofuran (THF). The filtered solids were extracted in a Soxhlet extractor overnight. The THF insoluble fraction was dried in a vacuum oven and weighed. The soluble fraction was distilled under vacuum (modified ASTM D-1160-87) to an atmospheric equivalent end point of 524°C. Resid conversion was calculated as follows:

$$\text{Resid Conv} = \left(1 - \frac{524°C^+\ \text{Resid}_{out}}{524°C^+\ \text{Resid}_{Feed}\ (\text{madf})}\right) \times 100$$

where madf is moisture, ash and distillate free. Mayan resid was processed with precursors dispersed or supported on coal or Al_2O_3. Larger scale simulations were performed in a 300-cc autoclave.

RESULTS AND DISCUSSION

PMA is a unique Mo precursor since it is relatively stable even in the presence of hydrogen to temperatures in excess of 300 °C. The stability of PMA has been associated with the Keggin structure in which the 12 Mo atoms surround the central phosphorus atom. The catalytic activity of PMA in a number of oxidation reactions has been associated with the Keggin structure. Although H_2S causes limited sulfidation at somewhat lower temperatures, the limited introduction of sulfur in the structure suggests that some ionic features may still be intact at relatively high temperatures, though certainly not at liquefaction temperatures. Yong et al. recognized that, in some cases, associated cations impart additional thermal stability on the Keggin structure [22]. For this reason, the thermal and catalytic activity of three metallic salts of PMA were investigated, namely the Co, Ni and K, and compared with the activity of PMA.

The thermal stability of the three salts in He is shown in Figure 1. The endotherm associated with dehydration of these materials is quite different for these salts. The K salt appears to dehydrate most rapidly, even more rapidly than PMA. Dehydration of the Ni and Co salts occurs over a much wider temperature range. An endothermic spike appears for these two salts at 330-400 °C which is lower than for PMA. This has been ascribed to the loss of constitutional water and collapse of the Keggin structure. Such a spike is not observed in the K structure until 500 °C suggesting that the Keggin ion may be stable at this temperature. In H_2 (see Figure 2), the initial loss of water from KPM occurs over a more narrow temperature range than for PMA. The material formed at 150 °C is quite stable. By contrast, the Ni salt and, to a lesser extent, the Co salt appear to continually lose weight over the whole region suggesting that dehydration is quickly followed by further changes in the ionic structure. After dehydration, the K salt is unusually stable at temperatures beyond 450 °C suggesting that the Mo may have remained in the +6 oxidation state. When H_2S is added along with H_2 (Figure 3), the PMA and Ni salt show a major loss in weight at approximately 300 °C, probably indicating breakdown of the Keggin ion. The K salt showed initially a weight gain suggesting incorporation of sulfur into the structure. However, at 350 °C, a very significant loss in weight occurs in an exothermic reaction. This suggests formation of a significant amount of water, destruction of the Keggin structure and reduction of Mo, probably to the +4 state, although this has not been confirmed. Clearly, the H_2S leads to a significant change in the stability of the K salt.

Resid conversions in the absence of a catalyst (Table 2) after 30 min was 10.9%. When coal equivalent to the amount used as a carrier for the metal catalyst was added to the reaction mixture, conversion increased by 1%. Although the thermal conversions are still incomplete, they are essentially unaffected by the presence of the coal. The addition of PMA at the 1000 ppm for the 30 min runs increased resid conversion by about 2%, whereas at the 15 ppm level there was no change

(Table 3). Increasing the run time to 90 minutes gave [illegible]gnificant increase in the level of conversion, also for the thermal reaction. Since the 15 ppm metal addition probably had no effect, the 21-22% conversion observed for both PMA and CoPM at this level is probably indicative of the thermal reaction. Increasing the metal concentration to 1000 ppm gave a sizable increase in conversion. Both PMA and the CoPM gave 31% conversion of resid to distillate. Although this work is in progress, it will be used to guide processing runs to be performed in a continuous batch configuration. The results from the conversion of petroleum resids and larger scale simulations will be discussed.

CONCLUSION

Thermal stability tests of PMA and bimetallic phosphomolybdates showed that these materials are mostly stable up to 400-450°C in the presence of He or H_2. The H_2S leads to a significant change in the stability, but transforms these materials into an active form of catalyst. Catalytic activity tests of PMA and bimetallic phosphomolybdates also showed that they have significant effect on resid conversion.

REFERENCES

[1] Nelson, W. L., Petroleum Refinery Engineering, McGraw-Hill, NY, 1958.

[2] Curtis, C. W., Guin, J. A., Pass, M. C. and Tsai, K-J., *Prepr. Pap.- Amer. Chem. Soc., Div. Fuel Chem.* **1984**, 29 (5), 155.

[3] Curtis, C. W., Guin, J. A., Pass, M. C. and Tsai, K-J., *Fuel Sci. Technol. Int.* **1987**, 5, 245

[4] Moschopedis, S. E. and Hepler, L. G., *Fuel Sci. Technol. Int.* **1987**, 5, 1.

[5] Demirel, B. and Givens, E. N., *Energy and Fuels* (in print).

[6] Curtis, C. W., Tsai, K-J. and Guin, J. A., *Ind. Eng. Chem. Res* **1987**, 26, 12.

[7] Curtis, C. W., Tsai, K-J. and Guin, J. A., *Fuel Process. Technol.* 1987, , 16, 71

[8] Curtis, C. W. and Cassell, F. N., *Energy and Fuels* **1988**, 2, 1.

[9] Flyn, T., Kemp, W., Steedman, W., Bartle, K. D., Burke, M., Taylor, N. and Wallace, S., *Fuel Process, Technol.* **1989**, 23, 197.

[10] Steedman, W., Flynn, T, Kemp, W, Bartle, K. D., Taylor, N. and Wallace, S., *Int. J. Energy Research* **1994**, 18, 299.

[11] Huber, D. A., Lee, Q., Thomas, R. L., Frye, K. and Rudins, G., *Prepr. Pap.- Amer. Chem. Soc., Div. Fuel Chem.* **1986**, 31 (4), 227.

[12] Gray, M. R., Upgrading Petroleum Residues and Heavy Oils, Marcel Dekker, Inc., N.Y., 1994.

[13] Del Bianco, A., et al., *Appl. Cat. (A)* **1993**, 94, 1.

[14] Kim, H. et al., *Prepr. Pap.- Amer. Chem. Soc., Div. Fuel Chem.* **1989**, 34, 1431.

[15] Lopez, J. McKinney, J. D. and Pasek, E. A., U.S. Patent 4557821, Dec. 10, 1985.

[16] Bearden, R. and Aldridge, C. L., U. S. Patent 4,637,870, Jan. 20 1987.

[17] Aldridge, C. L. and Bearden, R., U. S. Patent 4196072, Apr. 1, 1980

[18] Gatsis, J. G. and Plaines, D., U. S. Patent 3331769, July 18, 1967.

[19] Demirel, B. and Givens, E. N., *Catalysis Today* (in print)

[20] Del Bianco, A., Panariti, N., Anelli, M., Beltrame, P. L. and Carniti, P., *Fuel* **1993**, 72, 75.

[21] Marchionna, M., Lami, M. and Ancillotti, F., *Fuel Process. Technol.* **1994**, 40, 1.

[22]Yong, W. J., Quan, X. X. and Zheng, J. T., *Thermochimica Acta* **1987**, 111, 325.

ACKNOWLEDGEMENT

The authors gratefully acknowledge financial support provided by the U.S. Department of Energy Federal Energy Technology Center under contract number DE-AC22-91PC91040.

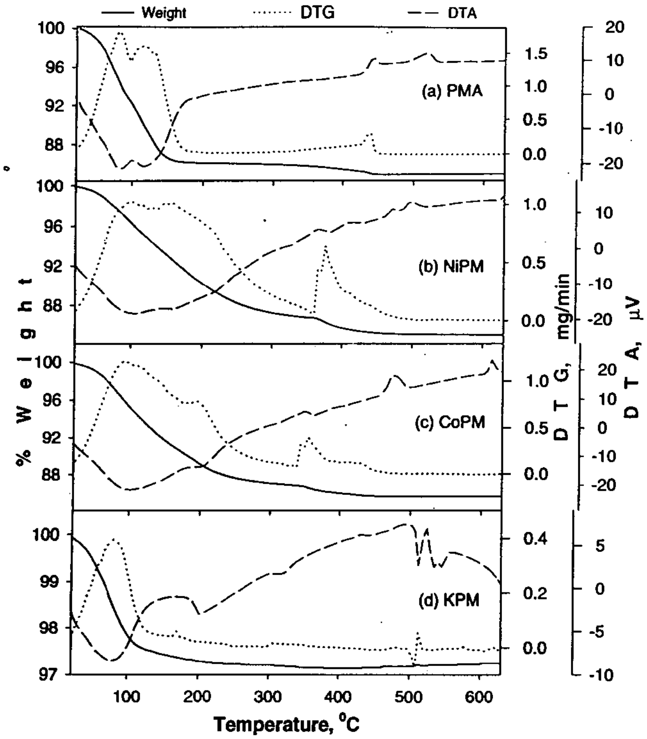

Figure 1. TG spectra of PMA and bimetallic phosphomolybdates in He.

Table 1. Analysis of Wyodak Black Thunder Coal.

Proximate Analysis	w%	Ultimate Analysis	w%(dry)	Sulfur Analysis	w%
Moisture	8.89	Carbon	70.62	Total	1.94
Ash	5.76	Hydrogen	5.03	Pyritic	0.80
Volatile matter	39.88	Nitrogen	1.13	Sulfate	0.80
Fixed carbon	45.47	Sulfur	0.52	Organic	0.34
		Oxygen (diff)	16.38		
		Ash	6.32		
		Ash, SO_3-free	5.47		

Table 2. Conversion of coal resid without catalyst.

	Resid conversion, wt%	
Reaction time, min	30	90
no catalyst, with coal	10.9	--
no catalyst, no coal	11.9	--

Table 3. Conversion of coal resid using PMA and CoPM.

	Resid Conversion, wt%			
Precursor	PMA		CoPM	
Reaction time, min	30	90	30	90
15 ppm Mo/g feed	11.9	22.2	12	21.1
1000 ppm Mo/g feed	14.3	31.2	--	31.4

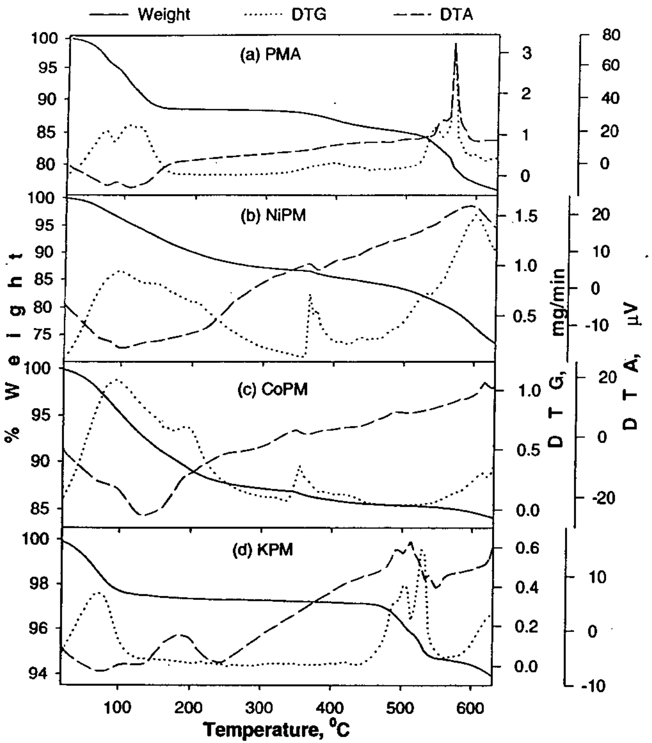

Figure 2. TG spectra of PMA and bimetallic phosphomolybdates in H_2.

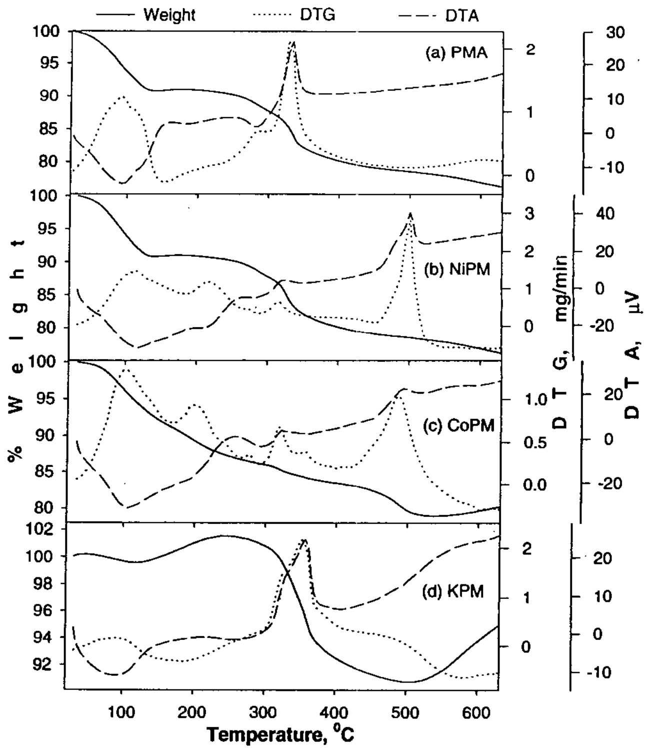

Figure 3. TG spectra of PMA and bimetallic phosphomolybdates in H_2S/H_2.

Upgrading a High Asphaltene Content Petroleum Residue by Hydrogenation with a NiMo-supported Catalyst

Ming-Gang Yang and Semih Eser

Fuel Science Program
and
The Energy Institute
209 Academic Projects Building
The Pennsylvania State University
University Park, PA 16802

INTRODUCTION

Upgrading petroleum heavy fractions has been increasingly important in petroleum refining for both economic benefit and environmental protection. Many technologies and strategies are now available for upgrading heavy residua. These processes can be divided into two broad categories: carbon rejection and hydrogen addition[1]. Carbon rejection processes redistribute hydrogen among the various components, resulting in fractions with increased or decreased H/C atomic. On the other hand, hydrogen addition processes involve external addition of hydrogen and result in an overall increase in H/C ratio of the products compared to that of the starting feedstocks. Hydroprocessing with NiMo (or CoMo)-supported catalysts has been widely used in commercial units because of high yields of liquid products and heteroatom removal[2-4]. Various heavy fractions have been used as feedstock for hydroprocessing. Process conditions depend on two major factors: feedstock properties and product specifications.

Catalyst deactivation in hydroprocessing is considered an important part of the process cost. Many deactivation processes, such as blocking of active sites by adsorption of asphaltenes, coke formation on the catalyst surface, pore blockage caused by metal accumulation, were researched[5,6]. Asphaltenes are considered to be responsible to the initial deactivation of the catalysts in heavy oil hydroprocessing[7,8], because of their adsorption on cobalt (or nickel) and molybdenum oxides and sulfides. At relatively high temperatures, asphaltenes are transformed to coke which deposits on the catalyst surface and causes deactivation of the catalysts. Therefore, the removal of asphaltenes is important for inhibiting catalyst deactivation and improving the downstream operating severity in a refinery.

Hydrogen-carbon atomic ratio (H/C) of feedstock is one of important factors determining the operation conditions. High H/C ratio means the feedstock has high hydrogen saturation and can be processed at relatively severe operation conditions. The change in H/C atomic ratio during the upgrading process can be used to measure the hydrogenation activity of a catalyst.

The present work explores the effects of a NiMo-supported catalyst and reaction conditions on upgrading a petroleum heavy residue, a ROSE pitch, which has high asphaltene and sulfur contents. Specifically, asphaltene conversion, sulfur removal, change in H/C atomic ratio, coke formation, and distillate production were investigated.

EXPERIMENTAL

The properties of the ROSE pitch used in the present work are listed in Table 1. The asphaltene and sulfur contents of the pitch are 29, and 6.0 wt%, respectively, and its H/C atomic ratio is 1.27. A simulated distillation analysis showed that the vacuum residue fraction (b.p.>525 °C) comprises more than 95 wt% of the pitch. A commercial catalyst, $NiMo/SiO_2\text{-}Al_2O_3$, was used hydrogenation experiments. The catalyst was sulfided in a batch reactor with CS_2 (anhydrous, > 99 %) as sulfur agent in *n*-dodecane (anhydrous, > 99 %) in two temperature stages: 200 °C for 2 h, and, then ,350 °C for 3 h before it was used in the experiments.

Reactions were carried out in 316 stainless steel batch reactors (25 mL) heated in a fluidized-sand bath. After adding the pitch and the catalyst, the headspace gas in the reactor was replaced three times with hydrogen before the reactor was charged with hydrogen to the desired cold pressure. Then, the reactor was plunged into a preheated sand bath. The experiments were carried out in the following range of conditions: 375 to 425 °C, initial H_2 pressure of 600-1250 psig, catalyst concentration of 10 - 20 wt%, and time periods of 30 – 90 min. The reactor contents reached the desired reaction temperature within 3 minutes. At the end of the reaction, the reactor was quenched in cold water. Liquid products (THF soluble) and solids (catalyst and deposited coke, THF insoluble) mixtures were washed with THF (Tetrahydrofuran, purity > 99.9 %). After separation of the solids from the mixture, the liquid products were recovered by evaporation of THF.

Asphaltene contents of the pitch and the liquid products were measured by treating the samples (0.2 ± 0.02 g) with *n*-hexane (20 mL) in an ultrasonic bath for 5 minutes, followed by settling for another 10 minutes before vacuum filtration through a previously weighed GF/A filter paper. The filtration residue was washed with excess hexane (about 30 mL). The solid residue and vial (as some residue remains adhered to the vial surface) were dried in a vacuum oven and weighed to determine the asphaltene content of the sample. The H/C atomic ratio and sulfur content of the feedstock or liquid products were measured by CHN–600 elemental analyzer and LECO sulfur analyzer, respectively. The coke on the catalys was defined as the difference in weight between the solid products (THF insoluble materials and catalyst) and the fresh catalyst. The fractional distribution of liquid products with repect to boiling point ranges was determined by Simulated Distillation gas chromatography (Hewlett Packard Series II 5890) with a high-temperature Megabore column P/N SD-002 HTC and a flame ionization detector.

RESULTS AND DISCUSSION

In order to investigate the effect of the catalyst on asphaltene conversion, the experiments were carried out either with or without the catalyst, but in the presence of hydrogen at the same initial pressure for both reaction systems. As shown in Figure 1, in the absence of the catalyst, both at 400 and 425 °C, the asphaltene conversion showed negative values, indicating an increase in asphaltene content after thermal reactions. In the same reaction system, the H/C ratio also decreased from 1.27 for the feedstock to 1.20 for the liquid products. The coke formation increased from 2 wt% of the feedstock at 400 °C to 10 wt% at 425 °C, as shown in Figure 2.

When the catalyst was present in the reaction system, both the asphaltene conversion and the H/C atomic ratio of the products increased. An asphaltene conversion of 44 and 46 wt % was achieved at 400 and 425 °C with the liquid product H/C of 1.35 and 1.37 at the corresponding reaction temperatures, respectively. These results are attributed to hydrogenation activity of the catalyst. The catalyst also showed high hydrodesulfurization (HDS) activity and suppressed coke formation (Figure 2). At 425 °C, more than 65 wt% sulfur was removed from the liquid products with only 1.5 wt% of the feedstock transformed to coke, compared to approximately 10 wt% coke obtained without the catalyst.

Figure 3 shows the change in asphaltene conversion and H/C ratio with increasing the temperature from 375 to 425 °C for 45 minute reaction. A significant increase in both parameters was observed upon increasing the temperature from 375 to 400 °C, with slight changes upon further increase in temperature from 400 to 425 °C. It appears that the thermal reactions, e.g., cracking and polymerization, become significant enough above 400 °C to offset the increase in hydrogenation activity of the catalyst. With the increasing reaction temperature from 375 to 425 °C, sulfur conversion increased proportionally from 13.5 to 45.7 wt %, and coke formation increased from 0.58 to1.3 wt%, as shown in Figure 4.

Figure 5 shows the effect of hydrogen pressure on asphaltene conversion and H/C ratio at 425 °C for 90 min with a catalyst concentration 20 wt %. Both parameters increased almost linearly with the increasing cold hydrogen pressure from 600 to 1250 psig. An asphaltene conversion of 92 wt% and a H/C ratio of 1.51 were achieved at the highest pressure used in the experiments. High hydrogen pressure also promoted sulfur removal, as shown in Figure 6, but it did not affect the coke formation to any significant extent in the range of 600-1250 psig initial H_2 pressure.

Increasing the reaction time from 30 to 45 min increased the asphaltene conversion from 31 to 46 wt% at 425 °C, 1000 psig initial H_2 pressure and 10 wt % catalyst concentration. Further increase in reaction time to 90 min did not cause any significant change in asphaltene conversion or in the H/C ratio of the liquid products. These observations can also be explained by the competing catalytic and thermal reactions, as discussed before for high temperature experiments.

Figures 7 shows the simulated distillation curves of the liquid products as a function of reaction temperature at 1000 psig initial hydrogen pressure, 45 min and 10 wt % catalyst. The distillation curve for the starting residue is also shown in Figure 7 for comparison. With the increasing reaction temperature, the curve shifts to lower temperatures, indicating the production of lower boiling-point material. The conversion of 525 °C$^+$ fraction was 5.2, 12.2 and 35.5 wt% at 375, 400 and 425 °C, respectively. The conversion increased nearly three times when the reaction temperature increased from 400 to 425 °C. Increasing the reaction time to 90 min at 425 °C (not shown in the figure) gave approximately 50 wt% conversion of the 525 °C$^+$ fraction. This means that thermal reactions essentially controlled the cracking at higher reaction temperatures.

CONCLUSIONS

Hydrogenation of a ROSE pitch produced liquids with low asphaltene and sulfur content and high H/C atomic ratio because of the high hydrogenation activity the NiMo-supported catalyst used in this work. At both low and high reaction temperatures, the hydrogenation activity of the catalyst was predominantly responsible for the asphaltene conversion and increase in the H/C atomic ratio. High extents of sulfur removal and suppression of coke formation were also possible because of the high hydrogenation activity of the commercial catalyst.

ACKNOWLEDGMENTS

This work was supported by funds from USX Foundation at the Laboratory for Hydrocarbon Process Chemistry at Penn State University. We thank Dr. Mark Plummer and Mr. Rolf Schroeder of Marathon Oil Company for many helpful discussions. We thank Dr. Mark Badger of PSU for his help with experimental work during the initial phase of this study. The catalyst sample was provided by Criterion.

REFERENCES

1. Dickenson, R. L.; Biasca, F. E.; Schulman, B. L.; Johnson, H. E. *Hydrocarbon Processing* **1997**, *76*, 57.
2. Sonnemans, J. W. M. In *Catalysts in Petroleum Refining and Petrochemical Industries 1995*; Stud. Surf. Sci. Catal., Elsevier Sci. B. V. **1996**, Vol. 100, p 99-115.
3. Yang, M.-G.; Nakamura, I.; Fujimoto, K. *J. of The Japan Petroleum Institute* **1997**, *40*, 172.
4. Yang, M.-G.; Nakamura, I.; Fujimoto, K. *Catal. Today* **1998**, in press.
5. Oballa, M. C.; Wong, C.; Krzywicki, A. *In Catalytic Hydroprocessing of Petroleum and Distillates*, Marcel Dekker, New York, **1994**, p 33-54.
6. Richardson, S. M.; Nagaishi, H.; Gray, M. R. *Ind. Eng. Chem. Res.* **1996**, *35*, 3940.
7. Bartholomew, C. H. *In Catalytic Hydroprocessing of Petroleum and Distillates*, Marcel Dekker, New York, **1994**, p 1-13.
8. Trimm, D. L. In *Catalysts in Petroleum Refining and Petrochemical Industries 1995*; Stud. Surf. Sci. Catal., Elsevier Sci. B. V. **1996**, Vol. 100, p 65-76.

Table 1. Properties of ROSE Pitch Feedstock

Simulated distillation, wt %	
naphtha (IBP - 171 °C)	0.0
kerosene (171 - 232 °C)	0.0
gas oil (232 - 370 °C)	0.7
VGO (370 - 525 °C)	3.7
residue (525 °C+)	95.6
Asphaltene, wt %	29
Elemental analysis, wt %	
C	82.4
H	8.7
N	0.61
S	6.0
H/C atomic ratio	1.27

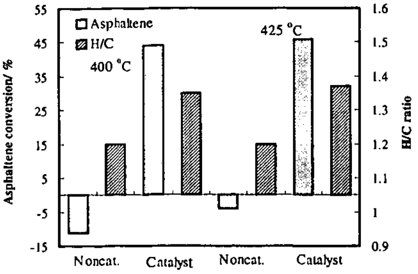

Figure 1. Comparison of thermal and catalytic reactions in asphaltene conversion and H/C atomic ratio change. 1000 psig H_2 pressure; 90 min; 10 wt % catalyst.

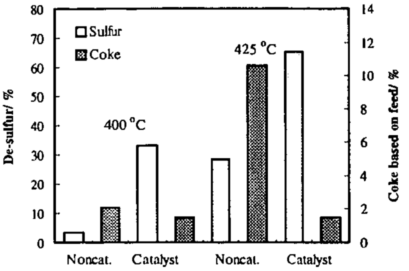

Figure 2. Comparison of thermal and catalytic reactions in sulfur conversion A nd coke deposits. 1000 psig H_2 pressure; 90 min; 10 wt % catalyst.

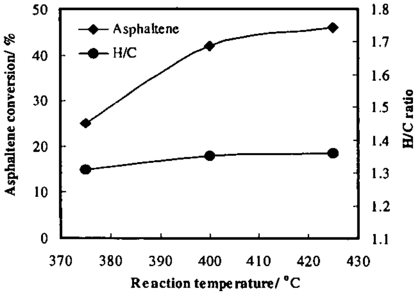

Figure 3. The effect of reaction temperature on asphaltene conversion and H/C atomic ratio increase. 1000 psig H_2 pressure; 45 min; 10 wt % catalyst.

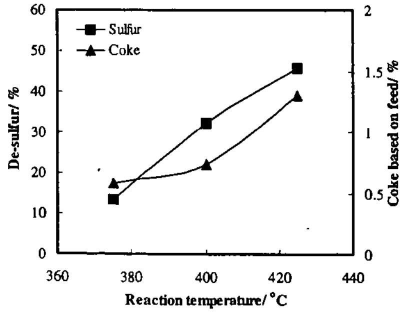

Figure 4. The effect of reaction temperature on sulfur conversion and coke deposits. 1000 psig H_2 pressure; 45 min; 10 wt % catalyst.

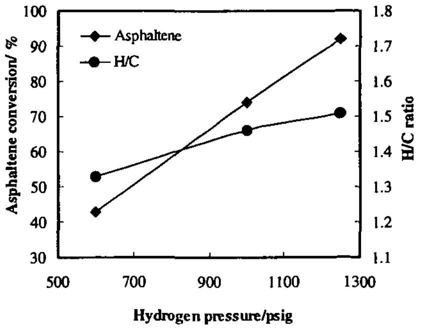

Figure 5. The effect of initial H_2 pressure on asphaltene conversion and H/C atomic ratio increase. 425 °C; 90 min; 20 wt % catalyst.

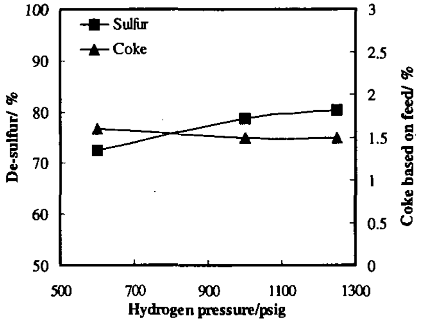

Figure 6. The effect of initial H_2 pressure on sulfur conversion and coke deposits. 425 °C; 90 min; 20 wt % catalyst.

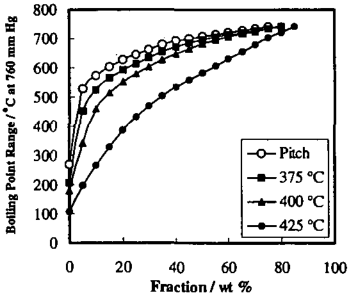

Figure 7. Distillation curves of feedstock and products at different reaction temperature. 1000 psig H_2 pressure; 45 min; 10 wt % catalyst.

THE USE OF METHANE AS SOURCE OF HIGHER HYDROCARBONS AND HYDROGEN FOR UPGRADING HEAVY OILS AND BITUMEN

Parviz Rahimi, Craig Fairbridge, National Centre for Upgrading Technology, 1 Oil Patch Drive, Suite A202, Devon, Alberta, Canada, T9G 1A8

Dennis Tanner, Department of Chemistry, University of Alberta, Edmonton, Alberta, T2G 2G2

Key words: Helium-methane plasma, helium-hydrogen plasma, hydrogen addition, methyl radicals, higher hydrocarbon from methane

ABSTRACT

Both the production of synthetic crude from the oil sands in Alberta and the upgrading of heavy oils to lighter products require hydrogen. The production of hydrogen by the steam reforming of methane is not only expensive but also contributes significantly to the production of greenhouse gases. Therefore, in bitumen and heavy oil upgrading, there is a major incentive to use methane directly. This paper describes the reactions of hydrogen and of methane plasma with olefin and aromatic model compounds and presents possible reaction mechanisms.

INTRODUCTION

Because of economic and environmental impacts, the direct use of methane or natural gas which contains 90 mole % methane in place of hydrogen has attracted considerable attention in recent years. It has been shown that different ranks of coal under coal liquefaction conditions and presence of methane produce more volatile products than under nitrogen.[1-3] Using model compounds such as benzene, naphthalene, toluene, bibenzyl and phenol, it has been demonstrated that a moderate degree of methylation can be achieved under certain conditions.[4-6] Recently, Pang et al.[7] concluded that, in the reaction of methane with petroleum and coal model compounds and the presence of catalyst, methylation yields are low because of the thermodynamics of the reaction is unfavorable. Ovalles et al.[8-9] reported the use of methane as a source of hydrogen for the upgrading of heavy oils. These authors reported a significant decrease in the viscosity of the crude and conversion of 540° C^+ with methane. Ilton and Maron have also demonstrated that the activity of methane can be enhanced in the presence of certain catalysts and their enhancement results in a high conversion of methane into higher hydrocarbons.[10]

Using microwave discharge, Mazur et al.[11] reported that atomic hydrogen can be generated from hydrogen gas and this atomic hydrogen can be reacted with olefins to form saturated and dimeric products. Tanner et al. [12] subsequently showed that the addition of hydrogen to olefins can be regiospecific.

The available data in the literature regarding the use of methane as a source of hydrogen indicate that methane is not useful for upgrading heavy hydrocarbons to lighter products because the use of methane results in low or no conversion. Other efficient methods for methane activation must be discovered in order to be able to use more or all of the available hydrogen in this molecule.

For the data reported in this paper, the use of methane as a source of hydrogen and higher hydrocarbons was investigated using microwave discharge. The objective was to follow the fate of methyl radicals and hydrogen atoms formed from methane under microwave discharge and reacted with model compounds containing double bonds. Furthermore, to shed light on the mechanism of dealkylation or cleavage of strong C-C bonds, the reaction of hydrogen atoms generated from hydrogen/helium plasma was investigated using toluene.

EXPERIMENTAL

General method for CH_3 radicals and H atoms reaction

Experimental details for H atom reactions with model compounds can be found elsewhere.[12] Similar Pyrex reactor and experimental conditions were used for the reaction of CH_4 with the model compounds. Briefly, the reactions with substrates (model compounds) were carried out in a Pyrex reactor neat or in acetone solution at -78°C. Helium-hydrogen or helium-methane was introduced into the reactor system at the desired flow rate. The pressure of the reactor was maintained at 3-4 Torr. H_2–He or H_2- CH_4 plasma was generated in the microwave cavity. Hydrogen atoms or methyl radicals were swept into the stirred solution. The reaction products were analysed and identified using GC/FTIR and GC/MS and quantified using a Varian Vista 6000, equipped with FID detector and a glass capilary column (PONA, 30 mx0.25mm, HP).

RESULTS AND DISCUSSION

Reaction of CH_4 with model compounds

In a previous study, the results of hydrogen radical addition to model compounds indicated that these molecules can be saturated at very low temperatures.[12] In the present study, the reaction of methane as a source of hydrogen with 1-octene and cyclohexane was investigated. The product distributions from He/CH_4 plasma are shown in Table 1 and Table 2. For comparison, the products from the reaction of He/H_2 plasma with these model compounds are also shown in these tables. No attempts were made to optimize the product yields. The results show that the products in the reaction of He/CH_4 plasma with both olefins are identical to those of the reaction of H_2/He plasma with the olefins. However, in the reaction with CH_4, a number of higher alkanes which were assumed to be resulting from the polymerization of methane could be identified (not quantified) in the reaction mixtures. Formation of higher hydrocarbons in these experiments was not quantified but their production signifies the possibility of the formation of higher hydrocarbons from methane. Although there was no evidence of the reaction of methyl radicals with the olefinic substrates, methyl radicals could be trapped by a spin trap such as tert-butylphenylnitron. This material was added to the reaction mixture before the plasma was activated; upon treatment with methane plasma the stable EPR spectra of the methyl radical spin adduct was observed.

The product distribution in the reaction of He/CH_4 plasma with toluene at –78°C is shown in Table 3. Beside hydrogenation products, addition of methyl radicals to toluene produced substituted toluene and combination reactions of benzyl and methyl radicals produced ethyl benzene. Formation of benzene in this reaction mixture has mechanistic significance since it indicates that hydrogen atoms had displaced methyl radical via ipso attack.

The mechanistic investigation of hydrogen addition to substituted aromatics was further continued by the reaction of H_2/He plasma with model compounds such as bibenzyl, 9-dodecylanthracene, dodecylbenzene, dibenzothiophene and 2-naphthalene thiol, but this investigation will be the subject of a later publication.

REFERENCES

1. Yang, K., Batts, B.D., Wilson, M.A., Gorbaty, M. L., Maa, P.S., Attalla, M.I., Long, M.A., and He, S.J.X., Fuel, 76, 1105 (1997).
2. Sundaram, M. S. and Steinberg, M., US Patent No. 4,687,570, 1987.
3. Egiebor, N.O. and Gray, M.R., Fuel, 69, 1276 (1990).
4. Wilson, M.A., Attalla, M.I., Yang, K., He, S.J.X., Long, M.A., Batts, B.D., Smith, J.W., Voigtmann, M.F. and Smith, D.R., Synthetic Fuels from Coal and Natural Gas, NERDPP End of Grant Report Project No. 1613, Canberra, Australia, 1993.
5. Scott, D.w., Bulletin 666, US Bureau of Mines, 1974.
6. He, S. X. J., Long, M.A., Wilson, M.A., Gorbaty, M. L., and Maa, P.S., Energy and Fuels, 9, 616 (1995).
7. Yang, K., Wilson, M.A., Quezada, R.A., Prochazka, J.L., Long, M.A., He, S.J.X., Gorbaty, M. L., and Maa, P.S., Fuel, 76, 1091 (1997).
8. Ovalles, C., Hamana, A., Rojas, I., and Bolivar, R., Proceedings of Eastern Oil Shel Symposium, 161, 1993.
9. Ovalles, C., Arias, E.S., Hamana, A., Badell, C.B., and Gonzalez, G., Fuel Chemistry preprints, 39, 973 (1994).
10. Ilton, L.E. and Maron, V.A., US Patent No. 5,068,485, 1991.
11. Berri, A., Berman, E., Vishkautsan, R., and Mazur, Y., J. Am. Chem. Soc., 108, 6413 (1986)
12. Tanner, D.D and Zhang, L. J. Am. Chem. Soc., 116, 6683 (1994)

Table 1. A comparison of the product distribution of the addition of atomic hydrogen (generated by microwave discharge of methane or H_2[a]) to 1-octene at ~78°C.

Reaction %	CH_4 Flow Rate ML/min (min)	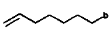	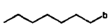	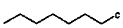	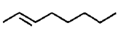	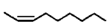	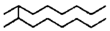	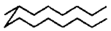
4.26	1 (30)	20.2	32.6	20.2	9.90	2.60	13.3	1.20
3.58	2 (35)	23.5	31.7	22.1	7.30	0.90	12.9	1.60
3.36	3 (30)	9.8	24.1	40.9	11.20	3.10	9.8	1.00
7.88	4 (30)	25.2	34.9	14.7	7.30	2.30	14.2	1.00
2.00	4 (30)	17.4	29.0	29.4	9.50	2.10	11.8	0.70
4.06[d]	4 (30)	22.9	34.9	14.8	9.20	2.90	14.3	0.90
	H_2 Flow Rate ML/min (min)							
3.09	4 (11)	16.4	27.7	29.8	10.9	2.54	11.7	0.92
8.05	4 (11)[d]	22.8	34.9	14.2	11.0	2.33	14.5	0.85

[a] See Ref. 12.

[b] Products formed by the disproportionation reactions.

[c] Products formed by the addition of hydrogen atom to a secondary alkyl radical.

[d] 1 M solution in acetone.

Table 2. A comparison of the product distribution of the addition of atomic hydrogen (generated by microwave discharge of methane or H_2) to cyclohexene at ~78°C.

Reaction %	CH_4 or H_2 Flow Rate (mL/min)	Time (min)	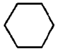	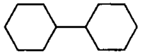	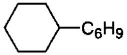
0.90	4	15	79.6	15.8	4.7
0.80	6	30	73.6	17.3	9.0
0.80	1	30	55.3	29.4	15.3
1.4[a]	4	20	91.8	5.9	2.3
2.1[a]	4	30	86.0	11.3	2.7

[a] Reaction with H_2.

Table 3. The Reaction of a CH_4 Plasma with Toluene (-78°C).

CH_4 (mole) Passed into The System	Reaction Time (min)	C_2H_6	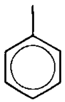	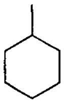	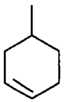	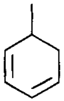	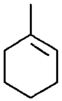	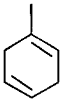	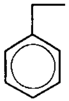	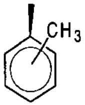 CH_3	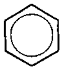	Dimer	% CH_4 Consumed
0.008	65	NQ	98.2				0.04	1.07	0.08	0.08	0.18	0.29	26
0.007	40		99.2	0.04			0.02	0.20	0.05	0.05	0.06	0.44	16.1
0.016	90		98.7	0.04			0.02	0.32	0.13	0.06	0.07	0.50	8.8
0.0018	10		99.4	0.03			0.08	0.10	0.04	0.05	0.05	0.13	37.9

NQ – not quantitated.

HYDROCRACKING OF LIAOHE VACUUM RESIDUE WITH BIMETALLIC OIL-SOLUBLE CATALYSTS

Ruihua Shen, Chenguang Liu and Guohe Que
Department of Chemical Engineering, University of Petroleum
Dongying, Shandong, 257062, P. R. China

ABSTRACT

Hydrocracking of Liaohe vacuum residue was investigated in an autoclave promoted by oil-soluble molybdenum dithiocarboxylate, nickel and iron naphthenates as well as their mixtures. The reaction was conducted at temperature of 430°C, residence time of 1 hour, catalyst concentration of 200ppm(based on metal in feed), and initial hydrogen pressure of 7.0MPa. It was found experimentally that high residue conversion, and low coke(toluene insoluble) and light gas yields were achieved in the presence of the mixed catalysts, indicating the mixed catalysts to be more active than the single one for the hydrocracking of vacuum residue. It was also discovered that the synergism was obviously present for the bimetallic catalysts when the weight ratio of molybdenum to nickel or iron was 3 to 2. X-ray diffraction(XRD) analyses of the toluene insolubles indicated that the active species of catalysts were non-stiochiometric metal sulfides, and no joint sulfides occurred in the presence of bimetallic catalysts. Microscopy and transmission electron microscopy(TEM) analyses further revealed that the dispersion of catalysts was improved in the presence of the second metal.

KEY WORDS: Hydrocracking, Bimetallic Oil-soluble Catalyst, Vacuum Residue

INTRODUCTION

The use of homogeneous oil-soluble metal compounds to enhance the liquid yield and to reduce coke formation has been explored extensively in the hydrocracking of heavy feedstocks. These compounds are based on transition metals, such as Mo, W, Co, Ni, V, and Fe[1]. It is well known and of great industrial importance that the addition of a second transition metal such as Co or Ni to a binary sulfide such as MoS_2 or WS_2 can give rise to an enhancement of HDS activity. In this paper we investigated the application of bimetallic oil-soluble catalysts and evaluated the relative activities of these homogeneous catalysts for liquid phase catalytic hydrocracking of Liaohe vacuum residue.

It is generally accepted that Mo-based catalysts give the best performances in terms of coke inhibition and product upgrading. On the other hand, Fe-based materials are often used in slurry processes because of their lower cost even though they show very low activity toward hydrogenation reactions.

The degree of dispersion of the catalyst strongly affects its activity. Although high levels of catalyst dispersion can be achieved by introducing some techniques[2,3,4], adding oil-soluble catalyst precursors seems the best way to promote a good dispersion. A systematic investigation showed that catalyst performances are almost independent of the organic group bonded to the metal as long as the organic group has provided oil solubility as well as the thermal lability to the precursor[5].

It is clear that the most promising new catalysts might stem from research on promoted or multicomponent systems. The objective of the present investigation was to develop bimetallic oil-soluble catalysts and to evaluate the relative activities of these homogeneous catalysts. The aim was to determine whether sufficiently small quantities of these catalysts could be used so that they would not need to be recovered after hydrocracking. The objective was to accelerate the rate of the hydrogenation reactions to permit them to keep pace with thermal cracking of the asphaltene and thus yield more stable distillates.

EXPERIMENTAL

The hydrogenation reactions were performed on a vacuum residue (500+) of Liaohe crude with bimetallic oil-soluble compounds as catalyst precursors. The vacuum residue feedstock used throughout the experiments was Liaohe Tuozili vacuum residue supplied by the Liaohe Petrochemical Refinery. The properties of this feedstock were reported in Table 1. These catalysts were mixtures of molybdenum dithiocarboxylate (MoDTC) and nickel or iron naphthenate (NiNaph or FeNaph) which was prepared from the commercially-available precursors. The weight ratio of the two metals varied from 1:4 to 4:1.

The hydrocracking experiments were all conducted with 35g Liaohe vacuum residue in a 100mL magnetically-stirred autoclave equipped with a thermocouple well. The weight of metal catalyst was calculated to give 200 ppm of metal based on the vacuum residue feed. The catalyst was weighed and added directly to the residue in the autoclave without vehicle or solvent. Then little elemental sulfur was added to promote the generation of the active form of the catalyst. Next, the autoclave was sealed, purged of air, and the hydrogen pressure brought up to 7.0MPa. The autoclave temperature was brought up to 300°C at a heating rate of 13°C min^{-1} and held at that temperature for half an hour to sulphidize the catalyst. Then the temperature was brought up to the reaction temperature of 430°C and holds for an hour.

After reaction the final autoclave pressure was measured and the autoclave was then cooled to room temperature. The gases in the autoclave were slowly vented to the fumehood and the autoclave was opened to permit the removal of the hydrocracked liquid product. The liquid products of the reactions were directly pumped into a weighed sample bottle and distilled using a modified ASTM D1160 procedure. Three distillate fractions were collected over three atmospheric boiling point ranges: initial boiling point (IBP) to 200°C, 200-350°C, 350-500°C and a residue of 500^{+}°C.

Duplicate autoclave experiments were performed for the characterization the percentage yields of the coke (toluene-insoluble). The coke was then characterized in terms of elemental analysis, x-ray diffraction (XRD) analysis and transmission electron microscopy (TEM) analysis.

RESULTS AND DISCUSSION

Influence of Catalysts on Yield and Product Distribution

In order to obtain a preliminary indication of the effect of the bimetallic catalysts, we carried out several experiments with one oil-soluble catalyst. All experiments with one or two oil-soluble catalysts and the results were shown in Table 2 and Table 3. Runs 1, 7 and 13 were processes with one oil-soluble catalystMo, Ni and Fe. Others were processes with two catalysts of different metal ratios. The yields of coke and hydrocarbon gas reflect the activity of the catalyst. In general the changes in the two criteria associated with the changes of the organic portion of the catalyst were relatively minor. So from these two criteria it appears that the metals gave the following order of activity: Mo symbol 62 \f "Symbol" \s 12> Ni symbol 62 \f "Symbol" \s 12> Fe.

When the mixture of two oil-soluble catalysts was used, the yields of coke and light gas were lower than either the nickel naphthenate or iron naphthenate was employed alone under the same hydrocracking operating conditions. The conversion of the residue (the yield of the distillates 500°C-) were higher than the molybdenum dithiocarboxylate was employed alone. Especially when the weight ratio of molybdenum to nickel or iron was 3 to 2, the yields of coke and gas were the lowest. A comparison on the basis of the percentage yield of coke of the performance of the bimetallic oil-soluble catalysts suggests that the activity of the catalysts of this ratio was approximately the equivalent to that of the molybdenum dithiocarboxylate and superior to that of nickel or iron naphthenate.

Characterization of Catalysts

Solids (coke + catalyst) obtained from hydroconversion were characterized by several techniques. At first, the x-ray diffraction data showed no evidence for the formation of a Ni-Mo (or Fe-Mo) sulfide. The two metals give rise to separate non-stiochiometric sulfides that may act as supplementary catalytic materials. Two metals bonded together, however, could produce a significantly modified Mo structure. When the ratio of the two metals was 3 to 2, the synergism was obvious.

From transmission electron microscopy (TEM) analysis, it appears that catalyst particles appears as irregular clusters of lamellas with a mean thickness of about 2-7nm (Figure 1). The size of the particles and irregular clusters in the presence of the bimetallic catalyst was smaller than that of the single-metal catalyst. This showed the dispersion of the promoted system was improved.

The microscopy analysis of the hydrocracked liquid phase verified previous conclusion (Figure 2). The very fine materials maybe catalyst particles absorbed with hydrocracked distillates. The mean size of the fine materials of the promoted system was much lower than that of the single-metal system. This indicated that the presence of the second metal improved the dispersion of the catalysts.

CONCLUSIONS

The results of this work demonstrate that the nature of the catalyst metal in the oil-soluble catalyst played a very significant role in governing the yields of coke and gaseous as well as liquid products. On improving the amount of hydrogen transfer under hydrocracking conditions by the using of mixtures of two oil-soluble catalysts, the coke yield decreased greatly. The bimetallic oil-soluble catalysts were superior in terms of residue conversion, as well as yield of coke and light gas, as compared to the use of single-metal catalysts. The synergism was especially obvious when the weight ratio of molybdenum to nickel or iron was 3 to 2.

X-ray analysis showed that, under the hydrocracking conditions, there is no evidence for the formation of a Ni-Mo (or Fe-Mo) sulfide. The synergism must stem from other causes. One reason maybe the improvement of the dispersion of the catalysts that was verified by TEM and microscopy analysis.

Promoted or multicomponent catalysts have excellent potential. If the concentration of the expensive metals can be decreased to an extremely low level, there is no necessary to recover the metals. However, further work is required to confirm these observations in a scaled-up operation. Additionally, it will be more advantageous to use the less expensive metal such as cobalt or nickel instead of the molybdenum for hydrocracking.

ACKNOWLEDGMENTS

We thank Biao Wang and Huaiping Wang for the XRD analyses and interpretaton and Ziping Ai for the TEM analyses and interpretation as well as Ping Wen for the microscopy analyses.

REFERENCES

1. Del Bianco, A.; Panariti, N.; Di Carlo, S.; Elmouchnino, J.; Fixari, B.; Le Perchec, P., Appl. Catal. 1993, 94, 1.
2. Hager, G.T.; Bi, X.X.; Derbyshire, F.J.; Eklund, P.C.; Stencel, J.M., Am. Chem. Soc. Div. Fuel Chem., Preprints, 1991, 36(4), 1900.
3. Rouleau, L.; Bacaud, R.; Breysse, M.; Dufour, J., Appl. Catal. 1991,104,137-149.
4. Ikura, M.; Stanciulescu, M.; Kelly, J.E., U.S. Patent 5,283,217, 1994.
5. Chen, H.H.; Montgomery, D.S.; Strausz, O.P., AOSTRA J. Res., 1989, 5(1), 33.

Table 1.
Liaohe 500^{+}°C Vacuum Residue Feed

Density(20°C)	0.9976	C,%	86.9
Viscosity(100°C),cSt	3380	H,%	11.0
CCR,%	19.0	S,%	0.4
SARA analysis,%		N,%	1.1
saturate	17.4	Ni,ppm	123
aromatic	30.3	V,ppm	2.9
resin	50.2	Fe,ppm	38
Asphaltene(n-C7)	2.1	Ca,ppm	96

Table 2.
Effect of the Mo/Ni Catalysts on Products and Distribution

Run No.	1	2	3	4	5	6	7
Ni/(Mo+Ni)	0.0	0.2	0.4	0.5	0.6	0.8	1.0
%Gas	5.4	5.6	4.8	5.4	6.0	6.7	6.5
%Coke	1.7	1.8	1.5	1.7	1.7	1.9	2.9
IBP-200°C(%)	5.3	3.0	3.4	3.4	4.4	3.1	6.6
200-350°C(%)	17.3	15.3	16.0	17.5	16.1	17.0	18.8
350-500°C(%)	28.5	27.0	26.9	27.4	28.3	28.7	26.1
500°C+(%)	41.8	47.3	47.4	44.6	43.5	42.6	39.1
Coke Quality							
H/C (at)	0.64	0.64	0.66	0.67	0.68	0.67	0.65
%N	3.5	3.3	3.2	3.5	3.5	3.4	3.5

Table 3.
Effect of the Mo/Fe Catalysts on Products and Distribution

Run No.	1	8	9	10	11	12	13
Fe/(Mo+Fe)	0.0	0.2	0.4	0.5	0.6	0.8	1.0
%Gas	5.4	5.6	5.8	6.2	7.0	7.1	10.0
%Coke	1.7	2.0	1.7	2.9	3.0	3.3	7.1
IBP-200°C(%)	5.3	5.1	5.6	5.9	6.1	7.1	7.3
200-350°C(%)	17.3	17.1	18.4	18.6	20.3	21.9	23.7
350-500°C(%)	28.5	28.8	26.7	28.1	27.2	25.4	28.4
500°C+(%)	41.8	41.4	41.8	38.3	36.4	35.2	23.5
Coke Quality							
H/C (at)	0.64	0.66	0.64	0.65	0.68	0.67	0.65
%N	3.5	3.5	3.3	3.5	3.3	3.2	3.5

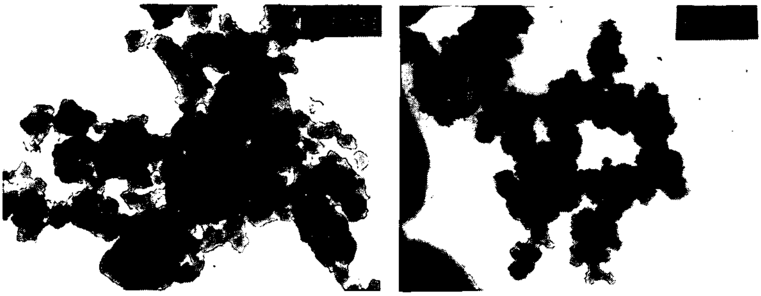

Figure 1. TEM micrograph of the solid obtained from Mo/Fe system (Mo:Fe=3:2, Magnification is × 19,000 and × 100,000 for left and right, respectively.)

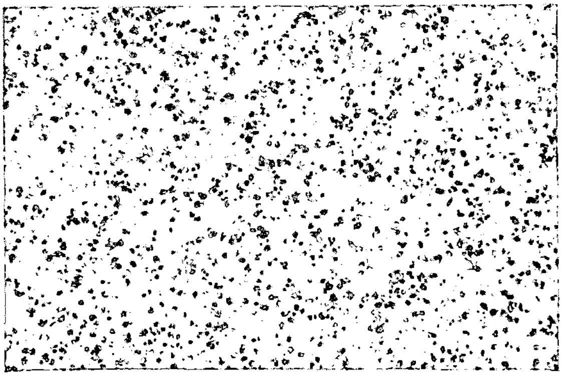

Figure 2. Micrograph of the hydrocracked liquid with Mo/Fe catalyst(Mo:Fe=3:2)

CATALYTIC HYDROCRACKING OF PETROLEUM VACUUM RESIDUE BY USING A COMBINATION OF MOLYBDENUM-BASED OIL-SOLUBLE AND IRON-BASED WATER-SOLUBLE CATALYSTS

Zong-Xian Wang, Hong-Yu Zhang, Ai-Jun Guo and Guo-He Que
National Heavy Oil Processing Laboratory, University of Petroleum (East China)
Dongying, Shandong 257062, P. R. China

ABSTRACT

Synergism was investigated of molybdenum-based oil-soluble catalyst and iron-based water-soluble catalyst in catalytic hydrocracking system of Liaohe vacuum residue. A combined use of water-soluble catalysts and active oil-soluble catalyst could enhance conversion and effectively inhibit coke formation, without much expense of relatively expensive oil-soluble catalysts. This can be explained by following reasons: (1) At early stage of hydrocracking, some kinds of poly-aromatics can be partially hydrogenated to hydroaromatics, which can act as hydrogen donors and can be a complement to the active hydrogen molecules directly activated by catalysts in the subsequent hydrocracking. (2) The cheap water-soluble catalyst can not only activate molecular hydrogen to inhibit coke formation, but also make the sacrifice of the sites of coke deposition, thus save partially the active Mo-based catalyst from deactivation by coke deposition.

Key words: synergism, oil-soluble and water-soluble catalysts, hydrocracking, vacuum residue

INTRODUCTION

The catalytic hydrocracking processes of heavy oils or bitumen concerning the use of dispersed catalysts (oil-soluble, water-soluble or fine particles of catalysts) have been extensively reported [1]. Nearly all these processes are operated at relatively high temperature, well above 430°C, and aim at high conversion to light products and low coke formation. The catalysts or additives used in these processes have little catalytic activity towards the cracking reactions; the conversion to lighter products is almost entirely a thermal process [2]. But these catalysts are more or less effective in inhibiting coke formation, some of which are even really effective [1-3], such as Mo-based oil-soluble catalysts used in M-coke process [4].

The chemical nature, the catalytic activity and the cost of these catalysts are the key factors for the optimization and development of efficient catalytic hydroconversion processes [2]. Some catalysts are active, but much expensive, such as Molybdenum, Nickel, and Vanadium -based oil-soluble catalysts. On considering their high price, a once-through scheme of hydrocracking process can be considered only in employing low catalyst concentrations (< 200ppm, base on metals); but if the catalyst concentration is too low under given hydrogen partial pressure, the large amount of coke formation may result. It is worth noting that higher H_2 partial pressure and higher concentrations of low active and not expensive catalysts, such as Fe-based oil soluble, water-soluble catalysts and powdered catalysts, can counter-balance the activity of Mo-based oil-soluble catalyst as used in trace concentration.

Generally, for the same metal, its oil-soluble salts can be distributed more well in heavy oil than its water-soluble salts and therefore, are usually more active than its water-soluble salts [1]; but may be more expensive than its water-soluble salts. Some oil-soluble catalysts are relatively expensive, but quite active, such as Molybdenum-based oil-soluble catalysts. Some water-soluble catalysts are relatively very cheap, but not quite active, such as iron-based water-soluble salts. To optimize the use of these catalysts, it is possible to use a mixture of these catalysts. If the concentration of a more expensive component can be reduced, the use of the second component could reduce catalyst cost. However, up to date, few studies have been carried out to investigate the synergism of the use of active oil-soluble catalysts and very cheap water-soluble catalysts (quite different solubility systems). In the presentation, a Molybdenum-based oil-soluble catalyst and an iron-based water-soluble catalyst are in combination used in hydrocracking of Liaohe vacuum residue to investigate the synergism of these two kinds of catalysts.

1. EXPERIMENTAL

1.1 *Sample*

Liaohe vacuum residue(>500°C) was collected from Liaohe Petrochemical Plant in March 1996. Carlo Erba 1160 elemental analyzer was used for C, H, N analysis; atomic absorption method was used to determine Ni, V, Fe and Ca contents. Average molecular weight was measured by using VPO method (benzene as solvent, 45°C) with Knauer molecular weight analyzer. The general properties of Liaohe vacuum residue are listed in Table 1. For comparison, the general properties of Gudao vacuum residue (the feed to VRDS unit at Qilu Oil Company) was also tabulated here.

Table 1 Properties of Liaohe vacuum residue (VR)

Property	Liaohe VR	Gudao VR
Density(20°), g./cm^3	0.9976	0.9998
Viscosity(100°)/mm^2.s^{-1}	3375	1710
Pour point, °C	42	41
Flash point, °C	312	327
Carbon residue, %	19.0	15.6
Elemental composition		
C, %	87.0	85.4
H, %	11.4	11.4
S, %	0.43	2.52
N, %	1.08	0.80
H/C(Atomic ratio)	1.50	1.60
Total Metal/PPM	258.6	131.6
Ni, ppm	122.6	48.0
V, ppm	2.9	2.2
Fe, ppm	37.5	13.8
Ca, ppm	95.6	33.8
Ash, %	0.06	0.03
SARA fractions:		
Saturates, %	17.4	14.5
Aromatics, %	30.3	34.8
Resins, %	50.2	47.2
nC7-Asphaltene, /%	2.1	3.5
Structural Parameters		
F_A	0.27	0.18
F_N	0.26	0.33
R_A/R_N	0.93	0.47

1.2 *Catalytic hydrocracking of Liaohe vacuum residue*

The experiments were carried in a 100ml FDW-01 autoclave reactor with an up-and-down stirrer at 120 times of reciprocation per minute. Initial pressure was 7.0MPa H_2 for catalytic hydrocracking. Catalyst used in the hydrocracking reaction was Molybdenum-based oil soluble and iron-based water-soluble catalyst (ca.50~1000 ppm based on metal concentration in feed). The former was compatible with the vacuum residue and gave rise to the homogeneous system with the vacuum residue, and the later was emulsified into the vacuum residue to form emulsion system. After sulphurization by elemental sulfur at 320°C for 30minute (S/Metal atomic ratio=3/1), these catalyst precursors were in situ reacted to real active catalysts. Then, the temperature was raised to 430°C for hydrocracking reaction. After 1-hour reaction time, the reactor was quenched (cooled) to room temperature, the reactor gas was vented, and toluene slurry was prepared from the reactor contents. Any solids adhering to the reactor walls or internals was carefully scraped off. The slurry was then centrifuged and the toluene insoluble (TI or coke) were separated and washed (extracted) with boiling toluene by using quantitative filter paper. The solids were dried and weighed. The toluene soluble was distilled into several fractions. The distillation scheme is as follows.

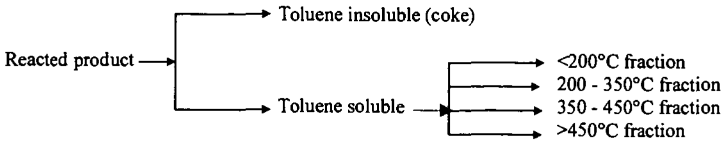

2. RESULTS AND DISCUSSION

2.1 *The activity of catalysts*

In order to make a comparison of catalytic activity between the Mo-based oil-soluble catalyst and the Fe-based water-soluble catalyst used in Liaohe vacuum residue hydroconversion processes, the same concentrations of these two kinds of catalysts were separately used in the hydrocracking tests, the results are listed in table 2. Both of the catalysts could suppress coke formation and cracking reactions in comparison with thermal cracking system without adding catalysts. The Mo-base oil soluble catalyst accounted for lower total conversion yield than the Fe-based water-soluble catalyst did; but the former gave rise to higher conversion per unit coke than the latter did. The conversion per unit coke was 53.1% for the Mo-based oil-soluble catalyst, 11.9% for Fe-based water-soluble catalyst and 8.8% for pure thermal cracking without added catalyst. In consideration of the over-cracking and condensation reactions during Liaohe vacuum residue hydrocracking, the following formula was proposed for evaluation of the catalytic activity of catalysts: R=(GL× Coke)/CP. Here, R is named coke and over-cracking suppressing index; GL is gas and light fraction yield, strictly the <200°C fraction yield; CP is the conversion per unit coke. Under the given reaction conditions, the R-value is 0.22 for the Mo-based catalyst, 10.7 for the Fe-based catalyst and 25.0 for thermal cracking without catalysts.

Table 2 Hydroconversion of Liaohe vacuum residue
by using different catalysts at 430°C, 7.0MPa initial H_2 pressure, 1hr

Cat., ppm	Conv. wt %	conv. per unit coke, wt %	200°C-, wt %	200-350°C, wt %	350-480°C, wt %	Coke, wt %
Mo, 470	49.4	54.9	13.4	11.1	24.0	0.9
Fe, 470	64.4	11.9	23.5	16.5	19.0	5.4
No cat.	69.2	8.8	27.9	12.5	20.9	7.9

Note: cat. ~ Catalyst; conv. ~ conversion; wt % ~ weight percent.

2.2 *Catalytic hydrocracking of Liaohe vacuum residue by using the Mo-based oil-soluble and Fe-based water-soluble catalysts*

As indicated in table 3, the combined use of Mo-based oil-soluble catalyst and the Fe-based water-soluble catalyst could really give rise to a synergetic effect on coke inhibition. With promotion of 400ppm Fe-based water-soluble catalyst, the relatively expensive Mo-based catalyst could be reduced from 470ppm to only 70 ppm without much loss of total catalytic activity. Under the given reaction conditions, the concentration of the more expensive component can be reduced to under 100ppm, the use of the second component (Fe-based water-soluble catalyst) could reduce total catalyst cost and hence avoid the catalyst recovery [1]. It seems that the synergism of these two kinds of catalysts can not be clearly understood simply by their complementary function; this will be further discussed in section 2.3.

Table 3 Synergetic effect of Mo-based oil-soluble and Fe-based water-soluble catalysts on hydroconversion of Liaohe vacuum residue (430°C, 7.0PMa H_2, 1 hr)

Cat., ppm		Conv. wt %	conv. per unit coke, wt %	200°C-, wt %	200-350°C, wt %	350-480°C, wt %	Coke, wt %	R
Mo	Fe							
470	0.0	49.4	54.9	13.4	11.0	24.0	0.9	0.22
70	400	48.7	48.7	15.5	10.0	22.1	1.0	0.32
25	445	56.4	25.6	18.4	13.0	22.8	2.2	1.58
0.0	470	64.4	11.9	23.5	16.5	19.0	5.4	10.7

Table 4 Synergetic effect of Mo-based oil-soluble and Fe-based water-soluble Catalysts on Hydroconversion of Liaohe vacuum residue

Cat., ppm		Conv. wt %	conv. per unit coke, wt %	200°C-, wt %	200-350°C, wt %	350-480°C, wt %	Coke, wt %	R
Fe	Mo							
0.0	70	50.0	35.7	13.4	8.9	26.3	1.4	0.53
100	70	52.8	33.0	17.7	10.4	23.1	1.6	0.85
200	70	55.9	32.9	18.4	11.4	24.4	1.7	0.95
400	70	48.7	48.7	15.5	10.0	22.2	1.0	0.32
600	70	47.0	52.2	14.4	9.9	21.8	0.9	0.25
800	70	52.0	74.3	15.2	10.5	25.6	0.7	0.14
1000	70	45.7	76.2	13.2	9.9	22.0	0.6	0.10
1000	0.0	56.4	17.8	16.6	12.9	23.7	3.2	2.98

With the Mo-based catalyst being kept in concentration of 70ppm and the Fe-based catalyst being increasingly added from 0ppm to 1000ppm, the coke suppressing ability is at first getting down, and then becoming higher and higher from 400 ppm to 1000ppm of Fe-based catalyst in use. The results were listed in table 4. When Fe-based catalyst added in the hydrocracking system was above 600ppm(total 670ppm Mo and Fe), the performance of the Mo-Fe catalysts in coke inhibition and over-cracking suppression was better than that of pure Mo-based catalyst used in 470ppm; this could be interpreted by their R values.

2.3 *The synergism of active oil-soluble catalyst and water-soluble catalyst in the catalytic hydroconversion of Liaohe vacuum residue*

At early stage of catalytic hydrocracking of vacuum residue, the oil soluble and water-soluble catalyst precursors are sulphidized, by indigenous sulfur or pre-added sulfur, to dispersed fine molybdenum sulfide and iron sulfide particles, which are real active catalysts. During the stage, the catalytic hydrocracking system was of following characters:

- High activity of the catalysts
- high hydrogen partial pressure
- Low cracking reactions and low free radical concentration

The former two characters could give rise to high concentration of active hydrogen surrounding catalyst fine particles. Therefore, little coke would be formed through polyaromatic radical combination or condensation because active radicals would be timely scavenged or hydrogenated by active hydrogen before their combination. However, condensed phase of asphaltene might be formed because of the adsorption of catalyst fine particles to asphaltene molecules. The latter character along with former two would lead to an excess of active hydrogen beside the active hydrogen used to scavenge polyaromatic free radicals. The excessive active hydrogen would hydrogenate some active polyaromatics to hydroaromatic species, which could act as hydrogen donors in subsequent reactions. This kind of hydrogen donors might be more active in coke suppression than directly activated hydrogen by catalysts because there would exist a higher compatibility and an easier hydrogen transfer between the hydrogen donors and coke precursors.

In fact, there may be large differences between catalysts in the abilities to generate these kinds of hydroaromatics---secondary hydrogen donors. Some catalysts may be not active enough to hydrogenate polyaromatics to hydroaromatics. With Mo-based additives, the reaction system can not only inhibit coke formation through shutting coke precursor radicals by catalytic active hydrogen but also develop a reservoir of active hydrogen---hydroaromatics. However, the less active Fe-based catalyst could not create so active hydrogen. But the less active catalyst could be a promoter of Mo-based catalyst to effectively inhibit coke formation during severe cracking stage. Meanwhile, if used alone, a large amount of less active additives would be needed to reach effective coke inhibition. Besides, some synergism may come from in situ formed combined Mo-Fe bimetal catalysts as the supported catalysts (such as $Mo/Ni/Al_2O_3$) do. But, in the authors' opinion, even there exists the kind of synergism; it may not be the main synergetic effect in the slurry-phase hydrocracking system.

3. CONCLUSION

The synergetic effect of active Mo-based oil-soluble catalyst and Fe-based water-soluble catalyst is concluded here:

- Active Mo-based catalyst is used for:
  (1) Inhibiting coke formation of the species with high coke formation tendency especially at the early stage.
  (2) Creating the secondary hydrogen donors--hydroaromatics that may be quite active in coke suppression.
  (3) Playing a great role in coke inhibition during the whole hydrocracking process.
- Less active Fe-based catalyst for:
  (1) Making the sacrifice of the sites of coke deposition, thus partially saving the active Mo-based catalyst from deactivation by coke deposition.
  (2) Playing significant role in coke suppression during the severe cracking stage when used in relatively large amount.

Therefor, the synergism of Mo-based oil-soluble catalyst and Fe-based water-soluble catalyst in catalytic hydrocracking of Liaohe vacuum residue is not only simple complementary effect, but also comprehensive promotion effect.

REFERENCES

(1)Del Bianco, A., Panariti, N., Di Carlo, S., Elmouchnino, J., Fixari, B. and Le Perchec, P., Applied Catalysis, A: General, 94, 1-16(1993)

(2)Del Bianco, A., Panariti, N., Marchionna, M. Am. Chem. Soc., Preprints, Div. Petrol. 40(4),743-746(1995)

(3)Le Perchee, P., Fixari, B., Vrinta, M., Morel, F., Am. Chem. Soc., Preprints, Div. Petrol. 40(4)747-751(1995)

(4)Bearden, R. and Aldrdge, C. L., Energ. Progress, 1(1-4), 44(1981)

THIRD-BODY ENHANCED METHANE CONVERSION IN A DIELECTRIC-BARRIER DISCHARGE REACTOR

Terence A. Caldwell, Pattama Poonphatanaricha, Sumaeth Chavadej, Richard G. Mallinson, and
Lance L. Lobban, School of Chemical Engineering and Materials Science,
University of Oklahoma, Norman, OK 73019

ABTRACT

A great deal of recent research in fuel chemistry has been focused on the utilization of the vast global natural gas reserves. A dielectric barrier discharge has proven to be an effective method of activating methane, the primary component of natural gas, which leads to the formation of higher hydrocarbons with hydrogen as a byproduct. Carbon chain building begins with the combination of activated C_1 species to form C_2. C_2 can react with C_1 to form C_3 or react with another C_2 to form C_4. C_3 may also react with C_1 to form C_4 species. Hydrogen is produced when a carbon-carbon bond forms. The reverse "chain scission" reactions also occur. Olefin production becomes more likely when H_2 concentrations are reduced. Other species, such as helium, hydrogen, and light paraffins have been added to the methane feed stream to determine if they have any synergistic effects on methane conversion or if they alter product selectivity.

INTRODUCTION

Recent projections indicate that the majority of global oil reserves will be depleted within the next century. Therefore, it has become necessary to study new methods of obtaining the required fuels for the world's vehicles and energy suppliers and to find alternate sources of feedstocks for the petrochemical industry. One plentiful resource that has shown a great deal of promise in relieving the world's dependence upon rapidly diminishing oil reserves is natural gas. Natural gas, which is composed primarily of methane, exists in large quantities trapped within the Earth's crust. Large natural gas reservoirs are found in many different parts of the world, many of which are in very remote locations.

Presently, natural gas is used primarily as an environmentally friendly combustion fuel in industrial processes. Since methane is composed of carbon and hydrogen only, its potential as a building block to form synthetic, impurity-free fuels and chemical feedstocks is significant. Most of the proven technologies for methane conversion are processes that include the initial reaction of methane with high pressure steam to form a mixture of carbon monoxide (CO) and hydrogen (H_2) known as synthesis gas. The synthesis gas can then be converted to methanol using a nickel catalyst or to higher hydrocarbons using an iron or cobalt catalyst via Fischer-Tropsch synthesis. Unfortunately, the methods that require the initial formation of synthesis gas from methane are multi-step processes that have high capital costs that limit their application.

In recent years, extensive research has been conducted on the conversion of methane using single step processes. Some of these methods include the direct partial oxidation of methane to methanol and the oxidative coupling of methane to C_2 hydrocarbons. Each of these processes uses oxygen to activate the methane molecule at elevated temperatures and/or pressures to form the desired products. Unfortunately, these conditions not only result in higher utility and capital costs, the high temperatures tend to favor the oxidation of the desired intermediate species to undesired species such as carbon monoxide, carbon dioxide, and water.

The dielectric-barrier discharge, commonly referred to as a *silent electric discharge*, has proven to be an effective method of activating methane. The silent electric discharge occurs in the gas gap between a pair of electrodes that have the same geometry, that is, between two flat-plate electrodes or in the annulus between two concentric cylindrical electrodes. A dielectric barrier that is often made of glass covers at least one of the electrode surfaces. The dielectric controls the charge transfer within the reactor and promotes a uniform charge distribution. A high voltage alternating current is used to provide the electrical potential across the electrodes. When the potential across the gas gap exceeds the minimum breakdown voltage of the system, a large number of micro-discharges are formed. These discharges are spread uniformly over the electrode surface and in the reaction volume. The discharges produce high energy electrons that interact with the methane molecules and transform the methane into a reactive species.

$$CH_4 + e^- \Leftrightarrow CH_3* + H* + e^- \qquad (1)$$

The resulting reactions lead to the formation of higher hydrocarbons, primarily alkanes, with hydrogen as a byproduct. The carbon chain building begins with the coupling of activated C_1 species to form a C_2 species.

$$2\ CH_3* \Leftrightarrow C_2H_6 \qquad (2)$$

The C_2 species can then react with C_1 species to form C_3 or react with another C_2 species to form C_4. C_3 may also react with C_1 to form a C_4 species. Hydrogen (H_2) is produced when a carbon-carbon bond forms.

$$C_2H_6 + CH_3{*} \Leftrightarrow C_3H_8 + H{*} \qquad (3)$$

$$C_2H_6 + C_2H_5{*} \Leftrightarrow C_4H_{10} + H{*} \qquad (4)$$

$$C_3H_8 + CH_3{*} \Leftrightarrow C_4H_{10} + H{*} \qquad (5)$$

$$2\,H{*} \Leftrightarrow H_2 \qquad (6)$$

The high energy electrons within the reaction zone also cause the reverse "chain scission" reactions to occur. The listed equations are meant to illustrate possible chain building reactions and do not represent a complete and accurate mechanism.

The silent electric discharge reactor (SEDR) is capable of converting over 50% of the methane feed to higher hydrocarbons. Presently, this high conversion requires significant power and lengthy residence times. Since methane is a relatively stable molecule compared to the other species within the reaction environment, the rate limiting step for the chain building process appears to be the activation of the methane molecule. The activation of methane must become more efficient before a process based upon the SEDR can be cost effective.

In an attempt to enhance the activation of the methane molecule, other species have been added to the methane feed stream. Mallinson et al. (1987) and Bhatnager et al. (1995) conducted extensive research using oxygen in the methane feed stream. Oxygen is more easily activated in the electric discharge environment than methane. Therefore, a larger fraction of activated oxygen species would be present than activated methane species under the same discharge conditions. It was hoped that the activated oxygen would interact with methane causing it to activate and react more readily. Their work showed that the presence of oxygen did indeed increase the rate of methane conversion in a SEDR. However, the presence of oxygen also promoted the continued oxidation of the desired intermediate species, primarily methanol, to less valuable products like carbon monoxide, carbon dioxide, and water.

Other species, such as helium, hydrogen, and light paraffins have been added the methane feed stream to determine their effect on methane conversion and product selectivity. These other species were selected because the are either chemically inert or are already present in the product stream when pure methane is run as the feed.

EXPERIMENTAL

A schematic of the silent electric discharge reactor is shown in Figure 1. The reactor system consisted of two metal electrodes made from flat aluminum plates. A dielectric barrier made of glass covered one electrode surface. The dielectric had a thickness of 0.090 in. A Teflon spacer 0.070 in. thick was situated between the dielectric and the opposite electrode. The spacer provided a channel for the inlet gases to flow axially through the reaction zone. The spacer also provided an airtight seal. The total volume of the reaction zone was about 150 cm^3.

The back side of one electrode was in contact with cooling water that was maintained at a temperature between 10 and 20 °C. Thermocouples were placed at the inlet and outlet of the cooling water jacket to measure the heat given off by the reaction. No significant temperature change was ever measured in the cooling water. This means that the reactor generated little heat during operation.

Two different power supply systems were used for these experiments. The first system was powered by wall current with a voltage of 220 V and a frequency of 50 Hz that was connected to a step-down variable transformer. The transformer allowed the voltage to be varied from 0 to 110 V while the frequency remained at 50 Hz. The output line of the variable transformer was connected to a secondary high voltage AC (HVAC) transformer. The HVAC stepped up the voltage by a factor of 125. This allowed voltages as high as 15 kV to be generated. The output lines of the HVAC were then connected to the aluminum plate electrodes to generate the high potential required for electric breakdown.

The second power supply used a wall current with a voltage of 120 V and a frequency of 60 Hz. The wall current was used to supply power to an Elgar Model 501SL AC power supply that was able to generate potentials up to 250 V. Connected to the power supply was a BK Precision 5 MHz Function Generator. This instrument generated a sinusoidal waveform and allowed the frequency to be varied over the range used, from 50 to over 300 Hz. Also connected to the output line of the power supply was a Microvip MK 1.2 Energy Analyzer that was used to measure the voltage, current, power, power factor, and frequency generated by the power supply. The output of the power supply was connected to a Franceformer Gaseous Tube Transformer that has a voltage multiplying factor of 125. The high voltage cables from the transformer were then connected to the electrodes of the reactor system.

The volumetric flow rates of the feed and product gases were measured by using soap bubble flowmeters. The analysis of the gas stream was done using a Perkin-Elmer "Autosystem" Gas Chromatograph or a Carle 400 Series AGC. The latter also had the capability of measuring hydrogen. The resulting chromatogram peak areas were converted to mole fractions by correlating the individual gas concentrations to their component peak responses. The correlations were derived from calibrations using known gas compositions.

The pressure within the reactor system was assumed to be approximately atmospheric (1 atm ± 0.05 atm). Each experiment was conducted at ambient temperature (25°C ± 5°C). Any increase in the reactor temperature due to the electric discharge and any exothermic reactions was assumed to be negligible.

RESULTS

Previous experiments with the SEDR were conducted using a feed of pure methane at a flow rate of 20 ml/min. A typical plot of the methane conversion and product selectivity versus applied voltage is shown in Figure 2. The frequency of the alternating current for these initial experiments was 50 Hz. The methane conversion increases significantly as the applied voltage increases. However, the selectivities of the products remain essentially the same.

For the remaining experiments, the applied voltage was set at 4.5 kV and the frequency was adjusted to 100 Hz. The methane conversion was maximized at 100 Hz for this reactor configuration. The molar flow rates for the major chemical species produced from the conversion of pure methane are shown in Figure 3. Since the concentrations of the product species are much lower than that of the feed species, the product flow rates are displayed on an inset graph with a different scale for clarity. The major products for this reaction are ethane and hydrogen. For each carbon-carbon bond formed, a hydrogen molecule is produced. The propane concentration is about a third less than that of ethane while the butane production is about half that of propane. Only a trace of C_2 or higher olefins are produced using pure methane.

Figure 4 shows the molar flow rates of the species produced from the reaction of pure ethane in a SEDR. The overall conversion of ethane is greater than the conversion of pure methane. Ethylene formation is significantly higher than that seen for the pure methane reaction. Also, the concentrations of the higher paraffins, propane and butane, are greater as well. Chain scission to form methane is also significant.

The next test involved adding an ethane fraction to the methane feed stream. The methane to ethane feed ratio was maintained at 4:1. The resulting molar flow rates are displayed in Figure 5. The total conversion of methane was larger than was the case for pure methane. The production of C_2 olefins is much greater than that for pure methane as well. Also, the production rate of propane and butane nearly tripled.

Figure 6 shows the molar flow rates associated with the reaction of ethane and hydrogen at a 1:1 feed ratio. The overall hydrogen to carbon ratio is the same as that for the pure methane case. Like the pure methane experiment, olefin production was very low. However, the chain scission reaction did not completely dominate as one might expect. A significant fraction of methane was formed, but a greater fraction of higher paraffins was formed as well, particularly butane.

DISCUSSION

The product selectivities shown in Figure 2 for the pure methane experiments suggest the following predominant reaction pathway for this feed condition: an activated C_1 species reacts with another C_1 species to form ethane and hydrogen. The ethane may crack to reform methane, or it can react with a C_1 species to form propane or with another C_2 species to form butane. Since olefin production is very low, it is apparent that dehydrogenation reactions are not favored. Also, the reaction of activated species to form unsaturated products is not significant. The high methane to ethane ratios in the exit gas stream suggests that the activation and reaction of methane is the rate limiting step or that the cracking reactions of the C_2+ species dominate.

The data in Figure 4 for the pure ethane experiment shows that although the chain scission reactions are significant, they do not overwhelm the chain building steps. A significant fraction of C_3+ species were formed along with methane. Also, the lower hydrogen to carbon ratio in the feed stream resulted in the formation of a large fraction of unsaturated hydrocarbons through dehydrogenation.

Ethane was added to the pure methane feed to determine its effect on the activation of the methane molecule. The resulting methane conversion was significantly higher than that for the pure methane case. It appears that the active species derived from ethane assist in the activation of methane resulting in enhanced methane conversion to higher hydrocarbons. Again, the lower hydrogen to carbon ratio in the feed stream results in a larger fraction of unsaturated species.

To test the effect of the hydrogen to carbon feed ratio on product selectivity, a feed consisting of an equimolar mixture of ethane and hydrogen was reacted. The ethane conversion in this experiment was significantly higher than for the pure ethane experiment. Also, dehydrogenation was suppressed by the high hydrogen concentration. Judging from the relatively high ethane conversions for each of these experiments, it appears that ethane is activated and reacts much more readily than methane. These tests indicate that the low activation rate of the methane molecules limits the production of more valuable species for the pure methane feeds.

Several researchers have attempted to enhance the conversion of methane to higher hydrocarbons by adding a chemically inert species to the feed stream. The hope was to find a third-body that would lower the activation energy of the methane molecule without disrupting the conversion pathway to more valuable products. Thanyachotpaiboon et al. (1998) studied the synergistic effect of helium on methane conversion in a SEDR. A helium to methane feed ratio of 1:1 resulted in a significant increase in the methane conversion. If helium did not interact with the methane in the discharge environment, one might expect the helium to serve only as a diluent and cause a decrease in the overall methane conversion due to the decreased partial pressure of methane. These results suggest that some of the helium is "activated" within the discharge environment and aids the activation of methane molecules through a third-body energy transfer. Unfortunately, on an industrial scale, adding helium to the methane feed stream, removing it from the product gases, and recycling it back to the feed may prove to be costly. Therefore, experiments on methane conversion enhancement were conducted using chemical species that are already present in the pure methane reaction process.

Some preliminary experiments have been conducted using propane and butane in the methane feed stream. In these cases, it appears that chain scission begins to dominate the reaction. The product concentrations are similar to those produced from ethane enhanced methane conversion.

CONCLUSIONS

The silent electric discharge reaction has proven to be a relatively effective means of activating methane molecules allowing them to react to form more valuable products. However, the activation rate is presently too low to make this process economically feasible on a large scale. Therefore, attempts have been made to enhance the conversion of methane by adding other species to the methane feed stream. Oxygen, helium, hydrogen, and light paraffins have all aided the conversion of methane with varying degrees of success. With the exception of helium, these species also change the selectivities of the reaction products. These changes may prove beneficial depending on the nature of the application. For example, the formation of liquid oxygenates by using oxygen may be favored in areas where the transportation of liquids through pipelines is possible. Olefin formation by limiting the amount of hydrogen in the feed may be encouraged in industrialized areas where poly α-olefin production takes place.

ACKNOWLEDGEMENTS

The authors would like to express their appreciation to the National Research Council of Thailand, the National Science Foundation for sponsoring a Graduate Research Traineeship in Environmentally Friendly Natural Gas Technologies, and the United States Department of Energy (Contract DE-FG21-94MC31170).

REFERENCES

Bhatnager, R. and R.G. Mallinson, "The Partial Oxidation of Methane Under the Influence of an AC Electric Discharge," *Methane and Alkane Conversion Chemistry*, M.M. Bhasin and D.N. Slocum (eds.), Plenum Publishing, New York, 249 (1995)

Mallinson, R.G., C.M. Slipcevich, and S. Rusek, "Methane Partial Oxidation in Alternating Electric Fields," American Chemical Society National Meeting, New orleans, LA,August, 1987, Preprints:American Chemical Society Fuel Chemistry Division, Vol. 32, No. 3, 266 (1987)

Thanyachotpaiboon, K., T.A. Caldwell, L.L. Lobban, S. Chavadej, and R.G. Mallinson, "Conversion of Methane to Higher Hydrocarbons in AC Non-Equilibrium Plasmas," submitted to *AIChE Journal* (1998)

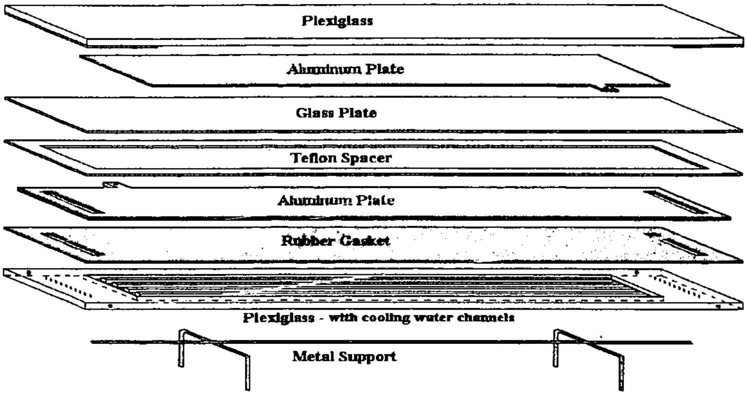
Plexiglass
Aluminum Plate
Glass Plate
Teflon Spacer
Aluminum Plate
Rubber Gasket
Plexiglass - with cooling water channels
Metal Support

FIGURE 1: A DIAGRAM OF THE SILENT ELECTRIC DISCHARGE REACTOR.

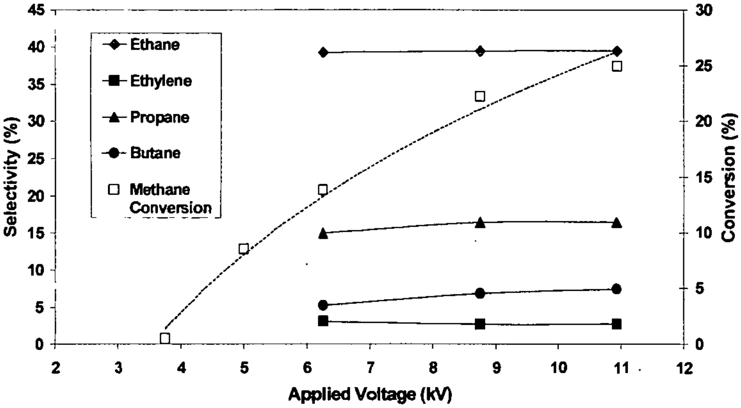

FIGURE 2: DISTRIBUTION OF PRODUCT SELECTIVITIES AS A FUNCTION OF THE APPLIED VOLTAGE. FREQUENCY = 50 HZ

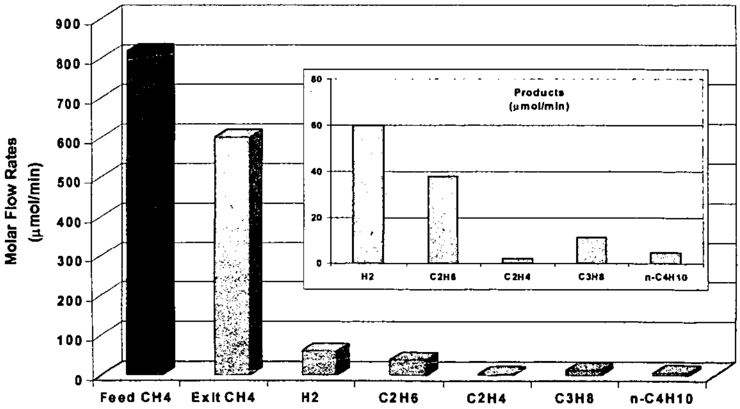

FIGURE 3: MOLAR FLOWRATES OF THE CHEMICAL SPECIES PRODUCED DURING THE REACTION OF PURE METHANE IN A SEDR. 4.5 KV 100 HZ

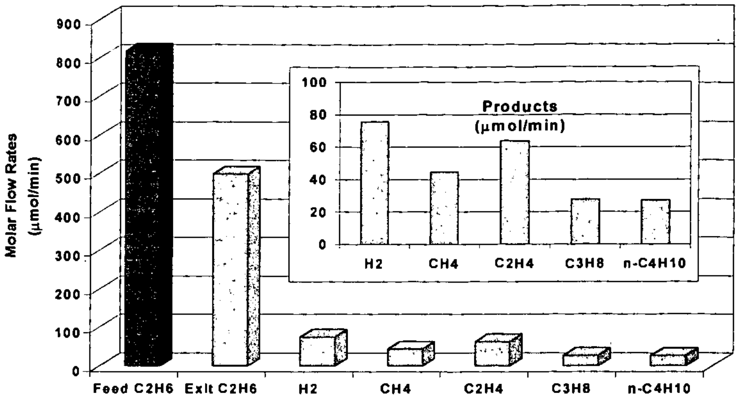

FIGURE 4: MOLAR FLOWRATES OF THE CHEMICAL SPECIES PRODUCED DURING THE REACTION OF PURE ETHANE IN A SEDR. 4.5 KV 100 HZ

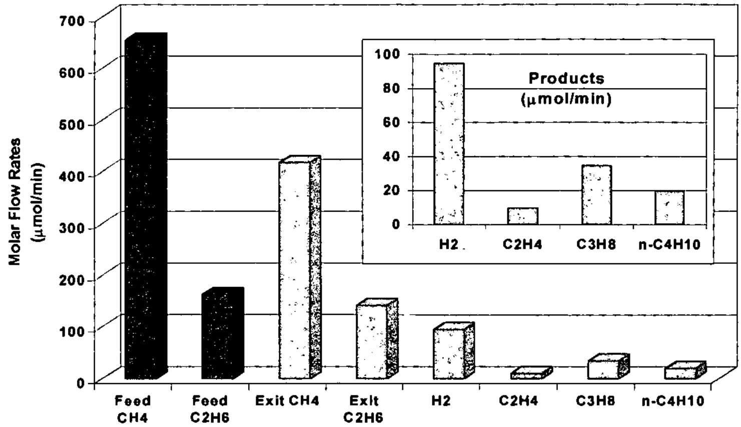

FIGURE 5: MOLAR FLOWRATES OF THE CHEMICAL SPECIES PRODUCED DURING THE REACTION OF A 4:1 MOLAR RATIO OF METHANE TO ETHANE IN A SEDR. 4.5 KV 100 HZ

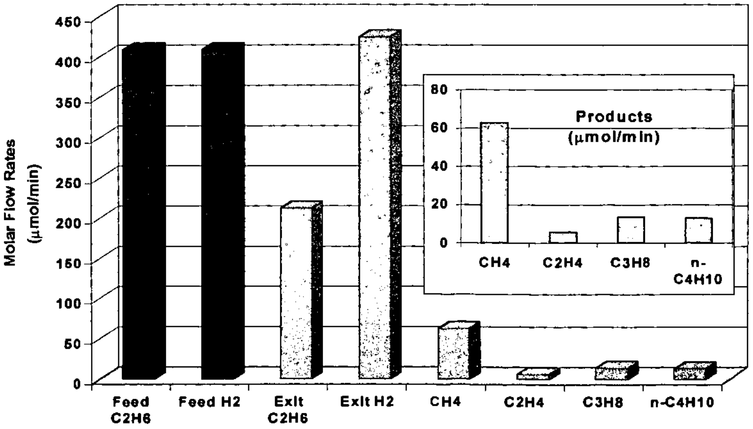

FIGURE 6: MOLAR FLOWRATES OF THE CHEMICAL SPECIES PRODUCED DURING THE REACTION OF AN EQUIMOLAR MIXTURE OF ETHANE AND HYDROGEN IN A SEDR. 4.5 KV 100 HZ

DISPERSION AND ACTIVITY OF INORGANIC CATALYST PRECURSOR IN HEAVY OIL

Richard A. McFarlane, Alberta Research Council, 250 Karl Clark Road, Edmonton, Alberta T6N 1E4, CANADA

Randall W.T. Hawkins, National Centre for Upgrading Technology, 1 Oil Patch Drive, Suite A202, Devon, Alberta T9G 1A8, CANADA

Ted Cyr, Alberta Department of Energy, 14th Floor Petroleum Plaza North, 9945- 108 Street, Edmonton, Alberta T5K 2G6, CANADA

Keywords: molybdenum sulphide, dispersion, heavy oil

ABSTRACT

Compared to supported catalysts, highly dispersed catalyst particles suspended in heavy oil are less susceptible to deactivation during heavy oil upgrading. Oil soluble catalyst precursors produce highly dispersed catalyst particles but can be expensive even when used at low concentrations. The dispersion of an aqueous catalyst precursor using an atomizing nozzle suspended in Cold Lake heavy oil has been carried out in the laboratory and the activity of the resulting catalyst was verified in semi-batch autoclave tests. The activation of the catalyst could be achieved simply by heating the heavy oil and catalyst precursor to reaction temperature. Although the catalyst particles are larger than those produced by oil soluble precursors their activities appear to be as good. The catalyst particles were shown to maintain their activity when recycled in sequential batch tests. Some details of the catalyst preparation, testing and properties are presented.

INTRODUCTION

Hydrocracking catalysts for upgrading heavy oil and bitumen are typically composed of metal sulphides dispersed on a porous oxide support in the form of extrudates. These types of catalysts suffer loss of activity due to the deposition of coke and metals, such as nickel and vanadium present in the heavy oil. Eventually, the fixed bed reactors employing these catalysts must be shut down and the catalyst replaced at a significant expense. Process technologies, such as moving bed and ebullated bed catalysts, which avoid shutdown by continuous addition of fresh catalyst are available but they can be expensive in capital and operating costs. Other processes have included the continuous addition of small amounts (< 5wt%) of finely dispersed catalysts and oil soluble catalyst precursors such as molybdenum naphthenate [1] to the heavy oil. The use of highly dispersed catalysts to upgrade heavy feeds has been recently reviewed by Del Bianco *et al.* [2]. The active catalysts are generally considered to be in a colloidal state and range in size from sub-micron to several microns. Typically, the concentration of catalyst on metal basis is 50 - 1000ppm but even at these concentrations they can be expensive to use. The ability to recycle the catalyst is important for the economics of the process especially if the metal catalyst is used in high concentrations (>100ppm).

Molybdenum is the basic constituent of the most active catalysts. The major source of molybdenum is the mineral molybdenite (crystalline molybdenum sulphide) which is roasted to produce molybdenum oxide, purified by dissolution in aqueous ammonia to produce ammonium heptamolybdate and separated by fraction crystallization. Thus, ammonium heptamolybdate is one of the cheapest sources of molybdenum. An active dispersed catalyst precursor produced from this material in a simple process could have low cost compared to oil soluble catalyst precursors.

EXPERIMENTAL

Catalyst Dispersion: An atomizing nozzle was used to sparge an aqueous solution of ammonium heptamolybdate into the heavy oil held in a stirred heated tank. The temperature and pressure of the aqueous solution and hydrocarbon were maintained such that the water was immediately vapourized during the injection. A nitrogen purge tube was inserted at the top of the tank to minimize air oxidation and to aid in removal of water vapour and ammonia liberated during the process. The degree of dispersion was controlled by adjustments in the solution concentration and, the pressure and flow rate of the atomizing nozzle.

By varying the concentration of Mo in the aqueous solutions while maintaining similar injection conditions, it is possible to produce products with suspended particulates having the same total surface area but different mass percent concentrations. Thus, two feeds were produced with different Mo concentration but with the same calculated total surface area for ammonium heptamolybdate particles and by extension MoS_2 surface areas.

Materials: The feedstock (F-0) used was Cold Lake heavy oil (Table 1). The catalyst precursor was ammonium heptamolybdate, $(NH_4)_6Mo_7O_{24}{\bullet}4H_2O$. This salt was dissolved in de-ionized distilled water to the desired concentration and then injected into the heavy oil. Two feeds, F-1 and F-2, were produced having Mo concentrations of 212 and 611ppm, respectively. The oil soluble catalyst used was molybdenum naphthenate obtained as a 6wt.% Mo solution in oil. The required amount was added to the heavy oil after dilution in 21g of a diluent (BP: 200-343°C).

Activity Testing: The feedstocks containing the dispersed catalysts were processed in a 2L semi-batch autoclave that was purged with N_2, charged with approximately 750g of the feedstock and pressurized to 1000psig with H_2 at room temperature. In order to ensure sulphiding of the catalyst before hydrocracking conditions were reached, the autoclave system was modified to allow the injection of dimethyldisulphide (DMDS) at high pressure. The autoclave was heated to 350°C at which point the pressure was about 2000psig. The flow of H_2 commenced at 2L/min., was maintained for 30 minutes then stopped. DMDS was introduced from the bottom of the reactor and the system held at 350°C for 30 minutes without H_2 flow. Following this period, H_2 flow was restarted and increased to 6.0sLpm as the temperature increased to 450°C. These final conditions were maintained for a fixed period and then the reaction was quenched in less then 5 minutes. A comparison test was also performed using molybdenum naphthenate as the catalyst precursor. Tests were also performed without this activation procedure and without addition of DMDS by heating straight to 450°C.

Vapour flow from the autoclave was passed through a series of three condensers, two held at 0°C and the third at –78°C. Dry gas (C_1-C_3) passing through these condensers was accumulated in a tank. C_4-C_5 product liquid was taken as the volatiles lost at atmospheric pressure and room temperature from the three condensers after let-down to sample collection bottles.

Asphaltene were determined by precipitation using n-pentane in a ratio of 40:1 with the oil. The 525°C+ pitch contents were determined by crude simulated distillation ASTM D5307.

RESULTS AND DISCUSSION

The results of autoclave tests are summarized in Table 2. The first three tests were carried out under identical conditions using the prepared feedstocks (Test-1 and -2) and the as-received heavy oil containing the oil soluble organometallic precursor (Test-3). In terms of coke and liquid yields, the catalyst formed from water-soluble precursor provided comparable performance to that from the oil soluble precursor. Slightly higher asphaltene and CCR conversions were obtained with the water soluble catalyst precursor.

Test -1 and -3 show that nearly identical product distributions can be obtained using similar Mo concentrations prepared from either water or oil soluble precursors. The small differences lie in the C_4-C_5 and C_{6+} liquid yields. Asphaltene conversion was 10% higher in Test-1 using the water-soluble precursor compared to Test-3 with the oil soluble precursor. Thus, if the dispersion can be made high enough water-soluble catalyst precursors can be used in place of more expensive organometallic precursors.

The flexibility of the injection process to achieve a range of dispersions is illustrated by Test-1 and -2. In this case, the feedstocks F-1 and F-2 were prepared so that the calculated total surface area of the precursor per gram of oil was identical but the Mo concentrations were different. Identical precursor and catalyst surface areas should exhibit the same activity. While the apparent catalyst activities were similar in Test-1 and -2, a slightly higher activity was exhibited in Test-2 which also had the higher Mo concentration. However, if feedstock F-2 was diluted with additional oil so as to make the Mo concentration similar to that of F-1, the lower activity per mass of Mo is evident in Test-4 where coke yield is higher while liquid yield and, CCR and asphaltene conversions, are lower than in Test-1.

As detailed in the experimental section, dimethyldisulphide (DMDS) was added to the feedstock in Tests 1-4 and a complex temperature program was used to ensure conversion of the catalyst precursor to the active MoS_2 phase. In Test-5, no DMDS was added and the feedstock was heated room temperature straight to 450°C. The results from Test-5 are almost identical to those from Test-2 and indicate that a complex sulphiding process is not required for proper catalyst activation.

Test-6 and –7a illustrate the performance of the catalyst at longer residence time and higher 525°C+ pitch conversion. Compared to Test-2, higher pitch conversions in Test-6 and –7a resulted in greater amounts of dry gas, naphtha and gas oil but solids increased from 0.5 to a maximum 0.8wt.% of feed. Liquid yield was reduced slightly at the highest conversion. In Test-6, the pitch conversion determined was 94.3%. This high value for pitch conversion is probably misleading and reflects the limitation of the crude simulated distillation. Based on the conversion in Table 2, the asphaltene content was 6.7wt.% whilst the 525°C+ pitch content was only 3.8wt.% and this is not reasonable. The true pitch conversion is probably between 78% and 90%.

Test-7a and -7b illustrate the performance of the catalyst in a simulated recycle operation. Following a run identical to that in Test-7a, the bottoms from this test were left in the autoclave and an additional amount of fresh oil equal to mass of liquid collected in the product condensers was added to the autoclave. The autoclave was then operated at the same conditions as before. The results for Test-7b presented in Table 2 represent the combined products from conversion of 290.33g of bottoms from Test-7a and 483.6g of fresh feed. As shown in Table 2, the amount of solids did not increase from Test-7a to Test-7b. Dry gas yield increased because of additional conversion of the recycled bottoms. This result suggests that this catalyst could be used effectively in a bottoms recycle process. This conclusion would have to be verified in a continuous true-recycle test.

The MoS_2 catalyst was found to be concentrated along with V and Ni in the product coke. The ash contents of the cokes listed in Table 2 varied from about 14wt.% to 33wt.% for runs using 212 and 611ppm Mo catalyst, respectively. Optical microscopy under cross-polarized light indicated that the coke in all cases except for Test-3 consisted of angular and rounded particles that possess a porous and isotropic matrix. The matrix was embedded with a varying amount of anisotropic mesospheres mostly 2 - 10 microns in diameter but occasionally larger. In the case of Test-3, the porous matrix showed an anisotropic (mosaic) texture and the mesospheres were larger, consisting of spheres approximately 30 microns in diameter.

Figure 1 shows the XRD spectrum of the coke produced in Test-2. The peak near 14° 2θ corresponds to scattering perpendicular to the (002) plane in hexagonal MoS_2. Other MoS_2 peaks include 33.0°, 39.5° and 58.5° attributable to scattering from the (100), (103) and (110) planes [3]. The two sharp peaks at 31.7° and 45.5° are due to sodium chloride that was present in the as received oil. Using the Debye-Scherrer equation, the width of the peak near 14° 2θ can be used to calculate the average stacking height of the hexagonal layers. In this case it corresponds to an average layer height of 35Å, i.e., 5.6 MoS_6 stacked layers. Daage and Chiannelli [4] have shown that the stacking height is related to catalyst hydrogenation activity and selectivity for hydrogenation compared to hydrodesulphurization. Scanning electron microscopy (SEM) showed that the MoS_2 crystallites are needle shaped and unencumbered with coke. The minor axis ranged from approx. 0.5 - 1.5 microns while the major axis varied from 5 to over 30 microns. The larger dimensions obtained by SEM compared to XRD indicate that the stacked layers that make up the crystallite were highly folded and disordered. This was confirmed with the aid of transmission electron microscopy (TEM) and selected area diffraction. The needle-like crystals were observed to be composed of a collection of rods that are less than 100nm in diameter. The composition and structure of the particles were confirmed by analysis using energy dispersive x-ray (EDX) analysis and selected area diffraction. The diffraction patterns indicated that the MoS_2 was polycrystalline but had some preferred orientation.

CONCLUSIONS

It has been show that a water soluble catalyst precursor, ammonium heptamolybdate, can produce highly dispersed and active MoS_2 catalyst. The activity of these catalyst approaches that achieved by oil soluble catalysts which are reported to be highly dispersed even though the catalyst particles were larger than those from the oil soluble catalyst. TEM confirmed that these large catalyst particles (5-30 microns) were made up of smaller particles (0.1 microns). The catalyst maintained its activity in a simulated recycle test. The lower cost of the water soluble catalyst, its larger aggregate size and its activity relative to the oil soluble catalyst make it a potential candidate for upgrading processes which use highly dispersed catalyst and employ bottoms recycle.

ACKNOWLEDGEMENTS

This work was sponsored and wholly supported by the Alberta Department of Energy and the Alberta Research Council for which the authors are grateful.

REFERENCES

1. R. Bearden and C.L. Aldrige, Energy Prog. 1984, Vol. 1, 44.
2. A. Del Bianco, N. Panariti, S. Di Carlo, J. Elmouchnino, B. Fixari and P. Le Perchec, Appl. Catal. A, 94, 1 (1993).
3. N. Rueda, R. Bacaud and M. Vrinat, J. Catal. 1997, Vol.169, 404.
4. M. Daage and R.R. Chianelli, J. Catal. 1994, Vol. 149, 414.

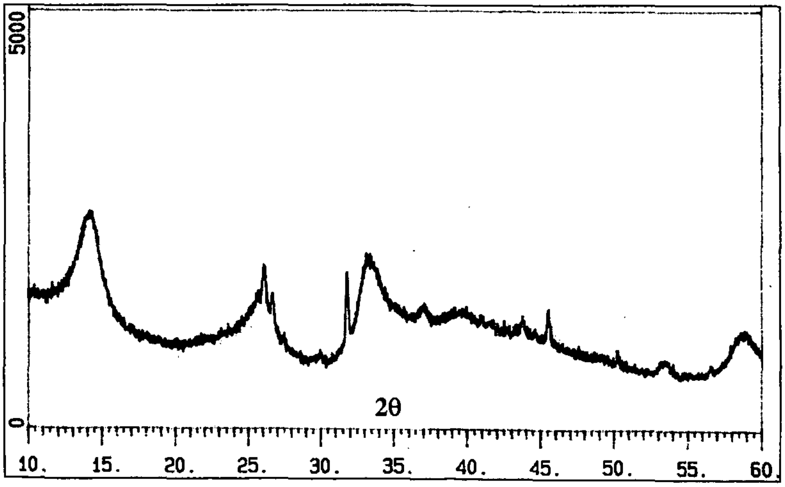

Figure 1. XRD of MoS_2 in coke from Test-2.

Table 1. Properties of Cold Lake heavy oil.

Carbon (wt.%)	82.8
Hydrogen (wt.%)	10.4
Nitrogen (wt.%)	0.40
Sulphur (wt.%)	4.60
Asphaltenes (wt.%)	16.9
CCR (wt.%)	12.6
H_2O (wt.%)	1.54
Nickel (ppm)	66
Vanadium (ppm)	178
°API Gravity	10.7
Viscosity @ 38°C (cP)	8,675
IBP – 200°C (wt.%)	0
200 – 343°C (wt.%)	10.7
343 – 525°C (wt.%)	35.5
525°C+ (wt.%)	53.8

Table 2. Results of autoclave activity tests.

Test	**1**	**2**	**3**[a]	**4**	**5**	**6**	**7a**	**7b**
Feedstock	F-1	F-2	F-0	F-2	F-2	F-2	F-2	F-2[c]
Mo Concentration (ppm)	212	611	200	200	611	611	611	611
Residence Time (min.)	45	45	45	45	45	90	70	70
C_{6+} Liquids (wt. % feed)	87.5	90.4	89.3	86.7	89.5	86.5	88.2	89.8
C_4–C_5 Liquid (wt. % feed)	5.6	4.6	4.4	4.5	4.3	3.8	4.0	1.6
Dry Gas (wt. % feed)[b]	4.6	4.2	4.7	5.3	3.7	5.9	4.8	6.7
H_2S (wt.% feed)[b]	2.4	2.3	2.1	2.2	1.9	2.3	2.0	1.9
Solids (wt. % feed)	0.7	0.5	0.9	2.1	0.6	0.8	0.5	0.5
Ash (wt.% of solids)	14.4	33.1	21.7	11.2	29.8	23.3	35.8	38.4
Simulated Distillation of C_{6+} Liquids								
IBP – 200°C (wt.%)	21.4	17.5	20.0	21.0	18.8	33.0	22.5	20.0
200 – 343°C (wt.%)	34.0	34.2	35.6	33.1	33.7	38.8	37.1	36.2
343 – 525°C (wt.%)	26.7	28.4	26.0	20.5	27.4	24.3	25.9	28.3
525°C+ (wt.%)	17.9	19.9	18.3	25.4	20.1	3.8	14.5	15.6
Conversions (%)								
Asphaltenes	65.7	72.3	56.3	41.3	67.5	66.7	71.0	45.9[d]
CCR	58.8	63.4	52.5	53.0	61.8	56.6	75.4	54.3[d]
525°C+	73.5	69.3	69.6	60.3	69.3	*94.3*[e]	78.2	60.8[d]

a. Product yield corrected for 21.7g of added diluent (BP: 200-343°C)

b. Values for Tests 1 to 4 include CH_4 and H_2S products from 10.0g of dimethyldisulphide.

c. Includes a calculated 290.3g of reactor bottoms (containing coke and catalyst) from Test-7a and 483.6g of virgin oil.

d. Conversions based on composite composition of virgin oil and reactor bottoms used in Test-7b.

e. Determined by crude simulated distillation ASTM D5307. See text.

Activities of Molybdenum Based Dispersed Catalyst Precursors

X. Zhan, M. Dieterle, B. Demirel, E.N. Givens

Center for Applied Energy Research
University of Kentucky
2540 Research Park Dr.
Lexington, KY 40511-8410

Keyword: Molybdenum Catalyst, Coal Liquefaction

ABSTRACT

This paper discusses the activation of several Mo-based precursors for coal liquefaction, including various molybdate salts (ammonium, potassium, and nickel), phosphmolybdic acid, and an oil soluble Mo complex (Molyvan L). Except for nickel molybdate which was essentially inactive, the activities of the other precursors towards coal and resid conversions were basically the same. Presulfiding promoted the activity of ammonium molybdate but had almost no effect on the other precursors. The low activity of nickel molybdate is attributed to its stability under liquefaction conditions.

INTRODUCTION

Numerous molybdenum based compounds are readily converted to active dispersed catalysts for coal liquefaction and resid hydroprocessing. These include both inorganic and organic Mo based compounds. The oil soluble Mo precursors are usually dissolved in the reaction system and readily form highly dispersed catalysts. Alternatively, water soluble precursors are impregnated onto the feed coal. During reaction they decompose *in situ* to form an active phases.

Previous liquefaction work in this laboratory has shown that recycled Mo catalyst always gave higher coal and resid conversions than freshly added catalysts. [1] This conclusion was based upon recycled catalyst contained in ashy resid obtained from Wilsonville pilot plant when Wyodak coal was processed with Molyvan L catalyst. The higher activity of recycled Mo catalyst led to the speculation that activation was time dependent and the Mo based catalyst precursors had to experience a few cycles in a continuous process before it could be fully activated. Our recent studies have also indicated that, when sulfur-free ammonium heptamolybdate was used as precursor, complete transformation to active catalyst *in situ* did not occur.[2] However, coals impregnated with thiomolybdates were slightly more active than the oxomolybdates in the absence of added sulfur. We also found that presulfiding oxomolybdate impregnated coal quite significantly increased conversion.

Coal liquefaction using dispersed Mo based bimetallic catalysts has also been widely studied in laboratory-scale batch reactors. The promotional effects of Fe and Ni on Mo catalysts have been reported by a number of researchers using a variety of coals.[3,4,5,6] Synergism was typically explained by the complementary effect of the metals or the formation of a new phase which was responsible for the high activity. However, recent pilot scale test have indicated that introducing Ni and Fe to a molybdenum impregnated coal does not influence conversion.[7]

Although inorganic molybdates have been widely used as catalyst precursors, most of the works has concentrated on ammonium based compounds because of their easy decomposition under liquefaction conditions. The objective of this study is to examine the effectiveness of other non-ammonium based molybdate precursors. Also, since some of these compounds contain more than one type of metal in the molecule, another objective is to examine if there is any advantage to using a compound containing two active metals.

EXPERIMENTAL

Materials Elemental analysis of the Black Thunder Wyodak coal are presented in Table 1. The as-received coal was impregnated with an aqueous solution containing various concentrations of catalyst precursors at the level of 0.5 g solution/g coal. The concentration of the aqueous solution was varied so that desired Mo loadings on coal could be achieved. In all cases, the coal paste was dried at 125 Torr and 100°C for two days to completely remove water. Solvent used in this study comprised mixtures of heavy distillate and deashed resid from Run 262e made at the Advanced Coal Liquefaction R&D Facilities at Wilsonville, AL. The properties of these materials, which were produced when the plant was operated with the same coal, are also summarized in Table 1. The following materials were used as received: Molyvan L (8.1% Mo, 6.4% P, R.T. Vanderbilt Co.), ammonium heptamolybdate (AHM, Aldrich,), phosphomolybdic acid (PMA, Aldrich), potassium molybdate (KM, Alfa), nickel molybdate (NiM, Aldrich), and tetrahydrofuran (THF, Aldrich). In all experiments, catalyst loadings were reported as mg Mo per kg dry coal.

Catalyst Pretreatment In some experiments, the catalyst impregnated coal was treated with H_2 containing 8 vol% H_2S prior to reaction. In a typical run, the reactor was loaded with coal slurry and placed horizontally in a furnace after purging with H_2 to remove air. The pretreatment was conducted at 300 psig and a gas flowrate of 200 ml/min (STP). The furnace was heated to 120 °C and held for 30 min after which it was successively heated to 250 and 360 °C while holding for 30 minutes at each temperature. After pretreating at 360 °C, the reactor was cooled, vented and subjected to regular reaction procedures described in the following section.

Coal Liquefaction Reaction Procedures All of the experiments were conducted in a 65 ml microreactor which was agitated at 400 rpm in a fluidized sand bath (Techne, SBL-2D) maintained at 440°C with an Omega CN4600 temperature controller. In every run, 3 g dry coal, 1.8 g heavy distillate, and 3.6 g deashed resid were added to the reactor which was then pressurized to 1000 psig at room temperature with H_2 containing 3 vol% H_2S. After 30 minutes reaction time, the reactor was removed and quenched in ice water. The liquid and solid products were scraped from the reactor using THF and subjected to Soxhlet extraction for 18 hours. The THF soluble material was distilled at 1 Torr and an atmospheric equivalent cut point of 566°C according to ASTM method D-1160. This cut point corresponds to that used in the pilot plant where the solvent was generated. All experiments were replicated at least twice to assure the reproducibility.

THF coal conversion and resid conversion were defined below as a measure of catalyst activity on an maf coal basis.

$$Coal\ Conv. = 100\times(1-\frac{[IOM]_{product}}{Coal(maf)}) \tag{1}$$

$$Resid\ Conv. = 100\times(\frac{[Coal(maf)+Resid]_{feed}-[IOM+Resid]_{product}}{Coal(maf)}) \tag{2}$$

RESULTS AND DISCUSSION

The liquefaction experiments using these catalyst precursors were performed at Mo loadings of 100 ppm and 300 ppm with/without H_2S/H_2 pretreatment. Figure 1 shows that at the Mo loading of 300 ppm without pretreatment, there is essentially no difference toward both coal and resid conversions for Molyvan L, AHM, PMA, and KM. The mean THF coal conversion of these four Mo precursors was 90.1±0.6% and mean resid conversion was 81.1±1.0%. For the Mo catalyst loading of 100 ppm as shown in Figures 2-3, the mean THF and resid conversions were 85.5±0.3% and 74.4±1.2%, respectively. The similar activities of these catalyst precursors, both the oil-soluble organic complex and water-soluble inorganic salts, may imply the formation of a similar active phase under liquefaction conditions. Considering the research work in this laboratory in the past years and those in open literatures, it is suggested that the formation of dispersed molybdenum catalyst is relatively independent of the starting material, as long as they decompose.

When the metal impregnated coal slurry was pretreated with H_2S/H_2, however, the activities of these precursors varied. At Mo loading of 100 ppm with pretreatment, coal conversions with AHM and KM increased slightly while that with PMA decreased. For resid conversion, AHM gave about 9% increase but PMA decreased by 4%, in line with its performance for THF coal conversion. The behavior of PMA in this study is consistent with the observation when this material was presulfided separately and then impregnated on coal.[8] Overall, it appears that pretreatment with H_2S improves the activity of AHM for resid conversion, does not affect the activity of KM, and slightly reduces the activity of PMA for both coal and resid conversions.

The major difference between KM, AHM and PMA is the presence of an ammonium group in AHM. As already noted, the catalyst precursors can not be fully activated *in situ* during a 30 minutes batch liquefaction run. Only a fraction of the precursors are converted to an active phase. Thus, the differences in activities between precursors may not be distinguishable. When these precursors are subjected to pretreatment, AHM is converted to an active phase through loss of the ammonium group. Thus, AHM exhibited higher activity than the other two precursors. Of course, over a longer period of exposure, such as that in a continuous process with catalyst recycle, most of the precursor would have converted to an active phase. As a result, these precursors show similar activities, although their activation kinetics may be different. The pilot plant test results indicated essentially no activity difference between AHM and PMA precursors. [7]

An interesting observation was that NiM improved coal conversion by less than 5% and resid conversion by less than 3% at all conditions tested. The low activity of NiM can be attributed to its stability under liquefaction conditions. TG analysis of NiM showed that this material is very stable in He at temperatures up to 600 °C. In $H_2S/H_2/He$ containing 5 vol% H_2S, there was a 1.5% weight gain at 450 °C indicating insignificant addition of sulfur, which is necessary to create an active catalyst phase. Unlike other Mo-based precursors, NiM is not readily converted to nickel and molybdenum sulfides that are active toward coal liquefaction. Therefore, NiM showed almost no advantage over thermal runs. In contrast, AHM and PMA have both been reported to form active phases [8,9] and showed high activities for both coal and resid conversions.

CONCLUSIONS

The inorganic and organic molybdenum compounds tested in this study showed essentially the same activities towards coal liquefaction and resid conversion. The nature of catalyst precursors is different and their activation mechanism may vary. In batch reactors which are typical of short reaction time, these precursors may exhibit different activities. It is expected, however, that in a continuous process with Mo catalyst recycle, the catalyst activity will be independent on precursor type as long as they decompose under liquefaction conditions. The low activity of nickel molybdate is probably due to its stability under liquefaction conditions.

ACKNOWLEDGMENTS

This research project was supported by the U.S. Depart of Energy under contract number of DE-AC22-91PC91040.

REFERENCES

1. Rantell, T., Anderson, R., and Givens, E.N., *Prepr.-Am. Chem. So., Div. Fuel Chem.*, 1996, 41(3), 993-997
2. Zhan, X, Dieterle, M., Lucas, A., Van Woert, H.C., and Givens, E.N., *Prepr.-Am. Chem. So., Div. Fuel Chem.*, 1998, 43(2), 320-324
3. Garg, D., and Givens, E.N., *Prepr.-Am. Chem. So., Div. Fuel Chem.*, 1983, 28(5), 200-209
4. Hulston, C.K.J., Redlich, P.J., Jackson, W.R., Larkins, F.P., and Marshall, M., *Fuel*, 1996, 75(12), 1387-1392
5. Derbyshire, F., Davis, A., Schobert, H., and Stansberry, P., *Prepr.-Am. Chem. So., Div. Fuel Chem.*, 1990, 35(1), 51-60

6. Zhan, X, Shabel, M., Cash, R., and Givens, E.N., *Prepr.-Am. Chem. So., Div. Petro. Chem.*, 1997, 42(3), 639-642
7. Givens, E.N. et al. "Bench-scale Testing of Advanced Concepts for Direct Coal Liquefaction: Evaluation of Dispersed Mo Catalysts." Paper presented to the Pittsburgh Energy Technology Coal Liquefaction and Solids Fuel Contractor' s Review Conference, Pittsburgh, PA, Sept. 3-4, 1997.
8. Belma, D., and Givens, E.N. *Prepr.-Am. Chem. So., Div. Fuel Chem.*, 1998, 43(2), 325-329
9. Lopez, J., and Pasek, E.A., "Process for Preparing Heavy Oil Hydroprocessing Slurry Catalyst", *US Patent 4,710,486*, 1987.

Table 1. Properties of Wyodak Coal and Feed Solvent

	Coal	Solvent	
	Ultimate Analysis	Heavy Distillate	Deashed Resid
<566°C	-	96.9	14.7
Composition (wt%)			
Carbon	70.62	88.86	89.79
Hydrogen	5.03	9.91	7.26
Nitrogen	1.13	0.44	0.86
Sulfur	0.52	<0.03	0.03
Oxygen (diff)	16.38	0.79	1.33
Ash	6.32		0.73
Ash, SO_3-free	5.46		

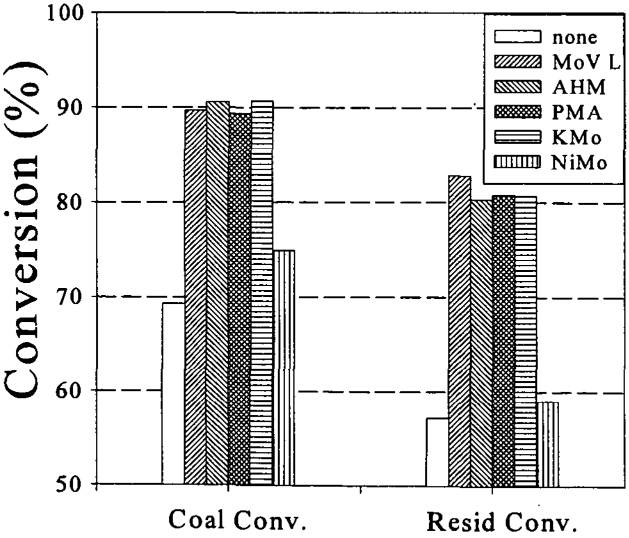

Figure 1 Effect of Various Mo Based Catalyst Precursors on THF Coal and Resid Conversions with Mo Loading of 300 ppm.

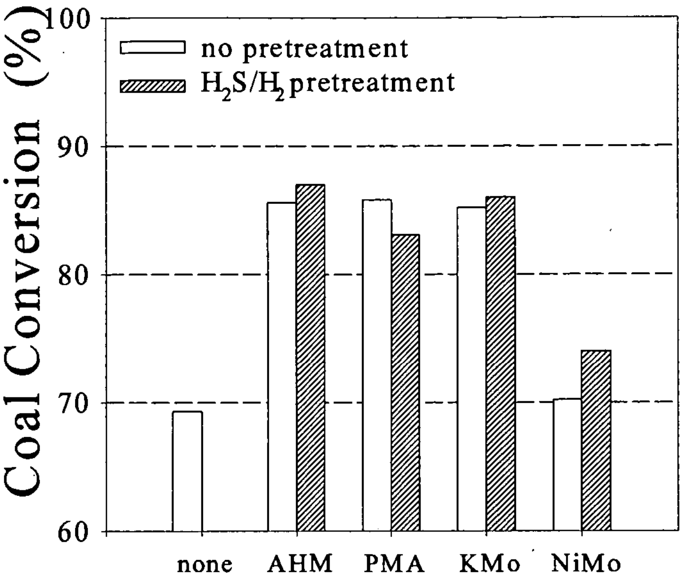

Figure 2 Effect of H_2S/H_2 Pretreatment on THF Coal Conversion with Mo Loading of 100 ppm

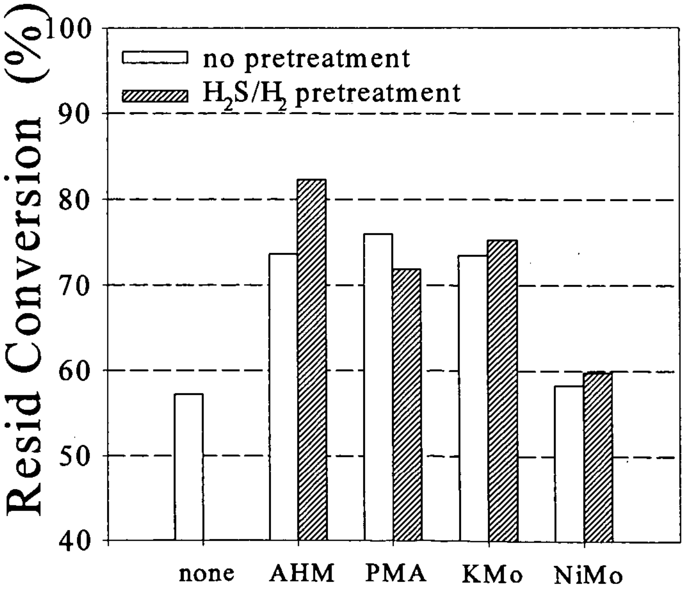

Figure 3 Effect of H_2S/H_2 Pretreatment on Resid Conversion with Mo Loading of 100 ppm

BIOPROCESSING OF CRUDE OILS AND DESULFURIZATION USING ELECTRO-SPRAY REACTORS

Eric N. Kaufman[*] and Abhijeet P. Borole
Bioprocessing Research and Development Center
Chemical Technology Division, Oak Ridge National Laboratory[†]
Oak Ridge, Tennessee, USA 37831-6226

"The submitted manuscript has been authored by a contractor of the U.S. Government under contract DE-AC05-96OR22464. *Accordingly, the U.S. Government retains a nonexclusive, royalty-free license to publish or reproduce the published form of this contribution, or allow others to do so, for U.S. Government purposes."*

ABSTRACT

Biological removal of organic sulfur from petroleum feedstocks offers an attractive alternative to conventional thermochemical treatment due to the mild operating conditions afforded by the biocatalyst. Electro-spray bioreactors were investigated for use in desulfurization due to their reported operational cost savings relative to mechanically agitated reactors and their capability of forming emulsions <5 μm. Here, the rates dibenzothiophene (DBT) oxidation to 2- hydroxybiphenyl (2-HBP) in hexadecane, by *Rhodococcus sp.* IGTS8 are compared in the two reactor systems. Desulfurization rates ranged from 1.0 and 5.0 mg 2-HBP/(dry g cells-h), independent of the reactor employed. The batch stirred reactor was capable of forming a very fine emulsion in the presence of the biocatalyst IGTS8, similar to that formed in the electro-spray reactors, presumably due to the fact that the biocatalyst produces its own surfactant. While electro-spray reactors did not prove to be advantageous for the IGTS8 desulfurization system, it may prove advantageous for systems which do not produce surface-active bioagents in addition to being mass transport limited.

KEY WORDS: oil desulfurization, *Rhodococcus*, electrostatic spraying, dibenzothiophene, biodesulfurization

INTRODUCTION

Biological refining of fossil fuel feedstocks offers an attractive alternative to conventional thermochemical treatment due to the mild operating conditions and greater reaction specificity afforded by the nature of biocatalysis. Efforts in microbial screening and development have identified microorganisms capable of petroleum desulfurization (see for example [1-12]), denitrification [6], demetalization [6], cracking [6, 13] and dewaxing. Further investigation and manipulation of enzymatic pathways responsible for these reactions [4, 14-17] has led to processes which are approaching commercial application, particularly in the area of biological desulfurization [7, 18]. Biological desulfurization of petroleum may occur either oxidatively (see for example [3, 5, 8, 9, 12, 17, 19-21], or reductively [2, 22-24]. In the oxidative approach, organic sulfur is converted to sulfate and may be removed in process water. This route is attractive due to the fact that it would not require further processing of the sulfur and may be amenable for use at the well head where process water may then be reinjected. In the reductive desulfurization scheme, organic sulfur is converted into hydrogen sulfide which may then be catalytically converted into elemental sulfur, an approach of utility at the refinery. A sampling of desulfurization rates achieved with oxidative and reductive microorganisms have been summarized in [25]. Regardless of the mode of biodesulfurization, key factors affecting the economic viability of such processes are biocatalyst activity and cost, differential in product selling price, sale or disposal of co-products or wastes from the treatment process, and the capital and operating costs of unit operations in the treatment scheme.

The selection of the petroleum feedstock in biodesulfurization will play a large role in the overall economic viability of the process. Biodesulfurization may be utilized as a pretreatment to crude oil before entering pipelines, may be applied as an alternative to hydrotreating the crude at the refinery, or may be applied in the polishing of refinery products such as diesel or gasoline. The particular application will determine the extent of desulfurization necessary and hence the treatment cost per barrel. At the wellhead, a biodesulfurization unit may be used to treat marginally sour crudes (0.6 - 0.7% S) converting them to sweet crudes (<0.5% S) and claiming the price differential in sweet versus sour crude in segregated pipeline systems (currently, the premium for sweet crude is ~$1/Bbl). For this application, the extent of desired desulfurization is quite low and this may serve as an attractive initial niche for biodesulfurization. When utilized for refinery applications, the biodesulfurization process must compete with conventional hydrotreating. Here the economic viability of biorefining will be based upon its competitiveness relative to the catalyst replacement, hydrogen, and octane penalty costs associated with hydrotreating.

[†] Research supported by the Office of Oil and Gas Processing, U.S. Department of Energy under contract DE-AC05-96OR22464 with Lockheed Martin Energy Research Corp.

While significant activity is progressing in the engineering and chemical modification of enzymes so that they may function in purely organic solutions [26-28], inherent to all of the current bioprocessing of fossil feedstocks schemes is the need to contact a biocatalyst containing aqueous phase with an immiscible or partially miscible organic substrate. Factors such as liquid / liquid and gas / liquid mass transport, amenability for continuous operation and high throughput, capital and operating costs, as well as ability for biocatalyst recovery and emulsion breaking are significant issues in the selection of a reactor for aqueous / organic contacting. Traditionally, impeller-based stirred reactors are utilized for such mixing due to their ease of operation and wide acceptance in the chemical and biological processing industries. Such mechanically stirred reactors contact the aqueous and organic phases by imparting energy to the entire bulk solution, i.e. the impeller must move the contents of the reactor. Energy input in the stirred reactor is a function of the phase ratio, oil viscosity, density, reactor size, impeller speed, etc. [29]. Typically, impeller based reactors are capable of achieving water or oil droplet sizes of 100 -300 μm in diameter when surfactants are not present [25] and require on the order of 1-6 W/L to do so based upon empirical correlation's [29]. It is estimated that if impeller based systems were capable of producing 5 μm droplets, it would require ~25 kW/L [30] if surfactants are not present. Furthermore, no capacity exists for biocatalyst separation or emulsion breakage within the reactor.

Alternative processing schemes [18] propose the use of "motionless mixers", in which the two phases are pumped over a reversing helical coil which creates turbulent eddies. While this method reduces the number of moving parts in the reactor, it does not reduce power requirements since costs are transferred from the impeller to the pumps required to move the liquids past the coil. Liquid velocities greater than 4 m/s are required to form emulsions (~10 μm) and one can not form emulsions in coil tubes greater than 3 mm in diameter [31]. For tubes greater than 10 cm in diameter one can not form droplets smaller than 1 mm. Like the stirred reactor, no capacity exists for emulsion breaking within the motionless mixer.

Recent advances in the area of contactors for solvent extraction have lead to the development of electrically driven emulsion phase contactors (EPC™) for efficient contact of immiscible phases [32-37]. In this concept, the differing electrical conductivity between the aqueous and organic phases causes electrical forces to be focused at the liquid / liquid interface, creating tremendous shear force (see for example [38]). This shear causes the conductive phase to be dispersed (5 μm droplet size - [30]) into the non-conductive phase, but does so with decreased energy requirements relative to mechanical agitators due to the fact that energy is imparted only at the liquid / liquid interface and not the entire bulk solution. Electrostatic crude oil desalters have been operated for several years [39]. More recently, devices based upon the EPC™ have been used commercially to water wash methyl tert-butyl ether feedstocks (with greater than 10-fold reduction in stage height [40]) and for organic extraction from aqueous analytical samples [41]. Energy consumption on a volumetric basis has been measured to be 2.4 W/L for a 30% tributyl phosphate / 70% dodecane / distilled water system, four orders of magnitude less than mechanical systems creating as fine an emulsion [30, 36].

The configuration of the EPC™ developed at the Oak Ridge National Laboratory is shown in Figure 1 where the contactor serves to disperse a liquid with a greater density than the continuous phase. The reactor employs two different types of electrode regions in order to increase liquid throughput. The first, termed the "nozzle region", provides a high capacity droplet dispersion by providing an electric field with a significant vertical component. This vertical field creates the dispersion at the nozzle entrance and accelerates it into the continuous phase. A second region termed the "operating channel" employs parallel plates carrying a modulated dc offset with high voltage spikes. This signal creates an oscillating horizontal electrical field which controls the residence time of the dispersed phase and serves to continuously coalesce and redisperse the droplets as they progress in a serpentine manner through the reactor. At the base of the reactor, an electrical field exists between the electrified central plate and the grounded aqueous phase, which accelerates the aqueous droplets to the organic / aqueous interface. In this manner, droplet coalescence and hence separation on the interface is enhanced. The EPC™ creates droplets of water containing biocatalyst ~5 μm in diameter within an organic phase, and does so with a power requirement of 3 W/L [25].

With the success the EPC™ has exhibited in the area of solvent extraction, it was proposed that it could be an efficient reactor system for aqueous / oil contacting in biorefining [42]. In our previous work [25], we characterized the emulsion quality and power requirements of the EPC™, and demonstrated that there was no detrimental effect on the cells due to the electric fields. Here, we compare the performance of the EPC™ to that of a batch stirred reactor (BSR), investigate the required level of biocatalyst activity before the surface area afforded by the EPC™ becomes a factor in reactor performance, and characterize the emulsion formed by both reactors in the presence of bacteria.

MATERIALS AND METHODS

Biocatalyst and solvent systems

The oxidation of dibenzothiophene (DBT) in hexadecane was studied to investigate reactor design and performance in an easily tractable chemical system. *Rhodococcus sp.* wild strain IGTS8 (ATCC 53968) was provided by Energy BioSystems Corp. and served as the biocatalyst. The sequence of DBT oxidation by IGTS8 is shown in Figure 2, (Kilbane, 1989) and detailed enzymatic steps in the pathway are discussed in [17]. Cells were supplied as a frozen paste and had a cell dry weight of 0.28 g/g of original frozen material. The aqueous phase in all experiments consisted of 0.156M, pH 7.5 potassium phosphate buffer. DBT (Aldrich, D3,220-2), dissolved in n-hexadecane (Aldrich, H670-3), served as the organic phase, with typical initial DBT concentrations being 0.6 wt.%.

Analytical

Liquid samples collected from the reactors were centrifuged at 14,000 RPM for 5 minutes to separate the aqueous phase and cell debris. DBT and 2-hydroxybiphenyl (2-HBP) concentrations in n-hexadecane were measured by gas chromatography using a Hewlett Packard 5890 gas chromatograph equipped with a flame ionization detector. A 1μL sample was injected onto a 15 m DB-1 column (J&W Scientific, catalog number 125-1012) which was used with a helium carrier flow of 10 mL/min. The temperature program was 150°C for 1 min followed by an initial ramp rate of 5°C/min up to 200°C and a final ramp rate of 25°C/min to a final temperature of 280°C. The column was calibrated with DBT and 2-HBP (Aldrich, #24,021-4) standards. The injector was operated at 250°C and the detector was operated at 300°C. In the experiments reported here, DBT and 2-HBP concentrations in the aqueous phase were below our levels of detection. Hence only concentrations in the organic phase are reported.

Batch stirred reactor experiments

Experiments conducted in batch stirred reactors (BSR) typically utilized 50 g of frozen *Rhodococcus sp.* wild type strain IGTS8 (ATCC 53968) cell paste which were brought up to 750 mL with 0.156M (pH 7.5) phosphate buffer (1X cell density) and added to 250 mL of 0.6wt% DBT in n-hexadecane. The reactor vessel was a 1-L VirTis Omni-Culture fermentor (model 178657, Gardiner, NY), utilizing a 6-bladed Rushton-type impeller with 2 baffles. The impeller was mounted on the shaft 0.5 inches from the aerator and 2 inches from the bottom of the vessel. The reactor was kept at 30°C, agitated at 800 RPM, and aerated with either room air or pure oxygen at a rates of either 0.2 or 1.0 SLPM. Specific aeration procedures are noted in the text. To collect samples, agitation and aeration were ceased for 5 min to allow the aqueous and organic phases to separate. A 1.5 mL sample from the top of the organic phase was then taken for analysis.

Mass transport experiments were conducted in the BSR to determine if the desulfurization process was liquid-liquid (l-l) or gas-liquid (g-l) mass transfer limited. The mass transport experiments were conducted as above except that aeration was performed using 1/4 " stainless steel tubing rather than the aerator supplied by the manufacturer. Unlike the previous experiments, the mass transport experiments were organic continuous as 250 mL of aqueous phase was dispersed into 750 mL of hexadecane containing 0.6wt% DBT. Five batch stirred reactors were run simultaneously with different quantities of *Rhodococcus sp.* wild type strain IGTS8 (ATCC 53968) cell paste added to each reactor. Using a 250 mL basis for the aqueous phase, the quantities of frozen biocatalyst added to the 0.156 M (pH 7.5) phosphate buffer in each reactor were 8.3, 16.7, 83.3, 166.7, and 250 g respectively. The cell density corresponding to 16.7 g frozen biocatalyst in 250 mL aqueous phase was considered as 1X cell concentration. Thus, the cell density was varied from 0.5X to 15X in this experiment. To collect samples, agitation and aeration were ceased for 5 min to allow the aqueous and organic phases to separate. A 1.5 mL sample was taken from the top of the organic phase in each reactor every hour for 10 h, and again at 24 h into the experiment.

Gas – liquid mass transport experiments were conducted using air and oxygen at 0.2 and 1.0 slpm. In order to determine whether or not an oxygen mass transport limitation was a factor in the experiments using different cell densities, two batch stirred reactors were run at 800 RPM, 30°C, containing 750 mL hexadecane with 0.6 wt.% DBT, 166.7 g biocatalyst (10X cell density) in 250 mL of phosphate buffer. The aeration rate was 1.0 slpm of room air for the control condition, and 1.0 splm pure oxygen in the experimental condition. Samples were collected every hour for 8 h using the procedure described above.

EPC™ experiments

The design and operation of the EPC™ utilized in these experiments are adaptations of those described by Scott *et al.* [36]. A schematic of EPC™ operation is shown in Figure 3. The Teflon body of the EPC™ measured 10 cm x 10 cm x 61 cm. The front and rear plates were made of clear Lexan, allowing for visual inspection of reactor operation. A thin sheet of Teflon was placed between the body and the front and rear plates to prevent wetting and current leakage to the Lexan. Three stainless steel electrodes, placed parallel to each other, measured 30 cm x 6 cm. The center electrode was charged, while the two outer electrodes were grounded. This adaptation to the original EPC™ design was found to minimize biomass fouling of the reactor. The center electrode was connected to the high-voltage electric supply through a supporting steel rod to avoid disturbance of electrostatic-spraying in the nozzle region. High-voltage (up to 40 kV) was generated using a pulsed DC power supply and automobile ignition parts. A power supply (Hewlett Packard 6653A, Avondale, PA) and two sweep/function generators (BK Precision 3030, Chicago, IL) were used to produce the signal which was then passed through an ignition coil (Mallory Promaster 29901, Carson City, NV) to step up the signal. In order to prevent discharge of the electrodes through the circuit, a high-voltage diode (Collmer Semiconductor CS4107X30, Dallas, TX) was placed between the coil and the EPC™. From the diode, the positively charged terminal was connected to the rings surrounding the capillary tubes, and the negative lead was attached to the center electrode. The charged rings created an initial dispersion of biocatalyst as the aqueous phase emerged from the capillary tubes. The parallel electrodes lower in the reactor enhanced droplet dispersion as the more dense aqueous phase descended to the bottom of the reactor.

In EPC™ experiments, the organic liquid served as the continuous phase into which an aqueous biocatalyst was dispersed. The organic phase consisted of 2,400 mL n-hexadecane containing 0.6 wt.% dibenzothiophene. The temperature of the organic phase was controlled at 30°C by pumping the liquid from the top of the EPC™, through a stainless steel coil submerged in a heated bath, and then returning the hexadecane to the bottom of the EPC™. Typically, biocatalyst (26.7 g of frozen cell paste was brought to a volume of 100 mL with potassium phosphate buffer) was recirculated through the reactor at 5.0 mL/min using a peristaltic pump. The cell density with respect to the amount of aqueous phase used in these EPC™ experiments corresponded to a 4X concentration. A higher cell density was used in the EPC™ as compared to the BSR experiments due to the lower aqueous:organic phase ratio in the EPC™ and to enable DBT conversion significant enough to be observed by the analytical procedure employed. Aqueous phase containing the biocatalyst was sprayed into the reactor at the nozzle region, was continuously coalesced and redispersed in the operating region, and coalesced at the base of the EPC™. To better aerate, sample, and control the aqueous phase, it was circulated from the reactor base to an external reservoir at a rate of 5.0 mL/min. The external container allowed for temperature control, pH and O_2 measurement, agitation, and aeration of the biocatalyst. The liquid was then returned to the top of the reactor through two 1.6-mm-OD, 1-mm-ID capillary tubes (U-140, Upchurch Scientific, Oak Harbor, WA) where it was again sprayed into the hexadecane. A water bath controlled the temperature of the jacketed aqueous reservoir at 30°C. The pH was monitored throughout the experiment, and remained in the pH range of 7.0 to 7.5. Agitation of the aqueous reservoir from a magnetic stirrer and room air aeration through a diffuser at 20 mL/min permitted more favorable conditions for the biocatalyst than did the long residence time at the bottom of the EPC™, a location which lacked both aeration and agitation. In order to help alleviate possible oxygen deficiency inside the reactor, another diffuser was introduced 3 cm from the bottom of the EPC™ at airflow rate of 36 mL/min. Samples from the EPC™ were drawn hourly for twelve hours through a 2m x 3.175mm Teflon tube placed 10cm through the top of the reactor against a sidewall. Using a 30mL glass-bodied syringe, the tubing was flushed with liquid from the EPC™ three times before a 1.5mL sample was drawn. Samples were centrifuged as described above. Due to the small amount of 2-HBP production in the EPC™, and hence greater associated error in GC analysis, samples were run in triplicate.

In experiments to determine possible mass transport limitations in the EPC™, 66.7 g of frozen cell paste was brought to 100 mL with potassium phosphate buffer (10X cell density) and used as the aqueous phase. In order to evaluate if oxygen mass transfer was a limiting factor, the aqueous reservoir used for recirculating the aqueous phase was sparged with pure oxygen at a flow rate of 50 mL/min. This experiment was also conducted at a 10X cell density.

RESULTS AND DISCUSSION

2-HBP production in the EPC™ and BSR

Desulfurization activity of the *Rhodococcus sp.* in both reactors was typically between 1 and 5 mg 2-HBP produced per dry g of biocatalyst per hour. Rates of 2-HBP production in the two reactor systems were within experimental variance and no appreciable difference in desulfurization rates were seen between the two reactors. Note that in the experiments reported here, the only available carbon and energy source for the biocatalyst other than what may be carried over in the frozen cell paste, was hexadecane and DBT. Other studies (outlined in [25]) have utilized additional external carbon and energy sources and have reported higher activities with *Rhodococcus sp.* Due to the high surface area reported in the EPC™ [25], higher rates were expected in the EPC™, however, similar performance was observed in both reactors. Experiments were conducted with higher cell densities to determine at what point the BSR becomes mass transfer limited and the high surface area afforded by the EPC™ would become beneficial.

Mass transport limitations

Results of the DBT desulfurization experiments conducted at varying cell densities in BSR's are given in Figure 4. The rate of desulfurization, when normalized with respect to cell mass, was found to decrease with increasing cell density indicating that mass transfer resistance was the controlling process in desulfurization. A statistical analysis of the data was conducted using the analysis of variance (ANOVA) test and the t-test (Table 1). Based on a 95% confidence interval, a significant difference in the rates of HBP production was observed between 5X and 10X cell density BSR's. This suggests that the desulfurization process becomes mass transfer limited at a cell density of 10X. The mass transfer limitation may be due to gas-liquid or liquid-liquid mass transport resistance.

The results of experiments conducted in the BSR at 10X cell density to evaluate possible gas-liquid mass transfer limitations are given in Figure 5. Increasing the rate of air supply or increasing the oxygen tension in the reactor through the use of pure oxygen rather than air was not seen to affect HBP production. It was determined that oxygen mass transfer was not the limiting factor in the desulfurization of DBT even at 10X cell density. This suggests that the system may be limited by liquid-liquid mass transfer. Since the EPC™ reportedly provides larger liquid-liquid interfacial area, the BSR was compared with the EPC™ for desulfurization activity at equal cell density.

EPC™ vs BSR at 10X cell density

Comparison of the EPC™ and BSR at 10X cell density is given in Figure 6. As shown, no difference was observed in the desulfurization rates between the two reactors. Thus, either the system is not truly mass transport limited or the EPC™ does not provide a larger surface area for reaction under the present conditions.

Emulsion characterization

To determine whether the EPC™ offers larger surface area than BSR, samples were collected from the reactors and observed under a microscope using a 100x oil emersion objective. Due to the opaqueness rendered by high cell densities employed, observations could not be made *in situ* during reactor operation. Samples collected during the run were immediately mounted on a slide and observed under a microscope. In addition to sampling conducted during a run, samples were also collected at the end of a run from a cuff layer formed after gravity settling of the aqueous and organic phases. The cuff layer (which was previously characterized as being 92.7% hexadecane) was observed to contain a major portion of the biocatalyst. In addition, a significant amount of the biocatalyst was extracted and existed in the organic phase. Microscopic examination of samples from the cuff layer of the BSR showed a very fine emulsion with droplet sizes ranging from 1 to 10 μm. A similar cuff layer was also formed during EPC™ experiments. Average droplet size for EPC™ and BSR samples collected at 4 hours during normal operation were 2.54 ± 2.40 μm and 3.08 ± 1.78 μm, respectively (n>300). Figure 7 shows a micrograph of the emulsion obtained in an EPC. Thus, a very fine emulsion is formed in the EPC™ as well as the BSR, and it appears that it is for this reason that an augmentation in desulfurization rate is not seen in the EPC™ relative to the BSR. Formation of such an emulsion in the BSR may be presumed due to production of biosurfactants by the biocatalyst IGTS8. Other *Rhodococcus sp.* have been previously reported to produce glycolipids in the presence of hexadecane as well as some crude oils [43]. Earlier characterization of droplet size in a BSR [25] was performed either with no biocatalyst present, or with an extremely small amount to allow in situ observation of the droplets in the reactor. Our previous work revealed a decrease in droplet size from 210 to 118 μm when adding just 5 g of cells in 750 mL aqueous phase. Thus, the emulsion characterization reported here (with 67 g of cells in 250 mL aqueous phase) is in no way contradictory to our previous reports. Preliminary experiments varying the concentration of DBT ten-fold did not affect the rate of desulfurization, indicating that the aqueous side liquid mass transfer may be controlling.

CONCLUSIONS

The performance of EPC™ was similar to BSR for desulfurization of a model system containing DBT in hexadecane treated with biocatalyst *Rhodococcus rhodochrous* IGTS8. The system was not limited by gas-liquid oxygen mass transfer at high cell densities (10X). The equal desulfurization rates in two reactors were due to almost equal interfacial area and the high degree of cell extraction into the organic phase. Higher interfacial area than normally expected in mechanically stirred reactors were realized in BSR, presumably due to formation of surfactants by the biocatalyst present. While EPC™ did not prove to be advantageous for the IGTS8 desulfurization system in terms of rates of desulfurization, it may prove advantageous for electro-static emulsion breaking, in reducing power requirements for mixing, and for creating large amounts of surface area for systems that do not produce surface active bioagents.

ACKNOWLEDGMENTS

This work was supported by the Office of Oil & Gas Processing, U.S. Department of Energy under contract DE-AC05-96OR22464 with Lockheed Martin Energy Research Corp. The authors acknowledge the material contributions of Energy BioSystems Corp., and the technical assistance of Drs. Punjai Selvaraj and Costas Tsouris at the Oak Ridge National Laboratory.

REFERENCES

1. Constanti, M., Giralt, J. and Bordons, A., "Desulfurization of dibenzothiophene by bacteria," *World Journal of Microbiology and Biotechnology*, **10**, 510-516 (1994).
2. Finnerty, W.R., "Organic sulfur desulfurization in non-aqueous media," *Fuel*, **72**, 1631-1634 (1993).
3. Kayser, K.J., Bielaga-Jones, B.A., Jackowski, K., Odusan, O. and Kilbane, J.J., "Utilization of organosulfur compounds by axenic and mixed cultures of Rhodococcus rhodochrous IGTS8," *Journal of General Microbiology*, **139**, 3123-3129 (1993).
4. Kim, T.S., Kim, H.Y. and Kim, B.H., "Petroleum desulfurization by desulfovibrio desulfuricans m6 using electrochemically supplied reducing equivalent," *Biotechnology Letters*, **12**, 757-760 (1990).
5. Lee, M.K., J.D., S. and Grossman, M.J., "Sulfur-specific microbial desulfurization of sterically hindered analogs of dibenzothiophene," *Applied and Environmental Microbiology*, **61**, 4362-4366 (1995).
6. Lin, M.S., Premuzic, E.T., Yablon, J.H. and Zhou, W.M., "Biochemical processing of heavy oils and residuum," *Applied Biochemistry and Biotechnology*, **57/58**, 659-664 (1996).
7. Monticello, D.J., "Biocatalytic desulfurization," *Hydrocarbon Processing*, **February** 1994, 39-45 (1994).
8. Ohshiro, T., Hine, Y. and Izumi, Y., "Enzymatic desulfurization of dibenzothiophene by a cell free system of Rhodococcus erythropolis D-1," *FEMS Microbiology Letters*, **118**, 341-344 (1994).
9. Ohshiro, T., Hirata, T. and Izumi, "Microbial desulfurization of dibenzothiophene in the presence of hydrocarbon," *Appl. Microbiol. Biotechnol.*, **44**, 249-252 (1995).
10. Shennan, J.L., "Microbial attack on sulfur-containing hydrocarbons: Implications for the desulfurization of oils and coals.," *J. Chem. Tech. Biotechnol.*, **67**, 109-123 (1996).
11. Sorokin, D.Y., "Biological oxidation of sulfur atoms in C1-sulfur and other organosulfur compounds," *Microbiology (NY)*, **62**, 575-581 (1993).
12. Wang, P. and Krawiec, S., "Desulfurization of dibenzothiophene to 2-hydroxybiphenyl by some newly isolated bacterial strains," *Arch. Microbiol.*, **161**, 266-271 (1994).
13. Premuzic, E.T., Lin, M.S., Jin, J.Z., Manowitz, B. and Racaniello, L., *Biochemical Alteration of Crude Oils in Microbial Enhanced Oil Recovery*, in *Biohydrometallurgical Technologies*, Torma, A.E., Apel, M.L. and Briarley, C.L., Editors. 1993, The Minerals, Metals, and Materials Society. p. 401-413.
14. Denome, S.A., Oldfield, C., Nash, L.J. and Young, K.D., "Characterization of the desulfurization genes from Rhodococcus sp. strain IGTS8," *Journal of Bacteriology*, **176**, 6707-6716 (1994).
15. Ohshiro, T., Kanbayashi, Y., Hine, Y. and Izumi, Y., "Involvement of Flavin coenzyme in dibenzothiophene degrading enzyme system from *Rhodococcus erythropolis* D-1.," *Biosci. Biotech. Biochem.*, **59**, 1349-1351 (1995).
16. Vazquez-Duhalt, R., Westlake, D.W.S. and Fedorak, P.M., "Cytrochrome *c* as a biocatalyst for the oxidation of thiophenes and organosulfides," *Enzyme Microb. Technol.*, **15**, 494-499 (1993).
17. Gray, K.A., Pogrebinsky, O.S., Mrachko, G.T., Xi, L., Monticello, D.J. and Squires, C., "Molecular mechanisms of biocatalytic desulfurization of fossil fuels," *Nature Biotechnology*, **14**, 1705-1709 (1996).
18. Dounias, G.A. and Stavropoulos, K.D., *Economic Feasibility of Biochemically Upgrading Heavy Crudes*, . 1995, Brookhaven National Laboratory.
19. Kilbane, J.J. and Bielaga, B.A., "Toward sulfur-free fuels," *CHEMTECH*, **december**, 747-751 (1990).
20. Olson, E.S., Stanley, D.C. and Gallagher, J.R., "Characterization of intermediates in the microbial desulfurization of dibenzothiophene," *Energy and Fuels*, **7**, 159-164 (1993).
21. Omori, T., Saiki, Y., Kasuga, K. and Kodama, T., "Desulfurization of akyl and aromatic sulfides and sulfonates by dibenzothiophene desulfurizing Rhodococcus sp. strain SY1," *Biosci. Biotech. Biochem.*, **59**, 1195-1198 (1995).
22. Kim, H.Y., Kim, T.S. and Kim, B.H., "Degradation of organic sulfur compounds and the reduction of dibenzothiophene to biphenyl and hydrogen sulfide," *Biotechnology Letters*, **12**, 761-764 (1990).
23. Lizama, H.M., Wilkins, L.A. and Scott, T.C., "Dibenzothiophene sulfur can serve as the sole electron acceptor during growth by sulfate reducing bacteria," *Biotechnology Letters*, **17**, 113-116 (1995).
24. Kim, B.H., Kim, H.Y., Kim, T.S. and Park, D.H., "Selectivity of desulfurization activity of Desulfovibrio desulfuricans M6 on different petroleum products," *Fuel Processing Technology*, **43**, 87-94 (1995).

25. Kaufman, E.N., Harkins, J.B., Rodriguez, M., Selvaraj, P.T., Tsouris, C. and E., M.S., "Development of an electro-spray bioreactor for crude oil processing," *Fuel Processing Technology*, **52**, in press (1997).
26. Almarsson, O. and Klibanov, A.M., "Remarkable activation of enzymes in nonaqueous media by denaturing organic solvents," *Biotechnology and Bioengineering*, **49**, 87-92 (1996).
27. Scott, C.D., Scott, T.C., Blanch, H.W., Klibanov, A.M. and Russel, A.J., *Bioprocessing in Nonaqueous Media Critical Needs and Opportunities*, . 1995, Oak Ridge National Laboratory.
28. Woodward, C.A. and Kaufman, E.N., "Enzymatic catalysis in organic solvents: polyethylene glycol modified hydrogenase retains its sulfhydrogenase activity in toluene," *Biotechnology and Bioengineering*, **52**, 423-428 (1996).
29. Perry, R.H., Green, D.W. and Maloney, J.O., *Perry's Chemical Engineering Handbook*, . 1984, McGraw-Hill: New York. p. 2336.
30. Scott, T.C. and Sisson, W.G., "Droplet size characteristics and energy input requirements of emulsions formed using high intensity pulsed electric fields," *Separation Science and Technology*, **23**, 1541-1550 (1988).
31. Chemineer, *Kenics Static Mixers KTEK Series*, . 1988: North Andover, MA. p. 32.
32. Byers, C.H. and Ammi, A., "Understand the potential of electro-separations," *Chemical Engineering Progress*, 91, 63 (1995).
33. Kowalski, W. and Ziolkowski, Z., "Increase in rate of mass transfer in extraction columns by means of an electric field," *Int. Chem. Eng.*, **21**, 323 (1981).
34. Martin, L., Vignet, P., Fombarlet, C. and Lancelot, F., "Electrical field contactor for solvent extraction," *Sep. Sci. Technol.*, **18**, 1455 (1983).
35. Scott, T.C. and Wham, R.M., "An electrically driven multistage countercurrent solvent extraction device: the emulsion phase contactor," *Ind. Eng. Chem. Res.*, **28**, 94 *(1989)*.
36. Scott, T.C., DePaoli, D.W. and Sisson, W.G., "Further development of the electrically driven emulsion phase contactor," *Ind. Eng. Chem. Res.*, **33**, 1237-1244 (1994).
37. Thorton, J.D., "The application of electrical energy to chemical and physical rate processes," *Rev. Pure and Appl. Chem.*, **18**, 197 (1968).
38. Ptasinski, K.J. and Kerkhof, P.J., "Electric field driven separations: phenomena and applications," *Sep. Sci. Technol.*, **27**, 995 (1992).
39. Warren, K.W. and Prestridge, F.L., "Crude oil desalting by counterflow electrostatic mixing," in proceedings of the National Petroleum Refiners Association Annual Meeting, San Antonio, TX, (1988).
40. Schwartz, E., Rock, K., Byeseda, J. and Pehler, R., "An improved process for MTBE unit feed pretreatment," in proceedings of the First Separations Division Topical Conference on Separations technologies: New developments and Opportunities, (1992).
41. Wood, T.S., Cernohlavek, L.G., Grant, D.T., Kelly, K.P., Lochhaas, P.D., Maynard, A.E., Ragsdale, D.N., Schrier, L.C., Stalling, D.L., Strumpf, D.M. and Tsang, A.Y., "Rapid, automated liquid / liquid extraction of contaminants from aqueous samples containing suspended solids," in proceedings of the First Separations Division Topical Conference on Separations technologies: New developments and Opportunities, (1992).
42. Lizama, H.M., Scott, T.C. and Scott, C.D., *Apparatus and Method for the Desulfurization of Petroleum by Bacteria*, . 1995, United States Patent Number 5,458,752.
43. Finnerty, W.R. and Singer, M.E., "A microbial biosurfactant-physiology, biochemistry and applications.," *Developments in Industrial Microbiology*, **25**, 31-46 (1984).

Table 1. Results of analysis of variance (ANOVA) and t-Test (assuming unequal variance) comparing desulfurization rates over a range of cell densities. The second column gives p values for an analysis of variance over the complete range of data. The 3rd through 6th column gives p values for t-Tests comparing two experiments at a time. Numbers in parentheses indicate the cell densities compared. The p values comparing the data at 5X and 10X cell densities are all below 0.05, showing a significant difference between the two sets. This suggests that the desulfurization process may be mass-transfer limited at 10X cell density with statistical certainty.

Time, hr	**ANOVA (p)**	**p (0.5 & 1)**	**p (1 & 5)**	**p (5 & 10)**	**p (0.5 & 5)**
1hr	3.62E-10	0.2170	0.7420	0.0010	0.0739
2hr	4.53E-02	0.2150	0.0953	0.0177	0.1820
3hr	2.60E-03	0.0787	0.3380	0.0066	0.0600
4hr	5.40E-03	0.4706	0.3340	0.0006	0.0950
5hr	5.30E-03	0.3250	0.4600	0.0146	0.2190
6hr	3.89E-05	0.7440	0.3580	0.0370	0.1310
7hr	3.00E-03	0.0750	0.0384	0.0025	0.0390
8hr	2.00E-04	0.0328	0.0510	0.0190	0.0180
9hr	6.00E-05	0.0951	0.1984	0.0031	0.0110
10hr	1.18E-02	0.5820	0.1458	0.0066	0.1920
24hr	9.00E-07	0.1343	0.0301	0.0005	0.0110

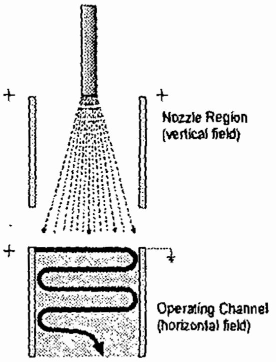
+
+
Nozzle Region
(vertical field)
+
+
Operating Channel
(horizontal field)

Figure 1: Dual electrode region concept for the emulsion phase contactor. The nozzle region disperses the aqueous phase into the organic and the operating channel serves to control droplet residence time within the reactor. Figure adapted from [36].

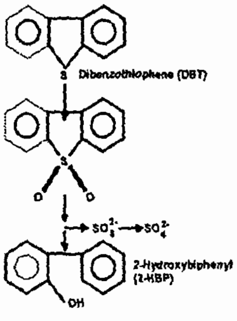
S Dibenzothiophene (DBT)
S
O
O
SO$_3^{2-}$ → SO$_4^{2-}$
2-Hydroxybiphenyl
(2-HBP)
OH

Rhodococcus sp. strain IGTS8 Pathway

Figure 2: Biochemical pathway showing the sequence of DBT oxidation by IGTS8.

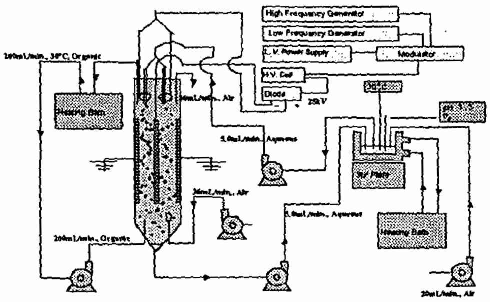
High Frequency Generator
Low Frequency Generator
L.V. Power Supply
Modulator
H.V. Coil
Diode
25kV
200ml/min., 30°C, Organic
Heating Bath
5.0ml/min., Aqueous
30ml/min., Air
30ml/min., Air
30°C
Stir Plate
5.0ml/min., Aqueous
Heating Bath
200ml/min., Organic
20ml/min., Air

Figure 3: Schematic of the emulsion phase contactor and ancillary equipment.

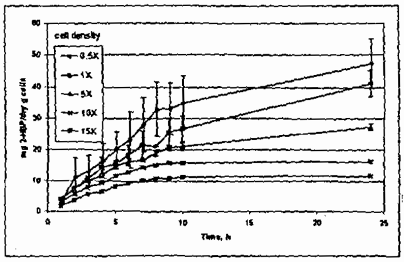

Figure 4: Effect of cell density on 2-HBP production rate. The 0.5X – 15X refers to cell density and 1X corresponds to 16.7 g cell paste in 250 mL aqueous phase. As observed from this plot, mass transfer may be a limiting factor in the DBT desulfurization process.

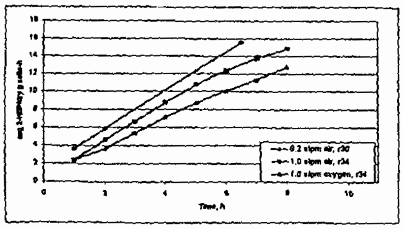

Figure 5: Effect of aeration rate and oxygen tension on 2-HBP production in batch stirred reactor. The experiment was conducted by dispersing 250 mL aqueous phase containing 166.7 g cell paste (10X cell density) in 750 mL hexadecane containing 0.6 wt% DBT.

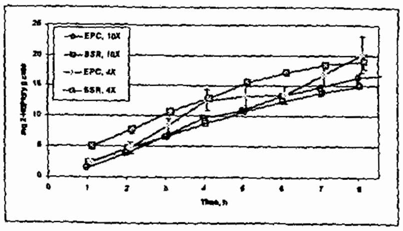

Figure 6: Comparison of 2-HBP production rate in EPC™ and BSR. The BSR experiment was conducted by contacting 250 mL aqueous phase containing 166.7 g cell paste (10X cell density) in 750 mL hexadecane containing 0.6 wt. DBT. In the EPC™ experiment, 107 mL aqueous phase containing 66.7 g cell paste (10X) was contacted with 2400 mL organic phase.

Figure 7: Micrograph of an EPC™ sample collected at 4 hours after beginning of reactor operation. The sample was collected from the central region between the electrodes using a Teflon tubing connected to a syringe and observed under a microscope as described earlier. The average droplet size was measured to be 2.54 ± 2.40 μm (n=300).

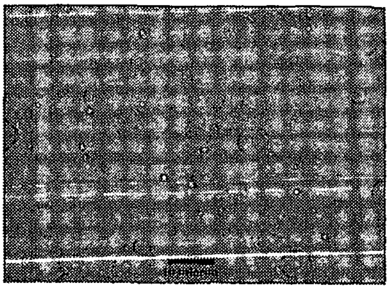

Biocatalytic Ring Cleavage of Aromatic Hydrocarbons and Heterocycles Commonly Present in Petroleum Distillates.

Q. Wu*, P.M. Fedorak, M.A. Pickard, M.R. Gray, and J.M. Foght
Univ. of Alberta, Edmonton, Alberta CANADA.

Keywords: Biotransformation, fused-ring aromatics, distillates

ABSTRACT

A potential alternative to conventional fuel upgrading techniques is to use bacteria under near-ambient conditions to catalyze aromatic ring cleavage in the first step of a two-stage upgrading process. The resulting biocatalytic products would be chemically hydrogenated under mild conditions in the second stage to produce the desired alkylbenzenes. Experiments testing biocatalytic ring cleavage of aromatic hydrocarbons are described in this study.

Pseudomonas fluorescens LP6a was chosen as the biocatalyst because of its broad-specificity aromatic hydrocarbon-degrading enzymes which confer the ability to oxidize a wide range of polycyclic aromatic hydrocarbons and heterocycles commonly present in petroleum middle distillates. Pre-grown, induced whole cell biocatalysts in aqueous suspension produced the predicted polar intermediates from aromatic substrates without altering the aliphatic carrier and without carbon loss from the aromatic substrate. Quantitative studies with ^{14}C-labeled aromatic substrates incorporated into synthetic and authentic distillates were carried out to reveal potential process-limiting factors. Parallel studies were performed using gas chromatography with a flame ionization detector to quantify aromatic ring cleavage in authentic distillates.

INTRODUCTION

Chemical hydrogenation processes are currently used to upgrade middle distillates produced by thermochemical cracking of heavy oils and bitumen. These distillates have a high content of low fuel value di- and tricyclic aromatics, which are reduced by expensive high temperature-high pressure hydrogenation to compounds such as alkylbenzenes. The catalysts involved are frequently deactivated by sulfur- and nitrogen-containing compounds in the feedstocks. These expenses make it desirable to explore an alternative to conventional upgrading techniques. An attractive alternative is to use bacteria to enzymatically cleave the fused-ring aromatics under near-ambient conditions, followed by mild chemical hydrogenation to produce the desired alkyl aromatics.

Biocatalytic technology has been used widely in crude oil biodegradation and is being assessed for biodesulfurization. It can be cost effective, competitive or compatible with current technology. It is well known that one ring of the di- and tricyclic aromatics can be opened selectively by bacterial enzymes. Although the oxygenated ring cleavage products are themselves undesirable, they may be converted to alkylaromatics under milder hydrogenation conditions than the parent feedstocks, resulting in cost savings.

Besides yielding the desired ring fission products, two primary requirements of the biological process are essential. First, the biocatalytic activity must be restricted to aromatic compounds and must be effective over the wide range of di- and tricyclic aromatic hydrocarbons, heterocycles and alkyl-substituted homologues common to middle distillates. Second, there should be no carbon loss from the aromatic substrates as a consequence of microbial oxidation; that is, the process has to be blocked at certain stage to prevent complete oxidation. Other advantages such as the ability of the cells to catalyze ring cleavage in a resting state and to be pre-grown quickly to high density in an active state would greatly benefit the process.

The research project described here deals with the biocatalytic stage for ring cleavage of aromatics in the middle distillates. *Pseudomonas fluorescens* LP6a was previously reported to possess several of the properties listed above and thus was chosen for this study. For example, LP6a mutant 21-41 has been shown to accumulate the expected ring cleavage products from a variety of pure aromatic compounds commonly present in petroleum distillates (Foght et al. 1997). In the experiments reported here, ^{14}C-labeled phenanthrene was incorporated into synthetic and authentic distillates to detect biotransformation of the substrate into water-soluble ring cleavage products. Parallel studies were performed using gas chromatography (GC) with a flame ionization detector (FID) to quantify aromatic ring cleavage in authentic distillates. These results are leading towards optimization of biocatalytic ring cleavage for bio-upgrading of petroleum distillates.

METHODS AND MATERIALS

Preparation of biocatalyst

Transposon mutants of *P. fluorescens* LP6a were generated by conjugation using a suitable Tn5 donor plasmid with subsequent screening for desired phenotypic changes (Foght and Westlake, 1996). Cultures of *P. fluorescens* LP6a mutants were incubated to high density in Tryptic Soy Broth (Difco; typically 200 mL) containing kanamycin (to maintain the transposon) at 30°C with agitation for 24 h. Enzymatic activity was specifically induced with salicylic acid (Yen and Serdar, 1988), and the cells were harvested by centrifugation and resuspension in 3 mM potassium phosphate buffer (pH 7). The protein content of biocatalyst suspensions was determined using the biocinchoninic acid assay (Pierce, Rockford IL).

Substrates and middle distillates

Seventeen aromatic compounds including naphthalene and its methyl-, ethyl- and dimethyl-substituted homologues, phenanthrene and dibenzothiophene (DBT) have been tested for ring cleavage with the chosen mutant 21-41 (Foght et al. 1997). Selected aromatic model compounds were dissolved in the aliphatic carriers *n*-hexadecane or heptamethylnonane (HMN; Efroymson and Alexander 1991) to provide a two-phase system referred to as a "synthetic distillate," or presented directly in authentic distillates. A brief description of the distillates used in this study is summarized in Table 1. The substrate solution was then added to the suspension of induced biocatalyst and incubated for 24 h to effect biotransformation of the substrates. Parallel sterile controls were also prepared.

Table 1. Brief description of authentic distillates used in this study

SOURCE	TYPE	Boiling point range	S content * (mol% of cut)
3HPP0015	Middle distillate	177-343°C	0.118
3HPP0016	Middle distillate	177-343°C	0.319
3HPP0017	Middle distillate	177-343°C	0.407
3HPP0018	Middle distillate	177-343°C	0.359
E #1	Distillate cut	177-343°C	NA
LCGO	Gas oil	NA	NA

* the 3HPP series was subjected to various hydrogenation conditions; elemental analyses were performed, with only the sulfur content reported here.
NA = not available

Radioactive and chemical analysis

To determine the biotransformation of the aromatic compounds quantitatively, ^{14}C-labeled phenanthrene (Amersham) was incorporated into synthetic and authentic distillates and incubated with the biocatalyst as described above. A two-step extraction procedure was used to extract and recover the radioactivity. First, unaltered non-polar substrates and distillates were recovered by extraction with pentane in the presence of the cells at neutral pH. Second, after the cells had been removed by centrifugation and the supernatant acidified to pH < 2, ethyl acetate was used to recover the polar ring fission products. Radioactivity was measured by liquid scintillation (Beckman model LS 3801) and the ratio of radiolabel recovered from the polar phase to that of total added was calculated as the percent converted to polar metabolites ("biotransformation percentage").

Similar extraction procedures were applied to the incubated cultures in quantitative GC experiments. Phenanthrene was usually used as the model substrate and biphenyl and benzothiophene were added as the internal standards to determine the relative residual mass of the model substrate in the pentane extracts. The biotransformation percentage was determined by comparing the relative residual mass of the model substrate incubated with the biocatalyst with that of the model compound in a parallel sterile control.

A silica gel column fractionation technique (Fedorak and Westlake 1981) was used to characterize the composition of the authentic distillates. The saturates and aromatics fractions were studied in detail to determine their susceptibility to microbial transformation by the biocatalyst compared with the whole distillate. Routine GC analysis of fractions and distillates was performed on a Hewlett-Packard model 5890 GC system equipped with a FID and a sulfur-selective flame photometric ionization detector. Chromatography conditions have been described previously (Foght and Westlake 1996).

RESULTS AND DISCUSSION

Radiometric determination of substrate biotransformation

Radiolabeled phenanthrene was incorporated into an aliphatic carrier or an authentic distillate to serve as a surrogate substrate for biotransformation. The radioactivity of the corresponding extracts was measured by liquid scintillation and the total recovery of the radiolabel and the conversion percentage were calculated. In this way, conversion of a specific compound can be monitored in the context of a complex mixture of substrates. Results are shown in Table 2.

Table 2. Transformation of [9-^{14}C]-phenanthrene presented in a hydrocarbon carrier: synthetic or authentic distillates or fractions of authentic disillates. Percent biotransformation is the fraction of added radiolabel recovered from the polar phase. Total recovery is expressed as a percentage of the radiolabel added.

	Radioactivity	
Presentation of ^{14}C-phenanthrene in:	**% biotransformed**	**% recovery**
Heptamethylnonane (HMN)	80	100
Mixture of HMN and the aromatics fraction of 3HPP0015 (2:1 V/V)	76	90
Aromatics fraction of 3HPP0015	68	91
Saturates fraction of 3HPP0015	72	91
Whole authentic distillate 3HPP0015	16	99
Whole authentic distillate 3HPP0016	58	102

The total recovery of the radiolabel was ≥90% for all experiments. Biotransformation of phenanthrene in HMN and the individual distillate fractions was relatively high, but biotransformation was substantially lower for whole 3HPP0015 than for whole 3HPP0016; the reason for this observation is unknown at present.

Gas chromatographic quantitation of biotransformation

In general, biotransformation levels of >80% can be obtained either for pure phenanthrene or phenanthrene presented in a synthetic distillate, and quantitation by GC is relatively easy because of the simplicity of the samples. However, quantitative GC analysis in the presence of the authentic distillates is difficult, with the results being semi-quantitative due to the complexity of the substrates.

A silica gel column fractionation technique was used to gravimetrically determine the composition of selected distillates (Table 3). Some fractions then were used as carriers for presentation of radiolabeled or unlabeled phenanthrene to investigate whether specific fractions or the whole distillate were inhibitory to biocatalysis. Biotransformation was analyzed radiometrically or by GC as reported in Table 4.

It can be seen from Table 4 that distillate saturates fractions did not inhibit biotransformation of phenanthrene. The saturates fractions were not oxidized by the biocatalyst, as determined by GC analysis (data not shown). However, certain aromatics fractions, especially the aromatics fraction of LCGO, had an inhibitory effect on phenanthrene bioconversion. The aromatics in the authentic distillates may compete with the analyte substrate (phenanthrene) for enzyme activity, or may inhibit the conversion of phenanthrene through toxicity to the biocatalyst directly or via their metabolites. Alternatively, inhibition may be a reflection of poor mass transfer during the biotransformation process.

Table 3. Fraction composition of selected distillates, prepared by silica gel column fractionation; mean ± 1 standard deviation, n=2

Distillate	Distillate composition (weight % of fraction)			
	Saturates	Aromatics	Polar	Asphaltenes
3HPP0015	55.4 ± 4.7	26.2 ± 2.2	0.80 ± 0	0.5 ± 0.4
3HPP0016	41.2 ± 2.6	41.2 ± 4.8	2.2 ± 0.6	ND
3HPP0018	59.7 ± 0.4	33.3 ± 0.1	1.2 ± 0.3	ND
E #1	59.0 ± 2.9	27.2 ± 1.6	6.2 + 0.6	ND
LCGO	36.4 ± 3.7	55.5 ± 3.5	5.4 ± 0.2	ND

ND = not determined

Table 4. Summary of biotransformation of phenanthrene presented in different carriers and incubated under standard conditions. Fractions were obtained by silica gel column chromatography of the authentic distillates listed in Table 3. The biotransformation percentage was determined either radiometrically or by quantitative GC, compared with parallel sterile controls.

Distillate	Presentation of phenanthrene in:	% Biotransformation	Analytical method
3HPP0015	Saturates fraction	72	Radiometric
	Aromatics fraction	76	Radiometric
	Whole distillate	36	GC-FID
3HPP0016	Whole distillate	60	GC-FID
E #1	Saturates fraction	74	GC-FID
	Aromatics fraction	64	GC-FID
	Whole distillate	62	GC-FID
LCGO	Saturates fraction	94	GC-FID
	Aromatics fraction	43	Radiometric
	Whole distillate	53	GC-FID

To distinguish among these possibilities, experiments were designed to elucidate limiting factor(s), using phenanthrene presented in the aromatics fraction of LCGO, an inhibitory carrier. In the first experiment, replicate samples of biocatalyst were suspended in different volumes of phosphate buffer to yield cell suspensions covering a 10-fold range of biomass density (measured as mg protein per ml suspension). To these suspensions, a constant volume of carrier containing 8.9 mg of phenanthrene was added, so that the only variable among tests was the biomass density. Biotransformation of the phenanthrene was calculated in either absolute units (percentage of phenanthrene biotransformed) or specific units, obtained by dividing the absolute units by the biomass density. Results are shown in Figure 1.

If the inhibitory effect of the carrier was due to competition for enzyme activity between phenanthrene and alternate substrates in the carrier, a constant specific % biotransformation would have resulted (i.e. a horizontal line) because the ratio of phenanthrene to the carrier was constant in the flasks and the same total biomass was present in all flasks. The results in Figure 1 are best explained if toxicity is the predominant inhibitory factor, because increasing biotransformation was observed as the volume ratio of cell suspension to carrier increased. That is, with increasing biocatalyst suspension volumes, the concentration of toxic compounds would decrease regardlessof whether these toxic compounds were the parent aromatics or their metabolites.

Figure 1. Specific biotransformation (% biotransformation of phenanthrene per mg biomass protein per ml biocatalyst suspension) as a function of the volume ratio of biocatalyst suspension to carrier. Phenanthrene was presented in the aromatics fraction of LCGO and measured by quantitative GC-FID.

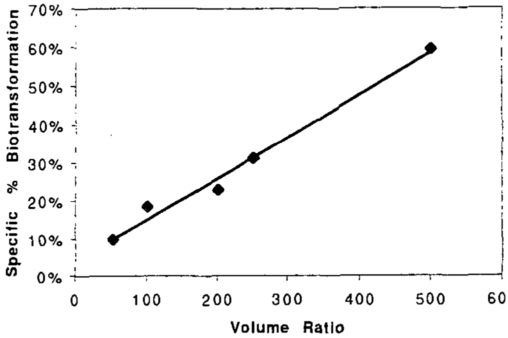

In the second set of experiments, the biomass density was varied over a 10-fold range by resuspending different amounts of biocatalyst in a constant volume of phosphate buffer, keeping the phenanthrene concentration and carrier volume constant. That is, the volume ratio of cell suspension to carrier was kept constant with only the biomass density varying. Phenanthrene bioconversion is presented in Figure 2 both as the absolute % biotransformation in a flask and as the specific % biotransformation, calculated per mg biomass protein. These values were plotted against the relative biomass density, with 1.0 being the cell density of an overnight culture and 0.1 being one-tenth this cell density.

Figure 2. Absolute % biotransformation of phenanthrene and specific % biotransformation of phenanthrene as a function of the relative biomass density, with 1.0 being the biomass density of an overnight culture. Phenanthrene was presented in the aromatics fraction of LCGO and measured by quantitative GC-FID.

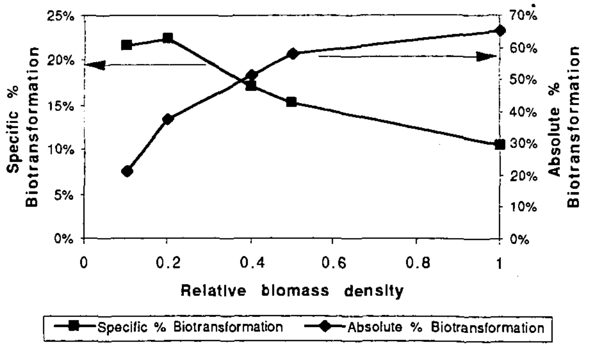

The absolute % biotransformation increased as the biomass density increased. This is as predicted, because the total amount of phenanthrene converted to polar metabolites should be greater if more cells are present. This biotransformation begins to plateau at about 60% when the relative biomass is approximately 1.0. In contrast, the "efficiency" of biocatalyst activity, calculated as specific % biotransformation, decreased above a relative biomass density of 0.2. That is, as the cell density increased, the biotransformation activity per mg biomass protein decreased. This may be due to mass transfer effects as the substrate has less access to individual cells due to "crowding" of the biocatalyst in suspension, or due to limitation of oxygen diffusion in the suspension, or it may be due to increased accumulation of toxic metabolites by the increased mass of cells. We cannot discriminate among these possibilities at present, although mass transfer seems unlikely to be a significant factor at the relatively low cell densities used in these experiments, and it seems unlikely that oxygen is limited under the fairly vigorous aeration conditions provided in the flasks (200 rpm agitation).

Figure 3. Relative rates of DBT ring cleavage at increasing incubation temperatures, normalized to enzyme activity at 30°C.

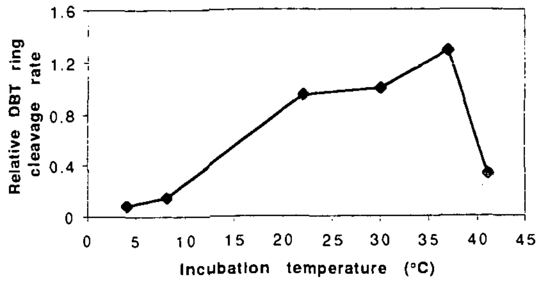

The effect of incubation temperature on biocatalysis was determined at six temperatures by incubating replicate batches of biocatalyst with DBT, a heterocyclic aromatic substrate. Rates of DBT ring cleavage were calculated spectrophotometrically (Foght et al. 1997) as Absorbance Units at 475 nm (the maximum absorption wavelength for the DBT ring cleavage product) produced per min incubation. Rates were normalized to the rate at 30°C as the indicator of relative enzyme activity, as shown in Figure 3. The ring cleavage rate increased with temperature, reaching maximum activity around 37°C, typical for a mesophilic bacterium like *P. fluorescens* LP6a.

CONCLUSIONS

- *P. fluorescens* LP6a biocatalyzes ring cleavage of the substrate phenanthrene when presented in several water-immiscible carriers including heptamethylnonane, various whole authentic distillates, and the saturates and aromatics fractions of those authentic distillates.
- Greater than 80% of the substrate can be biotransformed by the biocatalyst into polar ring cleavage products within a 24-h contact period.
- Ring cleavage activity is influenced by toxicity of some component(s) of the authentic distillates or their metabolites, particularly in the aromatics fraction. This knowledge may lead to general rules of distillate susceptibility to ring cleavage biocatalysis.
- Ring cleavage activity is influenced by temperature, with an optimum of ca. 37°C

ACKNOWLEDGMENTS

Grateful acknowledgment is made of funding from Texaco Group, Inc., Imperial Oil Resources Ltd., the National Centre for Upgrading Technology (Canada), and the Natural Sciences and Engineering Research Council of Canada (Collaborative Research & Development Program).

REFERENCES

FOGHT, J. M., WU, Q., FEDORAK, P., PICKARD, M. and GRAY, M., *Proceedings of BIOMINET/NCUT Symposium at the 48th Annual Technical Meeting of the Petroleum Society*, June 9, 1997

FOGHT, J. M. and D. W. S. WESTLAKE, *Biodegradation* Vol. 7, pp. 353-366, 1996.

YEN, K. M. and C. M. SERDAR, *Critical Reviews in Microbiology* Vol. 15, pp. 247-268, 1988.

EFROYMSON, R. A. and M. ALEXANDER, *Applied and Environmental Microbiology* Vol. 57, pp. 1441-1447, 1991.

FEDORAK, P. M. and D. W. S. WESTLAKE, *Canadian Journal of Microbiology* Vol. 27, pp. 432-443, 1981.

USE OF A DISPERSED IRON CATALYST FOR UPGRADING EXTRA-HEAVY CRUDE OIL USING METHANE AS SOURCE OF HYDROGEN.

Cesar Ovalles, Eduardo Filgueiras, Alfredo Morales, PDVSA-INTEVEP, Apdo. 76343,
Caracas 1070A, Venezuela.
Carlos E. Scott, Centro de Catálisis, Petróleo y Petroquímica. Facultad de Ciencias,
Universidad Central de Venezuela, Apdo. 47102, Caracas 1040A, Venezuela.
Fernando Gonzalez-Gimenez, B. Pierre Embaid, Depto. de Fisica, Ciencias, UCV, Apdo.
47586, Caracas 1041A, Venezuela.

Key Words: Extra-heavy Crude Oil, Upgrading, dispersed iron catalyst

INTRODUCTION

The use of natural gas (methane) as hydrogen source for the upgrading of extra-heavy crude oil [1-6] and coal [7-15] has been the subject of numerous studies during the last few years. In this particular, the reaction of Hamaca crude oil (°API = 8.3) under thermal conditions (380°C, 11.0 MPa of CH_4 for 4 hours residence time) and in the presence of water as additive, led to a decrease of two orders of magnitude in the viscosity of the upgraded product (from 500 to 1.99 Pa s at 30°C), conversion of the >540°C fraction of 60%, and 11.3% of reduction of sulfur with respect to the original crude [1-3]. By ^1H- and 2D-NMR analysis, the most probable pathway is a free-radical mechanism, which involves incorporation of methane via production of methyl radicals [3].

Using an alumina supported molybdenum-nickel catalyst and at similar conversion of the >540°C fraction, a relatively higher percentage of desulfurization (28%) and lower percentage of asphaltenes (9.3%) was obtained than those found in thermal reaction (11% and 11.8%, respectively) [1, 4]. These results indicate that methane can be catalytically activated and used for upgrading of extra-heavy crude oil. Furthermore, using a dispersed molybdenum catalyst, derived from $MoO_2(acac)_2$ (where acac = acetyl-acetonate) and by carbon isotope ratio mass spectrometry analysis, labeled methane ($^{13}CH_4$) was found to incorporate into the crude oil (estimated value 0.01% w/w) giving conclusive evidence on the involvement of CH_4 in the extra-heavy crude oil upgrading process [5-6].

In this work, we studied the use of an iron dispersed catalyst, derived from $Fe_3(CO)_{12}$ for extra-heavy crude oil upgrading using methane as source of hydrogen. The iron catalyst was isolated from the coke produced from the upgrading reaction and was analyzed by XPS, EDAX, and Mössbauer Spectroscopy. Also, the characterization of the products by ^1H-RMN were carried out in order to understand the methane activation processes that are occurring during the crude oil upgrading reactions.

EXPERIMENTAL

The crude oil employed in this work came from the Hamaca oil field in the Orinoco Belt and its analysis is as follows: API Gravity at 15.6°C = 8.7, Water (% w/w) = <1, H/C wt. Ratio = 0.115, Sulphur (% w/w) = 3.40, Nickel (ppm) = 91.9, Vanadium (ppm) = 412, Asphaltenes (% w/w) = 12.5, % of Residue (500^{+}°C) = 57%, Viscosity at 30°C (Pa s) = 500. The upgrading reactions were carried out batchwise in a stainless-steel 300 ml Parr reactor with 250 ppm of Fe at a temperature of 410-420°C, a pressure of 11 MPa of CH_4 and a residence time of one hour as described elsewhere [5-6].

The percentages of volatile material were determined by the method reported by Ceballo and coworkers using a Hewlet-Packard gas-chromatograph, model 5880 [16]. The percentage of conversion of the residue >500°C was defined elsewhere [3,5-6]. X-ray Photoelectron Spectroscopic (XPS) experiments were carried out in using a Leybold-Heraeus Surface Analysis System which was operated with an aluminium anode (1486.6 eV). Pass energy was set at a constant value of 50 eV and the data acquisition and manipulation were performed using a 486 IBM compatible computer. The instrument sensitivity factors used for scaling the photoelectron peak areas were calculated using the method reported by Leon and Carrazza [17]. The Mössbauer spectroscopy was carried out at room temperature, with a constant acceleration spectrometer, in the triangular symmetric mode for the velocity. The source was a ^{57}Co in palladium.

RESULTS AND DISCUSSION

The reaction of Hamaca extra-heavy crude oil (Table 1) at 11 MPa of methane and 410°C for 1 h (Table 1, control run) led to a reduction of two order of magnitude in the viscosity (from 500 to 2 Pa s), 10% of reduction in sulfur content and 41% conversion of the >500°C fraction in the upgraded product with respect to the original crude. Analogous reaction carried out in the presence of $Fe_3(CO)_{12}$ as dispersed catalyst (Table 1, run 1) yielded a product with further reduction in the viscosity (1.3 Pa s), higher reduction in sulfur content (14%) and similar value of conversion of the heavy fraction (40%). Additionally in the presence of the catalyst, a slightly reduction of coke formation (from 7.7 to 6.9%) was observed in comparison with the control experiment. These results indicate that the presence of the iron catalyst is necessary in order to enhance the upgrading of extra-heavy crude oil in the presence of methane

A reaction carried out in an inert argon atmosphere (Table 1, run 2) yielded a product with higher viscosity (2.7 Pa s), less reduction of sulfur content (8%) and lower conversion of the >500°C fraction (36%) with respect to the methane containing experiment (Table 1, run 1). These results indicate that methane is involved, as a source of hydrogen, in the upgrading reaction and that it can be activated by the metal catalyst.

An experiment (Table 2, run 3) conducted under hydrogen atmosphere afforded an upgraded product with slightly better properties (1.2 Pa s, 22% HDS, 40% conversion of >500°C fraction and 5% coke) than those obtained under methane (run 1) and argon (run 2) atmospheres. Thus, the order of reactivity is $H_2 > CH_4 > N_2$ as found by Ovalles *et al.* [3] and Sundaran [7] for thermally activated processes. Also, similar order of reactivity was reported by Egiebor and Gray in their iron catalyzed coal liquefaction experiments [9] and Ovalles *et al.* for $Mo\text{-}Ni/Al_2O_3$ catalyzed extra-heavy crude oil upgrading [4, 6].

From the methane upgrading reaction using $Fe_3(CO)_{12}$ as dispersed catalyst, the coke formed was characterized by EDAX, XPS and electron microscopy. X-ray diffraction and XPS analyses (after 1 h etching with Ar^+ ions) showed the presence of iron and sulfur.

Furthermore, the binding energy for the Fe 2p3/2 was found (Table 2) at 707.4 eV and can be assigned to Fe^{+2} according to the data reported in the literature [18]. Additionally, a sulfur species detected in the S2p region at 161.3 eV, which can be assigned to S^{-2} [19].

The ratio of the atomic percentages of Fe^{+2} (0.54) and S^{-2} (1.31) is 0.53, which is lower than that (1.1-1.4) reported by Reucroft and coworkers [19].To determine which type of Fe compound was present, a Mössbauer study was undertaken. The recorded spectrum is shown in Fig. 1A with the continuous line representing the result of a computer adjustment, which included, apart IS (Isomer Shift), FWHM and QS (quadrupole splitting), a hyperfine field distribution whose histogram is also shown in Fig.1B. Due to the small concentration of iron, the spectrum has a rather poor statistics, however the histogram obtained indicates the unambiguous presence of an Fe and V mixed sulfide, when compared with the spectra obtained in the systematic study of those sulfides [20-22]. According to the previous results, the composition of the present mixed sulfide should be near: $(Fe_{0.6}V_{0.4})_z$ S, where z is in the range of 0.8-0.9 .

The formation of the Fe-V mixed sulfide is certainly achieved *in situ*, by decomposition of the iron carbonyl ($Fe_3(CO)_{12}$) and subsequently the reaction of sulfur and vanadium coming from the feedstock [23]. A very similar mechanism, which demonstrated the appearance of those mixed-sulfides as the active phases, has been put in evidence in HDM reactions [24-25] undertaken with clay catalysts (the precursor is Fe_2O_3) acting on a Pao-X1 heavy crude from the Orinoco belt.

In order to gain mechanistic information, H-NMR analyses were carried out to the upgraded crude oil and the results are shown in Table 3. For $Fe_3(CO)_{12}$ soluble catalyst, an increase (17.2%) in the amount of α-hydrogen bonded to aromatic rings was observed in comparison with those observed for the control run (14.7%) and for the crude oil (15.5%). Similar catalytic runs carried out under argon and hydrogen atmospheres and $Fe_3(CO)_{12}$ led to lower amount of α-hydrogen bonded to aromatic rings (16 and 15 % for Ar- and H_2-containing experiments, respectively) than that found in the CH_4-containing experiment (17%).

Furthermore, an intense aromatization occurred for all the upgrading reactions as shown by the increase in the percentages of aromatic protons from 5.1% in the original crude to approximately 10% for runs 1-3. These results can be rationalized by incorporation of the methyl groups (or, in general, CH_x species where x = 1, 2, or 3) to the crude oil molecules, as shown in eq. 1 [6].

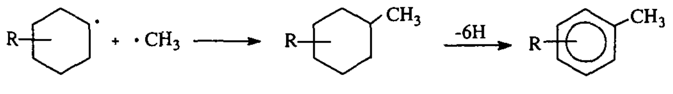
(1)

Where R = hydrocarbon (aliphatic or aromatic)

Naphtenic radicals shown in eq. 1 can be generated by either thermal or catalytic breaking of C-H bond under the reaction temperature (410°C). Egiebor and Gray found methyl and dimethyl products by GC analysis of the donor solvent (tetralin), which was attributed to direct alkylation by reaction with methane in their iron catalyzed coal liquefaction experiments [9]. Also, similar results were obtained previously for extra-heavy crude oil upgrading under thermal [3] and catalytic conditions [6]. The incorporation of CH_x species, coming from methane, into the crude oil molecules was confirmed by isotopic carbon distribution measurements ($^{13}C/^{12}C$) using $^{13}CH_4$ as a source of hydrogen [6].

REFERENCES

1) Ovalles, C.; Hamana, A., Bolivar, R. and Morales, A., U. S. Patent 5,269,909 **1993**.
2) Ovalles, C.; Arias E. S., Hamana, A.; Badell, C. B. and Gonzalez, G., *ACS Fuel Chem. Preprints* **1994**, 39: 973.
3) Ovalles, C.; Hamana, A., Rojas, I. and Bolivar, R., *Fuel* **1995**, 74, 1162.
4) Ovalles, C.; Hamana, A., Bolivar, R. and Morales, A. Proceeding X Conference of UNITAR, Houston , Texas, Feb. 1995.
5) Morales, A., Salazar, A., Ovalles, C. and Filgueiras, E., Procedings 11th International Congress. Catalysis-40th Anniversary. Studies in Surface and Catalysis, J. W. Hightower, E. Iglesia and A. T. Bell (Eds.), **101**, 1215 (1996).
6) Ovalles, C., Filgueiras, E., Morales, A., Rojas, I., de Jesus, J. C. and Berrios, I., to be published in Energy & Fuels.
7) Sundaram, M. U.S. Patent 4,687,570 (1987). b) Sundaram, M. and Steinberg, M. *ACS Fuel Chem. Preprints*, **1986**, 28: 77.
8) Steinberg, M., *Int. J. Hydrogen Energy* **1986**, 11: 715.
9) Egiebor, N. O., Gray, M. R., *Fuel* **1990**, 69: 1276.
10) Qin, Z. and Maier, W. F. *Energy & Fuels* **1994**, 8, 1033.
11) Maier, W. F. and Franke, R. *Fuel* **1994**, 73, 5.
12) Steinberg, M. and Fallon, P. T. *Hydrocarbon Process* 1982, Nov, 92.
13) Calkins, W. H. and Bonifaz, C. *Fuel* **1984**, 63, 1716.
14) Braekman-Danheux, C.; Cypres, R.; Fontana, A. and van Hoegaerden, M. *Fuel* **1995**, 74, 17.
15) Yang, K., Batts, B. D., Wilson, M. A., Gorbaty, M. L., Maa, P. S., Long, M. A., He, S. X., Atalla, M. I., *Fuel* **1997**, 76, 1105.
16) Ceballo, C. D., Bellet, A., Aranguren, S., Herrera, M., *Rev. Tec. INTEVEP*, **1987**, 7, 81.
17) Leon, V., Carrazza, J., *Rev. Tec. INTEVEP* **1989**, 9, 81.
18) Kim, J. Y., Reucroft, P. J., Taghiei, M., Pradhan, V. R., Wender, I., *Energy & Fuels* **1994**, 8, 886.
19) a) Des Marais, D. J., Hayes, J.M., *Anal. Chem.*, **1976**, 48, 1651. b) Gillet, S., Rubini, P., Delpuech, J-J, Escalier, J-C, Valentin, P. *Fuel* **1981**, 60, 221.
20) Embaid, B. F., Gonzalez-Jimenez, F., Scott, C. E., *Hyperfine Interactions* **1994**, 83, 385.
21) Scott, C. E., Embaid, B. P., Luis, M, A., Gonzalez-Jimenez, F., Gengembre, L., Hubaut, R., Grimblot, J., *Bull.Soc.Chim.Belg.*, **1995**, 104, 331.
22) Scott, C.E., Embaid, B.P., Gonzalez-Jimenez, F., Hubaut, R., Grimblot, J., *J. Catalysis*, **1997**, 166, 333.
23) Derbyshire, F. *CHEMTECH* **1990**, 20, 439 and references therein. b) Weller, S. W. *Energy & Fuels* **1994**, 8, 415 and references therein.
24) Gonzalez-Jimenez, F., Constant, H., Iraldi, R., Jaimes, E., Rosa-Brussin, M.. *Hyperfine Interactions*, **1986**, 28, 927.
25) Gonzalez-Jimenez, F., Bazin, D., Dexpert, H., Villain, F., Constant, H. Rosa-Brussin, M., *Physica B*, **1989**, 158, 215.

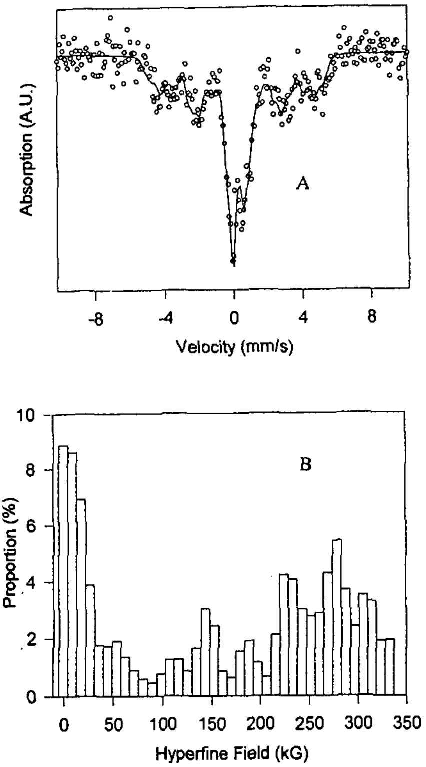

Fig. 1. A) Mössbauer spectrum with the continuous line representing the result of a computer adjustment including, IS (Isomer Shift), FWHM and QS (quadrupole splitting).

Table 1. Upgrading of Extra-Heavy Crude Oil using $Fe_3(CO)_{12}$ as Organometallic Precursor[a]

Run	Gas used	HDS[b] (wt%)	% Conv. >500°C[c]	Viscosity (Pa s)[d]	Coke (wt%)	Gases (wt%)	Liquids (wt%)
Hamaca crude oil	-	(3.40% S)	-	(500)	-	-	-
Control[e]	CH_4	10.0	41	1.99	7.7	4.6	87.7
1	CH_4	14	40.5	1.34	6.9	4.6	88.5
2	Argon	8	35.8	2.77	6.0	3.1	90.9
3	H_2	22	39.7	1.20	5.0	4.5	90.5

[a] The reactions were carried out in a 300-ml batch reactor at 410°C, 250 ppm of Fe, 11 MPa of final pressure for a 1-h period. The results are the average of at least two different reactions. [b] Percentage of desulfurization with respect to the starting crude oil. [c] Percentage of conversion of the residue >500°C as defined in ref. 3, 5-6. [d] Viscosity measured at 30°C. [e] Control experiment, i. e. **no catalyst** was used.

Table 2. Results of the XPS analysis of the coke isolated from upgraded Hamaca crude oil using $Fe_3(CO)_{12}$ as catalyst precursor after 1 h etching with Ar^+ ions[a]

Element	Binding energy (eV)	Atomic %[b]	Assignment[c]	Reference
Fe2p3/2	707.4	0.54	Fe^{+2} as in FeS	18-19
S 2p	161.3	1.31	S^{-2} as in FeS	20
C 1s	284.6	97.24	Adventitous carbon	18-20
O 1s	532.8	0.91	Organic Oxygen	18-20

[a] The reactions were carried out as described in Table 1. The coke was isolated by filtration after diluting the upgraded crude oil in toluene. [b] Atomic percentage on the surface. [c] Most probable assignment according to the published literature.

Table 3. Protons distributions for upgraded Hamaca crude oil measured by ^1H-NMR using $Fe_3(CO)_{12}$ as catalyst precursor[a].

Run	Gas used	H_{arom}[b]	H_{aliph}[c]	H_α[d]	H_β[e]	H_γ[f]
Hamaca crude oil	-	5.1	94.9	14.7	56.2	24.0
Control[g]	CH_4	9.0	91.0	15.5	52.0	23.5
1	CH_4	8.4	91.6	17.2	51.2	23.0
2	*Argon*	8.9	91.1	16.2	51.3	23.3
3	H_2	8.7	91.3	15.2	51.5	24.6

[a] The reactions were carried out as described in Table 1. [b] H_{arom} = Hydrogen bonded to aromatic carbons. [c] H_{ali} = Hydrogen bonded to aliphatic carbons. [d] H_α = Hydrogen bonded to aliphatic carbons in α position to an aromatic ring. [e] H_β = Hydrogen bonded to aliphatic carbons in β position to an aromatic ring. [f] $H\gamma$ = Hydrogen bonded to aliphatic carbons in γ or more position to an aromatic ring. [g] Control experiment, i. e. ***no catalyst*** was used.

UPGRADING OF ALBERTA HEAVY OILS
BY SUPERACID-CATALYZED HYDROCRACKING

Otto P. Strausz, Thomas W. Mojelsky, John D. Payzant, Department of Chemistry, University of Alberta, Edmonton, AB Canada T6G 2G2;
George A. Olah and G.K. Surya Prakash, Hydrocarbon Research Institute, University of Southern California, Los Angeles, CA 90089-11661.

Keywords: bitumen, asphaltene, hydrocracking, superacid

INTRODUCTION

An alternative to conventional catalytic hydrocracking of tar sand bitumens would be a superacid-catalyzed hydrocracking. Olah *et al.*[1] have shown the superacid HBF_4 to be an excellent catalyst at low temperatures (105–170°C) and hydrogen pressure (500 psi) for the depolymerization/liquefaction of coal. Superacids prepared from anhydrous HF and metal halides (*e.g.* TaF_5)[2] and Lewis acids[3] have also been used for the catalytic hydrocracking of petroleum. However, HBF_4, with activity function[4] $H_0 \sim -16$, offers the unique advantage, in addition to being non-reducible (hence would not oxidize products), of being a gas and readily falling apart to HF and BF_3, thus permitting the corrosive superacid components to be easily removed from the liquefaction/reaction mixture.

In Olah[1] *et al.'s* papers on the superacid treatment of coal, no product analysis data were reported. A study, however, was published on model compounds thought to represent the molecular bridging groups holding coal "monomers" together. Dibenzyl, diphenylmethane and biphenyl (along with their ether and sulfide analogs) were used. Under superacid conditions near quantitative conversions to products such as benzene, toluene, anthracene, p-xylene (phenol, benzenethiol) were obtained in high yields.

The aim of the present exploratory study was to assess the feasibility of employing HBF_4 for the deploymerization/hydrogenation of tar sand bitumens and asphaltenes. The characteristic features of this process can be summarized as follows:

- it involves ionic mechanisms, in contrast to the free radical mechanisms in thermocatalytic cracking and therefore may produce different, possibly more valuable, products than those obtained from the latter reactions;
- the temperature and hydrogen pressure required are much lower than in conventional hydrocracking;
- a gaseous catalyst is free of all the problems associated with solid catalysts (poisoning, core plugging, recovery);
- both HF and BF_3 can be readily separated from the product oil by distillation and recycled;
- neither HF nor BF_3 would cause any oxidative degradation of products; and
- the process is free of fluorine incorporation into products.

EXPERIMENTAL

Hydrocracking was done on 2.0–5.5 g samples of Athabasca or Cold Lake bitumen or asphaltene. Mixtures of the sample with 0–30 mL dry methylcyclohexane were placed in a 250-mL Parr autoclave under a dry nitrogen atmosphere. The autoclave was cooled to –78°C (in a dry ice–acetone bath) and 50-mL anhydrous HF was added. The vessel was closed tightly, warmed to room temperature and 500 psi BF_3 was introduced, followed by 500 psi H_2. Then the autoclave was heated to the desired reaction temperature and maintained at that temperature for 2–24 h. At the conclusion of the reaction, the autoclave was cooled to room temperature, depressurized, opened and the contents quenched with 500-mL ice water. The organic layer was separated and washed several times with a 10% sodium bicarbonate solution to remove traces of acid. The acid-free organic layer was then analyzed by conventional class separation and in some cases by capillary GC–MS, FTIR and ^1H and ^{13}C NMR spectroscopy.

RESULTS AND DISCUSSION

The HBF_4-catalyzed hydrocracking of Athabasca bitumen (5.5 g) was carried out in a 24-h reaction at 170°C using, as in all subsequent experiments, 50-mL HF and 500 psi pressure each, BF_3 and H_2. The reaction yielded 33.0% *n*-pentane solubles, 14.7% CH_2Cl_2 solubles ("asphaltene") and 1.8% CH_2Cl_2 insolubles, indicating the formation of 50.5% volatiles (which were not recovered). This experiment demonstrated the high efficiency of the $HBF_4 + H_2$ superacid system in causing deep-rooted chemical alterations in the bitumen. The extent of the alterations can be appreciated by keeping in mind that in thermocatalytic hydrocracking at 170°C practically no reaction would occur and the yield of volatiles would be only a few percent.

In previous studies on coal liquefaction Olah *et al.*[1] used methylcyclohexane (MCH) as a solvent and hydrogen transfer agent thought to facilitate the process. For this reason, in a series of experiments the effect of added MCH on the hydrocracking of Athabasca bitumen and asphaltene was next examined. The percentage recoveries of bitumen, maltene and asphaltene from the reactions are presented in Figure 1 and Table 1. The data show that under the reaction conditions indicated in Table 1, increasing the volume of added MCH increases the yield of recovered products, bitumen, maltene and asphaltene. The only exception is the asphaltene from the hydrocracking of asphaltene with 30-mL MCH. Total product yields above ~20-mL MCH exceed the amount of the initial feedstock from both bitumen and asphaltene and rapidly rise with further amounts of MCH. Thus, it is clear that the excess amount of products must be coming from the reactions of added MCH. Since neat MCH does not appear to react under similar reaction conditions, it must be concluded that the intermediates in the HBF_4-catalyzed hydrocracking of bitumen or asphaltene serve as initiators of the decomposition of MCH. At less than 5 mL, MCH does not appear to decompose or affect the hydrocracking of the bitumen or asphaltene feedstocks, except perhaps by the suppression of the small amount (1.8%) of coke which forms in long reactions. Five-mL MCH in short runs (≤ 2 h) and 30-mL MCH in long runs (24 h) suppressed formation of coke. Product yields with 5-mL MCH are about the same as without MCH.

Table 1. Superacid Treatment of Athabasca (Suncor Coker Feed) Bitumen and Asphaltene. Effect of the Quantity of Added MCH.

MCH (mL)	Asphaltene		Maltene	
	% recovered	% of starting material	% recovered	% of starting material
Bitumen				
5	18.5	8.1	81.5	35.7
15	13.1	9.4	86.9	62.3
30	5.8	11.7	94.2	191.6
Asphaltene				
5	57.1	44.6	42.9	33.5
15	54.6	49.2	45.3	40.8
30	19.1	38.4	80.9	161.6

[a] 500 psi H_2, 500 psi BF_3, 50-mL HF, 1 h, 190°C, reactor volume 250 mL, sample size 2.5–3.1 g. [b] The asphaltene content of the bitumen was 15.5%.

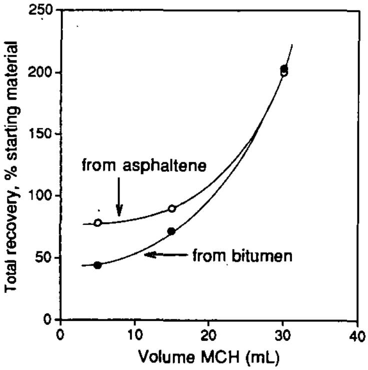

Figure 1. Product (bitumen) yields as a function of added MCH

The low yield of recovered products, Figure 1, in the reactions with 5-mL added MCH represents high conversions to volatiles, 56% from bitumen and 22% from asphaltene. At the same temperature, 190°C and 1-h reaction time, practically no decomposition takes place. With asphaltene, along with the volatiles, 30% conversion to *n*-pentane solubles also occurred. The results obtained from experiments with added MCH further validate the result obtained in the neat bitumen hydrocracking reaction.

Before progressing further, it is noted here that in the early stages of the investigations considerable difficulties were experienced with the lack of reproducibility. Moreover, it was noted that the maltene product—espeially from the asphaltene reactions with added MCH—was highly reactive and upon exposure to air it reacted with oxygen, transforming the colorless mobile liquid oil to a translucent gum. This observation suggested that conjugated alkenes may have been produced, providing a possible explanation for the lack of reproducibility. Next, it was found that the fresh maltene product from the hydrocracking of Cold Lake bitumen contained no oxygen, but after two days' exposure to air the oxygen content was 5.8%.

Comparison of the IR spectra of air-protected and air-exposed samples, Figures 2 and 3, revealed the absence and presence of intense carboxylic (1705 and 3440 cm^{-1}) and possibly alcoholic (1080 cm^{-1}) group absorptions and the presence and absence of conjugated triene absorptions (1500–1700 cm^{-1}). It was also found that the double bonds could be readily brominated. Oxidation with m-chloroperbenzoic acid converted the "saturate" fraction to some polar material in >98% yield, suggesting the absence of any paraffinic hydrocarbons.

Furthermore, the GC of the "saturate" fraction featured two broad humps superimposed by a large number of peaks corresponding to individual compounds. Four of six selected major peaks from GC–MS could be assigned to isomers of a $C_{16}H_{24}$, and the remainign two to some $C_{17}H_{26}$ hydrocarbons. These structures possess five C=C double bond equivalents. Next, in order to determine the number of double bonds in these structures, the "saturate" fraction was subjected to PtO_2-catalyzed hydrogenation which led to chemical changes. It is known that tetra-substituted double bonds are not affected under these conditions.

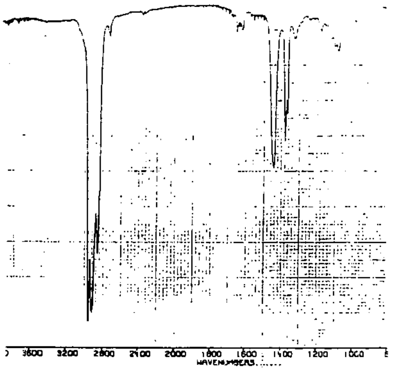

Figure 2. Infrared spectrum of the "saturate" fraction of Cold Lake superacid-treated asphaltene, stored under nitrogen.

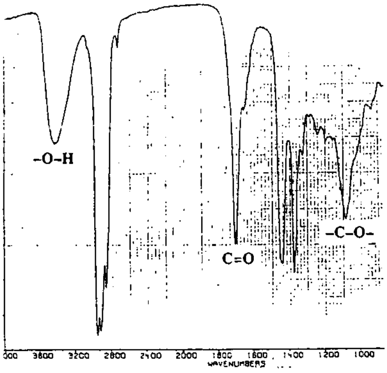

Figure 3. Infrared spectrum of the "saturate" fraction of Cold Lake superacid-treated asphaltene, exposed to air.

The ^1H NMR spectrum of the "saturates" consisted almost entirely of aliphatic hydrogens with a small contribution from alkene hydrogens. The ^{13}C NMR spectrum showed significant signals in the 125–135 ppm range which are due to alkene carbons and from the attached proton test it appeared that the carbons resonating in the 125–135 ppm range had no attached hydrogens. This suggests that, in agreement with the ^1H NMR spectrum, the resonances correspond to tetra-substituted alkenes.

In an attempt to obtain further structural information, the "saturate" fraction was subjected to ionic hydrogenation ($(Et)_3SiH$, CF_3CO_2H, $BF_3{\bullet}Et_2O$, 0°C, 1 h) which, after alumina chromatography, gave ~35% yield of hydrogenated product. GC–MS analysis of this material showed that the $C_{16}H_{24}$ and $C_{17}H_{26}$ compounds in ionic hydrogenation were converted to $C_{16}H_{30}$ and $C_{17}H_{32}$ compounds, both of which contain two saturated rings. Therefore, the original $C_{16}H_{24}$ and $C_{17}H_{26}$ compounds each contained three carbon-carbon double bonds which must have been conjugated in order to account for the high reactivity of these molecules, as manifested by their spontaneous rapid reaction with atmospheric oxygen. Moreover, from the NMR spectra it is clear that the alkene carbons are quaternary. Therefore, we are forced to conclude that under the experimental conditions of the superacid-catalyzed hydrogenation employed, the MCH solvent undergoes ionic rearrangement, degradation and oligomerization. Speculative structures and mechanisms for the formation of the bicyclic conjugated quaternary tri-olefins are shown in Scheme 1.

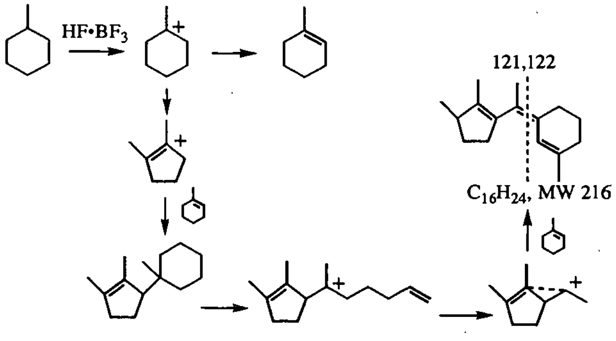

Scheme 1. Superacid-catalyzed solvent polymerization

Most of the peaks in the GC–MS of the "saturate" fraction correspond to molecules with structures analogous to the $C_{16}H_{24}$ and $C_{17}H_{26}$ compounds. Thus, for example, in the chemical ionization GC–MS of the "saturate" fraction three major selected peaks corresponded to isomeric $C_{24}H_{36}$ compounds which would fit the tricyclic conjugated tetra-alkene structure

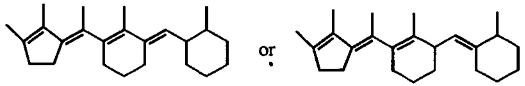

$C_{24}H_{36}$

Thus, the C_{24} compounds appear to be the homologs of the C_{16} and C_{17} compounds having one more MCH ring, with or without an extra carbon atom.

The results from studies on the HBF_4-catalyzed hydrocracking in the presence of MCH point to the general reactivity of the HBF_4 superacid system indicating that acyclic and cyclic hydrocarbons can be attacked. Indeed, the typical gas chromatograms of the saturates from the native bitumens displaying the series of biological markers are altered beyond recognition after the hydrocracking process (suggesting the destruction of cheilanthanes, hopanes, isoprenoids, etc.). Also, the monoaromatic subfraction after hydrocracking appears to be rich in 1-phenyl, 2,2-dimethyl-*n*-alkanes, whereas in the native asphaltene the aromatic-attached alkyl groups are *n*-alkyl, and branched alkyls are hardly present. The appearance of these products is consistent with the known tendency of superacids to catalyze the break-up of alkyl chains and bring about their isomerization to t-butyl structures. Superacids also catalyze the transalkylation of aromatic compounds which, together with the above isomerization reactions, could account for the generation of the branched alkyl products.

SUMMARY AND CONCLUSIONS

- It has been extablished that the superacid HBF_4 is a highly effective catalyst for the hydrocracking of bitumens and asphaltenes even under very mild conditions (170–190°C, 1 h or less);
- The reactions involved proceed with ionic mechanisms as opposed to the free radical mechanisms in thermal hydrocracking, resulting in deep-rooted alterations of the chemical composition of the bitumen, evidenced by the high (56%) conversion of the bitumen to volatiles, the drastic changes in the gas chromatograms of the various compound classes of the bitumen and the appearance of many prominent branched alkylbenzene peaks, etc.
- In asphaltene, parallel to depolymerization some secondary polymerization leading to the formation of asphaltene-like materials takes place upon prolongued reaction times. Therefore, establishing the optimal reaction time is essential to obtain the most favorable conversions.
- Methylcyclohexane exhibits high reactivity with respect to the $HF{\bullet}BF_3$ superacid under the conditions of the bitumen or asphaltene hydrocracking process—typifying the general reactivity of cycloalkanes—resulting in the oligomerization of methylcyclohexane to produce conjugated alkenes; this reaction also reflects some of the possible ways by which the superacid may react with the bitumen or asphaltene since both these materials are known to contain cycloalkane units.
- Fluorine incorporation into the bitumen does not take place and no evidence could be found for catalyst consumption.
- BF_3 is a gas and HF a low-boiling liquid (b.p. 20°); both are highly water-soluble and therefore should be readily separable from the hydrocracked bitumen and recycled for further use. Thus, taking the above results in conjunction with the ready recoverability of the catalyst, it can be concluded that $HF{\bullet}BF_3$ superacid catalysis has considerable potential for commercial application in the bitumen upgrading industry.

ACKNOWLEDGEMENTS

We thank the Alberta Oil Sands Technology and Research Authority for financial assistance.

REFERENCES

1. Olah, G.A.; Bruce, M.R.; Edelson, E.H.; Husain, A. *Fuel* **1984**, *63*, 1130–1137; Olah, G.A.; Husain, A., *Fuel* **1984**, *63*, 1427–1431; Olah, G.A.; Bruce, M.R.; Edelson, E.H.; Husain, A. *Fuel* **1984**, *63*, 1432–1435; Olah, G.A. US Pat. 4,394,247 (1983).
2. Siskin, M.; Wristers, J.P.; Purcelli, J.J., *US Patent 3,901,790* (1975).
3. Ignasiak, T; Bimer, J; Samman, N; Montgomery, D.S.; Strausz, O.P. In *Chemistry of Asphaltenes*, Advances in Chemistry Series 195, Bunger, J.W.; Li, N.C., Eds, American Chemical Society: Washington, D.C., 1981, pp 183–201.
4. Olah, G.A.; Prakash, G.K.S., *Superacids*, J. Wiley & Sons: New York, 1985.

STUDY ON HYDROGEN DONATION ABILITY OF RESIDUE HYDROCRACKING SYSTEM CATALYZED BY OIL-SOLUBLE AND WATER-SOLUBLE CATALYSTS

Zong-Xian Wang, Hong-Yu Zhang, Ai-Jun Guo, and Guo-He Que,
National Heavy Oil Processing Laboratory, University of Petroleum (East China),
Dongying, Shandong 257062, P. R. China

Molybdenum-based oil-soluble and iron-based water-soluble catalyst precursors were separately used in catalytic hydrocracking systems of Liaohe vacuum residue in order to investigate the hydrogen donation ability of mild hydrocracking products. The catalytic hydrocracking tests were conducted in an 100ml autoclave, at 430°C, 30min, 7.0MPa initial hydrogen and 50°C, 500ppm catalysts (based on metal in feed). Anthracene (ANT) was used as a hydrogen acceptor to react, under conditions of 405°C, 2MPa N_2 and 30 minutes, with the atmospheric residue (AR) of hydrocracking products to determine the hydrogen donation ability of the AR. Thus, the hydroaromatic species in the AR might donate active hydrogen to anthracene, which make anthracene change to dihydroanthracene (DHA). GC technique was used to quantify the DHA formation, which was indirectly indicative of the hydrogenation activity of different hydrocracking catalysts. The results showed that Fe-based water-soluble catalysts have little ability to hydrogenate the polycyclic aromatics to hydroaromatics, the hydrogen donors, though they could inhibit coke formation when used in relatively large amount. However, Mo-based oil-soluble catalyst has higher hydrogenation activity, and even could promote hydroaromatics generation. These secondary hydrogen donors could act as a reservoir of active hydrogen and a complement to the active hydrogen molecules activated directly by catalysts in the subsequent hydrocracking stage.

Key words: hydrogen donation, catalytic hydrocracking, vacuum residue

INTRODUCTION

Dispersed metal catalysts used in slurry phase hydrocracking of residue are commonly prepared either by the addition of finely divided inorganic powders to the residue, or by the addition of water- or oil-soluble metal salts to the heavy oils [1-8]. For the same metal, its oil-soluble salts seems more active than its water-soluble salts and its inorganic powders, as its oil-soluble salts can be homogeneously mixed into the heavy oil and can form superfine active catalyst particles after sulfidation [1,5]. For different metals, Mo, Ni, Co, Fe are most commonly used [1-8], of which Mo seems the most active in residue hydrocracking and Fe may be the lowest in their salt prices.

All these catalysts can suppress coke formation during residue hydrocracking by hydrogenating unstable polynuclear aromatic free radicals that are generated thermally [1,3]. Some may be quite active even in very low concentrations (100-200ppm, based on metal to residue), such as oil-soluble Mo-based catalysts [1,5]; some others can counterbalance the total catalytic activity only as in a large amount (1000-50000ppm), such as Fe-based water-soluble or powdered catalysts [1,6,7]. Hence, it seems that there is a little difference in coke suppression mechanism between these two relatively extreme catalysts. The present study uses anthracene (ANT) as a chemical probe to characterize the hydrogen donation ability of residue hydrocracking systems catalyzed respectively by Mo-based oil-soluble and Fe-based water-soluble catalysts. The hydroaromatic species in residue can donate hydrogen to anthracene and make the anthracene mainly change to dihydroanthracene (DHA) [9-12]. The hydrogen donation ability is indicative of inter- or intra-molecular hydrogen transfer between the donors and coke precursors free radicals. The higher is the hydrogen donation, the higher the coke suppression ability.

EXPERIMENTAL

Sample

Liaohe vacuum residue(>500°C) was collected from Liaohe Petrochemical Plant in March 1996. Carlo Erba 1160 elemental analyzer was used for C, H, N analysis; atomic absorption method was used to determine Ni, V, Fe and Ca contents. Average molecular weight was measured by using VPO method (benzene as solvent, 45°C) with Knauer molecular weight analyzer. The general properties of Liaohe vacuum residue are listed in Table 1.

Catalytic hydrocracking of Liaohe vacuum residue

The experiments were carried in a 100ml FDW-01 autoclave reactor with an up-and-down stirrer at 120 times of reciprocation per minute. Initial pressure was 7.0MPa H_2 for catalytic hydrocracking.

Catalyst used in the hydrocracking reaction was Molybdenum-based oil soluble and iron-based water-soluble catalyst (ca.50~1000 ppm based on metal concentration in feed). The former was compatible with the vacuum residue and gave rise to the homogeneous system with the vacuum residue, and the later was emulsified into the vacuum residue to form emulsion system. After sulfidation by elemental sulfur at 320°C for 30 minutes (S/Metal atomic ratio=3/1), these catalyst precursors were in situ reacted to real active catalysts. Then, the temperature was raised to 430°C and kept at the temperature just for 30 minutes for hydrocracking reaction. After that, the reactor was quenched (cooled) to room temperature, the reactor gas was vented, and toluene slurry was prepared from the reactor contents. Any solids adhering to the reactor walls or internals was carefully scraped off. The slurry was then centrifuged and the toluene insoluble (TI or coke) were separated and washed (extracted) with boiling toluene by using quantitative filter paper. The solids were dried and weighed. The toluene soluble was distilled into several fractions. The results were listed in table 2.

Measurement of hydrogen donation abilities of Liaohe vacuum residue hydrocracking products

Anthracene (ANT) was used as a hydrogen acceptor to react, in a 50 cm^3 stainless steel tubular reactor with a 30 cm^3 quartz inner tubular microreactor, with >350°C fraction of the hydrocracking products under 405°C and 2MPa N_2 atmosphere. The feed charge is a mixture of 1-gram oil sample and 2 gram anthracene. Thus, the secondary hydroaromatics in >350°C fraction of hydrocracking products can donate active hydrogen to anthracene, which make anthracene change to 9,10-dihydroanthracene (DHA)[9-12]. The reaction products were analyzed by gas chromatography using a Varian3400 chromatograph equipped with a 30m×2.65um HP-5 (crosslinked 5% Ph Me silicon) column and a FID detector and naphthalene and DHA as the internal standards. The contents of DHA generated in the thermal reaction system were listed in table 3. The quantity of molar hydrogen accepted from one gram of charged oil sample could be calculated by following equation:

$$MN=Y_{DHA}\times W_{mix}/(M_{DHA}\times W_{oil})$$

Here, MN is the moles of hydrogen accepted from 1 gram of oil sample, Y_{DHA} the yield of DHA in the thermal reaction system, W_{mix} the weight of charged mixture of oil and ANT, M_{DHA} the molecular weight of DHN and W_{oil} the weight of charged oil sample. The MN values for different oil samples were also tabulated in table3.

RESULTS AND DISCUSSION

Distribution of hydrocracking products

It seems that the coke formation has a tendency to increase with the Mo-based catalysts at the early stage of Liaohe vacuum residue hydrocracking as indicated in table 2. This coke may largely consist of condensed-asphaltene. Under the induction of polar catalyst particles, the structure of asphaltene micellae may become loose, and asphaltene may be adsorbed by MoS_2 particles (with relatively higher polarity) and may condense on the particles, leading to the formation of toluene insoluble materials, a physically condensed state of asphaltene of higher polarity, not a real chemical coke. The more the MoS_2 catalysts, the stronger the induction to polar asphaltene may be, the more the initial coke will form, but the less the ratio of the coke to MoS_2; and, relatively, the total catalyst activity is still high. The product distribution indicates that with increasing Mo-based catalyst, conversion to VGO seems to increase and the conversion to lighter product decreases, showing an increase in hydrogenation ability.

Hydrogen donation ability of Liaohe vacuum residue and its hydrocracking products

This work aimed at determining the hydrogen donation abilities of Liaohe vacuum residue and its hydrocracking products, VGO(350 - 480°C) and hydrocracked vacuum residues (HVR), processed under different conditions. As table 3 indicated, the Liaohe Atmospheric residue has higher hydrogen-donating ability than its vacuum residue. The hydrogen-donating abilities of thermal cracked products of Liaohe vacuum residue are less than those of its catalytic hydrocracking products, showing that the catalysts could, at least, suppress the cracking of hydrogen-donating species in the residue reaction system. In comparison, Mo-based oil-soluble catalyst could give rise to higher hydrogen-donating abilities of its catalyzed hydrocracking products than Fe-based water-soluble catalyst. It seems that the hydrogen activated by Fe-based catalyst was not enough high to hydrogenate polycyclic aromatics to hydroaromatics, leading to only a little difference in hydrogen-donating abilities between its catalyzed products and thermal cracking products. The Mo-based catalysts might catalyze hydrogenation of some active polycyclic aromatics to hydroaromatics beside its high coke suppression ability by directly catalyzing hydrogenation of polycyclic aromatic free radicals. The hydroaromatics generated in situ could act as hydrogen donors in subsequent reactions. The active hydrogen transfer from the hydrogen donors to polycyclic aromatic free radicals may be easier than the active hydrogen directly activated by the catalysts because the hydroaromatics are more compatible with the free aromatic radicals than the catalysts.

With the increase of Mo-based catalyst, the hydrogen-donating abilities of its catalyzed hydrocracking products increase. As Mo was over 160ppm, the hydrocracked vacuum residues were very near to Liaohe vacuum residue in hydrogen-donating ability. On the basis of one gram of Liaohe vacuum residue, the total hydrogen donations of its catalytically hydrocracked AR were 4.56×10^{-4}, 5.02×10^{-4},6.25×10^{-4}, 6.42×10^{-4}, 7.01×10^{-4}, 7.12×10^{-4}, and 7.14×10^{-4}moles for no catalyst, 470ppm Fe, 74ppm, 86ppm, 168ppm, 316ppm and 619ppm Mo respectively. In comparison to 470ppm Fe, 86ppm Mo could make the AR a net gain of 1.40×10^{-4} moles of hydrogen donation. Except for direct free radical hydrogenation ability of Mo catalyst, the net gain of hydrogen donation ability might play a great role in coke suppression during further hydrocracking process. For example, prolonging hydrocracking time from 30minutes to 1hour could make the coke formation to increase from 1.6% to 5.7% as 470ppm Fe catalyst was used, and make the coke formation to increase from 0.2% to only 1.3% when 86ppm Mo-based catalyst was used.

CONCLUSION

Anthracene was used as a chemical probe to determine the hydrogen donation ability of Liaohe vacuum residue and its mild catalytic hydrocracking products. In comparison to pure thermal cracking, the catalysis of Fe-based water-soluble catalysts was little in promoting the formation or in suppressing the cracking of the hydroaromatics--the secondary hydrogen donors, though Fe catalysts could inhibit coke formation when used in relatively large amount [1]. However, Mo-based oil-soluble catalyst has higher hydrogenation activity, and even could promote hydroaromatics generation in comparison to Fe-based catalyst. These secondary hydrogen donors could act as a reservoir of active hydrogen and a complement to the active hydrogen molecules activated directly by catalysts in the subsequent hydrocracking stage.

ACKNOWLEGEMENT

The authors thank Miss F. Gao and Mr. R-F. Liu for helpful experimental work, and Miss J-X Xing for GC analysis.

REFERENCES

(1)Del Bianco, A., Panariti, N., Di Carlo, S., Elmouchnino, J., Fixari, B. and Le Perchec, P., Applied Catalysis, A: General, 94, 1-16(1993)

(2)Del Bianco, A., Panariti, N., Marchionna, M. Am. Chem. Soc., Preprints, Div. Petrol. 40(4)743-746(1995)

(3)Le Perchec, P., Fixari, B., Vrinta, M., Morel, F., Am. Chem. Soc., Preprints, Div. Petrol. 40(4)747-751(1995)

(4)Bearden, R. and Aldrdge, C. L., Energ. Progress, 1(1-4), 44(1981)

(5)Strausz, O.P., Lown, E.M., Mojesky, T.W., Am. Chem. Soc., Preprints, Div. Petrol. 40(4)741-742(1995)

(6)Liu, C., Zhou, J., Que, G., Liang, W., Zhu,Y., Fuel, 73, 1545-1550(1994)

(7)Smith, K.J., Duangchan, A., Hall, A.G., Am. Chem. Soc., Preprints, Div. Petrol. 42(3)479-483(1997)

(8)Del Bianco, A., Panariti, N., Marchionna, M., Am. Chem. Soc., Preprints, Div. Petrol. 42(3)484-488(1997)

(9)Yokono, T., Marsh, H., Yokono, M., Fuel, 60, 607-611(1981)

(10)Yokono, T., Obara, T., Iyama, S., Sanada, Y., Carbon, 22(6)623-624(1984)

(11)Wang, S.L, Curtis, C.W., Energy & Fuels, 8, 446-454(1994)

(12)Pajak, J., Krebs, V., Mareche, J.F., Furdin, G., Fuel Processing Technology, 48, 73-81(1996)

Table 1 General properties of Liaohe vacuum residue (VR)

Density(20°), g./cm^3	0.9976	SARA fractions:	
Viscosity(100°)/mm^2.s^{-1}	3375	Saturates, %	17.4
Pour point, °C	42	Aromatics, %	30.3
Flash point, °C	312	Resins, %	50.2
Carbon residue, %	19.0	nC7-Asphaltene, %	2.1
Elemental composition		Total Metal/PPM	258.6
C, %	87.0	Ni, ppm	122.6
H, %	11.4	V, ppm	2.9
S, %	0.43	Fe, ppm	37.5
N, %	1.08	Ca, ppm	95.6
H/C(Atomic ratio)	1.50	Ash, %	0.06

Table 2 Effect of catalysts on Liaohe vacuum residue hydroconversion (430°C, 7MPa initial hydrogen pressure, reaction time 30 min.)

Catalyst., ppm	<350°C, %	350-480°C,% (VGO)	>480°C, % (HVR)	Coke, %
none	23.0	22.5	52.7	1.8
Fe, 470	21.5	20.1	56.8	1.6
Mo, 74	14.0	18.0	68.0	0.2
Mo, 86	14.3	17.0	68.5	0.2
Mo, 168	13.4	17.3	69.1	0.2
Mo, 316	13.1	18.4	68.2	0.3
Mo, 619	12.9	20.0	66.6	0.5

Table 3. Hydrogen transfer in thermal reaction system of initial hydrocracking products of Liaohe residue

Oil Sample/ANT (m/m)	DHA generated in thermal reaction system	MN ×10^4
LHVR, (0.2170: 1)	1.32%	8.22
LHAR , (0.1970:1)	1.26%	8.49
VGO(H2), (0.5042:1)	1.99%	6.60
VGO(H2,Fe470), (0.4879:1)	2.13%	7.22
VGO(H2,Mo74), (0.5032:1)	2.39%	7.93
VGO(H_2,Mo86), (0.5058:1)	2.42%	8.00
VGO (H_2,Mo168), (0.5143:1)	2.59%	8.47
VGO (H_2,Mo316), (0.5042:1)	2.75%	9.12
VGO (H_2,Mo619), (0.4938:1)	2.72%	9.14
HVR (H_2) , (0.5073:1)	1.79%	5.91
HVR (H_2,Fe470), (0.5083:1)	1.91%	6.30
HVR (H_2,Mo74), (0.5120:1)	2.16%	7.09
HVR (H_2,Mo86), (0.4742:1)	2.14%	7.39
HVR (H_2,Mo168), (0.5001:1)	2.41%	8.03
HVR (H_2,Mo316), (0.4934:1)	2.37%	7.97
HVR (H_2,Mo619), (0.4945:1)	2.42%	8.12

VGO--350-450°C fraction; HVR--hydrocracked vacuum residue.
LHVR--Liaohe vacuum residue; LHAR--Liaohe atmospheric residue.

Amorphous Microporous Mixed Oxides, New Selective Catalysts with Chemo- and Shape-Selective Properties

Wilhelm F. Maier
Max-Planck-Institut für Kohlenforschung
D-45470 Mülheim an der Ruhr, Germany

The increasing economical and ecological demands on chemical processes have led to a growing need for more selective heterogeneous catalysts. Selectivity based on hindered diffusion of molecules of different polarity or size in micropores, the so called shape selectivity, is key to the success of zeolites [1]. However, fundamental limitations with respect to chemical composition and pore architecture restrict general applications of these catalysts. Amorphous microporous mixed oxides (**AMM**) are promising new materials, whose catalytic properties can be controlled during a one-step preparation procedure of the sol-gel-type. By acid catalyzed co-polycondensation of an alkoxide of Si, Zr, Al or Ti with a soluble derivative of a catalytically active element, such as Mn, Mo, V, Ti, Sn, In, Cu, Fe, Cr, atomically distributed active centers in the oxide matrix can be obtained. In the absence of any template, the reaction conditions followed by drying and calzining provides a highly porous mixed oxide with a narrow pore size distribution around 0.6-0.9 nm. The surface polarity of such an oxide can be controlled by the addition of alkoxides containing a nonhydrolyzable alkylgroup, such a methyltriethoxysilane, to the copolycondensation reaction. The basic reaction for silica based AMM-8materials is shown below:

$$\mathbf{xM(OR)_n + yMeSi(OR)_3 + (RO)_4Si + H_2O \dashrightarrow (MO_{n/2})_x(Me\text{-}Si_{1.5})_ySiO_2 + ROH}$$

catalytic centers	*polarity modifier*	*microporous matrix*	*Amorphous Microporous Mixed oxide (AMM)*

The materials are denoted as AMM-M_xM', where M' stands for the base oxide and x for the atom% of the additional oxide M. After proper calzination, these materials remain amorphous and have a porosity of 10-35%. A typical pore size distribution and a high resolution TEM-micrograph (AMM-Ti_3Si = 3 % titania in 97 % silica) are shown in Figure 1.

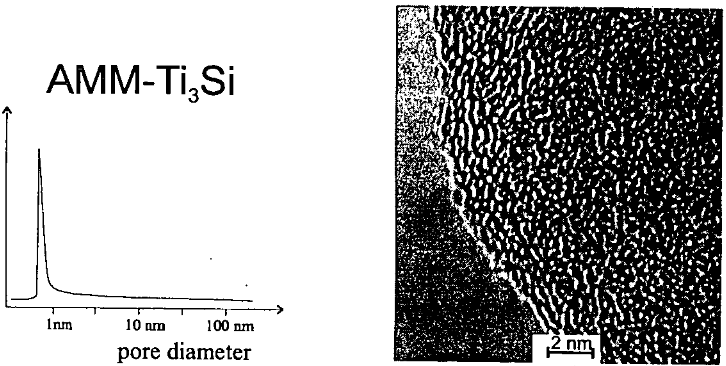

Fig. 1: Pore size distribution (Horvat-Kawazoe-method) and TEM-micrograph of a typical AMM-catalyst.

Rheological studies show a simultaneous increase in elasticity and viscosity under these sol-gel conditions indicative of a linear chain growth in the polycondensation process [2]. The porosity of these amorphous materials has been shown to be stable up to 800 °C. Diffuse reflectance IR, XANES [3] and diffuse reflectance UV [4] provide evidence for homogeneity and atomic isolation of the Ti-centers in AMM-Ti_xSi at Ti-concentrations < 5%. PFG-NMR studies on hydrophobic and hydrophilic AMM-Si-materials with small molecules show diffusion rates comparable to those observed in Y-zeolites. It was found, that the diffusion of unpolar molecules like hydrocarbons is not affected by the surface polarity, while the diffusion of polar molecules like water and butanol is strongly hindered in hydrophilic AMM-Si, while both molecules are not observable in the hydrophobic AMM-$^{Me}Si_xSi$ [5].

In general, AMM-materials can be described as catalysts prepared to contain isolated catalytically active centers in the shape selective environment of micropores. The lack of inherent limitations with respect to chemical composition and pore size makes AMM-materials versatile catalyst for many uses. AMM-materials have already shown promising properties as selective heterogeneous catalysts in a variety of applications:

Hydrocracking: Decane hydrocracking is an established test reaction for the precise assignment of pore structure and pore architecture of zeolites [6]. After impregnation with 0.5 % Pt, **AMM-Ti_3Si**, AMM-$Ti_{17}Si$ and AMM-$V_{10}Si$ have been exposed to the decane hydrocracking test under standard conditions. The product distribution positioned the Ti-containing AMMs in the range of large pore zeolites, while the **AMM-$V_{10}Si$** is positioned in the zeolite free range between the medium-pore 10-ring zeolites and the large pore 12-ring zeolites. The test furthermore identifies the AMM-materials as having a tubular pore system lacking larger cavities and pore intersections [7]. These results showed for the first time shape selective properties of amorphous materials. Therefore shape selective properties are not associated with crystallinity, but only with a small pore size and a narrow pores size distribution.

Redox-catalysis with organic hydroperoxides: With TBHP as oxidizing agent AMM-Ti_3Si catalyzes the selective epoxidation of alkenes. With linear and cyclic olefins, the rate of epoxidation decreases rapidly with increasing number of carbon atoms [7]. A similar decrease in the rate of epoxidation of alkenes with TS-1 has been ascribed to molecular shape selectivity [8]. AMM-V_xSi and AMM-Ti_xSi can selectively oxidatize olefins and saturated hydrocarbons [9]. Like other crystalline and amorphous Ti-silicates the catalysts are deactivated during epoxidation reactions by product inhibition, caused by pore- or surface blocking with the alcohol formed from the hydroperoxide. The catalysts are not active with hydrogen peroxide as oxidant.

Redox-catalysis with hydrogen peroxide: Due to unconnected surface coordination sites highly porous oxides are rich in surface hydroxyl groups and thus highly hydrophilic. By copolycondensation of increasing amounts of $Me\text{-}Si(OEt)_3$ with $Si(OEt)_4$ and 1% $(iPrO)_4Ti$ a series of AMM-materials with increasing hydrophobicity was prepared. The most hydrophobic materials (**AMM-$Ti_1{}^{Me}Si_{45}Si$**) show several interesting properties. The catalysts do not deactivate during epoxidation reactions and they can be reused. They can be used with hydrogen peroxide as oxidant. In fact, with H_2O_2 these hydrophobic amorphous microporous Ti-Si-oxides show comparable activities as Ti-containing zeolites for a wide range of selective oxidation reactions, such as ammoxidation, oxidation of alcohols, and oxidations of saturated hydrocarbons [11].

Acid catalyzed etherification and esterification reactions: Solid acid catalysts are of increasing importance as potential replacement of homogeneous acid catalysts in the production of fine and bulk chemicals. **AMM-Sn_xSi** with low Sn-content have been found to be very active and selective mild acid catalysts. The catalysts are Lewis-acidic, no evidence for Brønstedt acidity was obtained by IR-studies. The catalysts showed excellent catalytic activities for esterification reactions of pentaerythritol with stearic acid and for the formation of t-butylethers [12].

Oxidative dimerization of propene with air: Oxidative coupling of propene with air in the gas phase under selective formation of 1,5-hexadiene has been reported with diene selectivities peaking at 60 % at propene conversions far below 10 %. With **AMM-In_xSi** at 560 °C under continuous gas phase flow conditions propene (23 % conversion) is selectively converted with air to 1,5-hexadiene (selectivity 84 %). The unusual selectivity is attributed to the presence of isolated In-centers (confirmed by EXAFS-studies) in the shape selective environment of the micropores [13]. With **AMM-Cu_6Si** at 370 °C acrolein is formed with a remarkable selectivity of 93 % at a propene conversion of 10 % [14].

Selective Oxidation of toluene to benzaldehyde with air: In a gas phase flow reaction at continuous reaction conditions **AMM-Mn_3Si** selectively oxidizes toluene to benzaldehyde with air (normal pressure, 450 °C, toluene conversion 5 %, selectivity 83 %). EXAFS investigations identify the Mn as isolated centers of oxidation state II [15].

Selective aromatic alkylation: The isopropylation of naphthalene and biphenyl have been investigated with various AMM-catalysts. The **AMM-Al_xSi** materials show the most promising activity. After deactivation of external acid sites, AMM-Al_3Si exhibits highly selective alkylation behaviour. In the gas phase at continuous flow conditions at 250 °C 4,4'-diisopropylbiphenyl is formed directly from biphenyl with a selectivity of 61 % at a biphenyl conversion of over 7 %. At identical reaction conditions a H-Mordenite reaches 73 % selectivity. Isopropylation of naphthalene at unoptimized conditions at a conversion of 46 % produces only mono and diisoproylnaphthalene (ratio 2:1), the latter consists to 44.5 % of the 2,7- and to 50 % of the 2,6-isomer. This shows that AMM-catalysts can be modified to become selective dialkylation catalysts comparable to the best zeolites [16].

Microporous catalyst membranes: Another promising area is the application of catalytic membranes as a means to improve the selectivity of heterogeneously catalyzed reactions. The combination of permselectivity with catalysis opens a new field of reaction engineering and reactor design [17]. Due to the preparation process, which passes through a sol, thin AMM-catalyst films can be prepared by dip-coating [18]. With the use of proper support membranes, thin catalyst membranes have been prepared, characterized and applied in various heterogeneously catalyzed reactions. Poison resistant catalysis has been achieved in the hydrogenation of fatty esters by dosing the hydrogen through a microporous AMM-Pt_3Ti membrane catalyst. Addition of well known poison molecules like tetrahydroacridine or quinoline in equimolar amounts have no effect on the rate of hydrogenation, since the poison molecules are too large to penetrate the micropores of the membrane containing the catalytically active sites [19]. A higher turnover frequency (TOF) in the membrane relative to the batch reactor was noted. In a more detailed study of the rate of hydrogenation of 1-octene in the batch reactor relative to the membrane reactor, this higher TOF could be confirmed. It was shown, that comparable TOFs in the membrane reactor and in the batch reactor are obtained, when the hydrogen is dosed through the liquid sitting on top of the catalyst membrane, while the TOF increases by a factor of 10 when hydrogen is dosed through the catalyst membrane to the alkene containing solution. By competition experiments it is shown, that the normally occurring competitive adsorption of alkene and hydrogen on the Pt-sites does not seem to occur, when hydrogen is dosed through the membrane [20]. In another investigation a new way to prevent secondary reactions has been demonstrated. The basic scheme is to pass a solution of two reactants through a catalytically active microporous membrane. When the pores are so narrow, that molecular passing of reactants is hindered or inhibited during the diffusion through the pores (single file diffusion), secondary reactions cannot take place as long as the concentration of the limiting reactant does not allow a second reaction to ocurr. The action of the micropores is to provide a defined reaction zone and to completely prevent backmixing of the products formed with the reactants. With AMM-Pt_3Ti-membranes at proper reaction conditions 1,3-hexadiene can be hydrogenated selectively to monoenes at conversions of up to 40 %. At 20 % conversion 2-hexyne is selectivively hydrogenated to cis-2-hexene. In both reactions no n-hexane formation is detectable. However, when the hydrogen pressure is increased (increases the hydrogen concentration in the solution and the pores) n-hexane formation occurs. The same AMM-Pt_3Ti-catalysts is completely unselective in the batch reactor at identical reaction conditions [21]. The prevention of back-mixing by microporous catalyst membranes is a new means to avoid secondary reactions.

Clearly, amorphous microporous mixed oxides are a promising class of selective heterogeneous catalysts, ready and waiting for technical applications.

References:

[1] Zeolites and Related Materials: State of the Art 1994, (eds.: J. Weitkamp, H.G. Karge, H. Pfeifer, W. \tab Hölderich), Elsevier, Amsterdam 1994; W. Hölderich, M. Hesse, F. Näumann, Angew. Chem. Int. Ed. 1988, **27**, 226.
[2] Tilgner, I.-C., Fischer, P., Bohnen, F.M., Rehage, H., Maier, W.F., Microporous Materials, **5** (1995) 77.
[3] S. Klein, S. Thorimbert, W.F. Maier, J. Catal.,**163** (1996) 477.
[4] S. Klein, W.F. Maier, B.M. Weckhuysen, J.A. Martens, P.A. Jacobs, J. Catal.,**163** (1996) 489.
[5] C. Krause, S. Klein, J. Kärger, W.F. Maier, Advanced Mat. **8** (1996) 912.
[6] J.A. Martens, P.A. Jacobs, S. Cartlidge, Zeolites 1989, 9 423.
[7] W.F. Maier, S. Klein, J. Martens, J. Heilmann, R. Parton, K. Vercuysse, P.A. Jacobs, Angew. Chem. Int. Ed. **35** (1996) 180.
[8] A. Corma, P. Esteve, A: Martinez, S. Valencia, J. Catal 1995, **152**, 18.
[9] S. Klein, J. Martens, R. Parton, K. Vercuysse, P.A. Jacobs, W.F. Maier, Catal. Lett., **38** (1996) 209.
[10] S. Klein, W.F. Maier, Angew. Chem., 108 (1996) 2376; Int. Ed. 35 (1996) 2330.
[12] S. Storck, W.F. Maier, W. Ben-Mustafa, H. Bretinger, I.M.M. Salvado, J.M. Ferreira, D. Guhl, J.A \tab Martens, W. Souverijns, J. Catal., **172** (1997) 414.
[13] S. Bukeikanova, H. Orzesek, U. Kolb, K. Kühlein, W.F. Maier, Catal.Lett. **50** (1998) 93.
[14] H. Orzesek, PhD-Thesis, University of Essen, Germany, 1998.
[15] F. Konietzni, U. Kolb, U. Dingerdissen, W.F. Maier, J. Catal. in print.
[16] S. Neunerdt, PhD-Thesis, University of Essen, Germany, 1998.
[17] H.P. Hsieh, Catal. Rev. Sci. Eng. **33** (1997) 1.
[18] Maier, W.F.; Tilgner, I.-C-;, Wiedorn, M.; Ko, H.-C.; Ziehfreund, A.; Sell, R. Advanced Materials, **10** (1993) 730.
[19] Maier, W.F.; Ko, H.C. Catal. Today, **25** (1995) 429.
[20] I.-C. Tilgner, C. Lange, H-W. Schmidt, W. F. Maier, CIT, 69 (1997) 1776.
[21] C. Lange, B. Tesche, S. Stork, W. F. Maier, J. Catal. **175** (1998) 280.

THERMAL UPGRADING OF PETROLEUM RESIDS USING POLAR H-DONOR SOLVENTS

Richard Dutta[1], Shona Martin[2], Mark Plummer[3] and Harold H. Schobert[1]

[1]The Energy Institute, Penn State University, University Pk., PA 16802
[2]Dept. of Pure and Applied Chemistry, Univ. of Strathclyde, Glasgow G1 1XL, Scotland, UK
[3]Marathon Oil Co. PO Box 269, Littleton, CO 80180-0269

KEYWORDS: Petroleum resids, hydrogen donor solvents, tetrahydroquinoline

INTRODUCTION

As a novel approach to upgrading petroleum resids it was proposed that experiments should be carried out utilizing polar H-donor solvents (e.g. tetrahydroquinoline (THQ) and indoline) in an effort to increase H/C ratio, increase desulfurization and demetallation, and improve the boiling point distribution to 90% boiling below 1000°F.

The objectives of this project were as follows: 1) To identify potential hydrogen-donating solvents for upgrading petroleum resids. 2) To screen these solvents and compare their effectiveness in improving the boiling point distribution and elemental composition of the resids. 3) Once the initial screening has been done, to fully test one or two of the best solvents in larger batch reactors, to fully analyze the effectiveness of the solvent. 4) To undertake model compound and solvent reactions and modeling to understand the H-transfer efficiency, docking interactions etc.

This paper will discuss the major findings for these objectives and make conclusions as to the potential use of H-donors in upgrading heavy petroleum resids.

EXPERIMENTAL

All reactions were carried out in 25ml microautoclaves and a 300ml batch reactor (Marathon Oil Co.). Petroleum resids were obtained from Marathon Oil and potential solvents were obtained from various chemical companies. In each reaction, a measured amount of resid/pyrene was weighed into the reactor along with a carefully weighed amount of solvent in various wt/wt (or mol/mol) proportions. The reactor was purged twice with nitrogen and pressurized to either 200psi with nitrogen (inert atmosphere) or 500-1500psi hydrogen. The reactor was then lowered into a fluidized sand bath set at a pre-defined temperature (375-450°C) for a pre-determined reaction time (60-180 minutes). After the reaction time had expired, the reactor was removed from the sand bath and immediately quenched in cold water. The reaction products were extracted with THF and hexane to determine conversion of the asphaltene fraction of the resid. The products were analyzed by gas chromatography to determine conversion of the solvent, and simulated-distillation (SIMDIST) to determine the boiling point distribution. Elemental analysis was carried out to determine C, H, and S.

RESULTS AND DISCUSSION

Thermal Cracking of vacuum resid (VR1) using Donor/Non-donor Solvent

In order to stop retrogressive reactions that occur during thermal cracking of resids, several experimental approaches can be undertaken: 1) Use molecular hydrogen to try and cap the reactive radicals which are recombining, 2) Use molecular hydrogen and a catalyst to improve conversion levels, 3) Utilize solvents that can be a source of hydrogen for radical capping and hydrogenation of aromatic rings. In order to assess these approaches, a study into vacuum residue (VR1) upgrading using various donor/non-donor solvents, hydrogen vs. inert atmosphere, and the impact of a catalyst on the reaction, was undertaken. The major results are shown in Figure 1, which gives conversion of asphaltene data and boiling point (by simulated distillation) data (<400°C and <550°C). Use of non-donor solvents (naphthalene, toluene, quinoline) in the reaction leads to retrogressive reactions, similar to those seen when no solvent is used. Tetralin (low polarity H-donor) does give up some hydrogen to cap the reactive radicals but the asphaltene fraction is not converted as much as when THQ (highly polar H-donor) is used. Hydrogen atmosphere does increase conversion of asphaltenes, but the use of a catalyst precursor, ammonium tetrathiomolybdate (ATTM), does not significantly improve the results. Quinoline (polar non-donor) is effective only when ATTM and hydrogen are present. This is due to the hydrogenation of quinoline to THQ which then acts as a donor. This idea of hydrogen shuttling between gas phase hydrogen, quinoline, THQ and the resid molecules will be discussed in detail later in the paper. Figure 1 also shows the effect of increasing THQ concentration of the solvent system on conversion and boiling point distribution. When 100% toluene is used, retrogressive reactions are occurring, leading to a negative conversion of 36%. As THQ is added to the solvent, conversion increases. With 100% THQ, asphaltene conversion increases to +30%.

One of the interesting features of Figure 1 is that there appears to be a relationship between asphaltene conversion and conversion of the resid to <400°C and <550°C material. This can be seen more clearly in Figure 2, where these two parameters are plotted against each other. It can be seen that as the heavier asphaltene molecules are converted to hexane soluble material, the amount of cracking to lower boiling products, decreases. There are some exceptions, which are pointed out in Figure 2 as catalytic reactions. The results suggest that there may be two mechanisms that need to separately addressed when considering upgrading resids. Firstly, thermal cracking of side chains from the multicyclic compounds that make up a large proportion of these resids and cracking of smaller molecules to produce the distillable material, and secondly, hydrogenation and subsequent cracking of large polycyclic macromolecules that make up the asphaltene structure. To convert asphaltene requires hydrogen, which also reduces cracking of smaller compounds due to reactive radical capping. In a real process, it would be necessary to reach a compromise in conversion of asphaltenes and production of distillates. This would depend on the final product requirement. For example, in the case of resids, it may be important to produce a product that can be fed into the FCC for further treatment.

Thermal cracking of ROSE pitch using THQ

After the initial screening studies using VR1, it was decided to switch the initiative of the research to ROSE pitch. This was partly due to the fact that ROSE pitch is more difficult to upgrade and whatever we could achieve with this material we could probably repeat with the vacuum resid. ROSE pitch also contains a larger proportion of asphaltenes which have to be converted in order for the process to work efficiently.

The experimental approach was to determine the effect of temperature and hydrogen pressure on conversion of asphaltenes and cracking of the pitch to distillable products. Table 1 shows boiling point data, asphaltene conversion, solvent conversion and H/C ratio for ROSE pitch products under various reaction conditions. Asphaltene conversion is at a maximum at 425°C (33%). At 450°C, conversion drops to 24%. This is due to coking reactions occurring at this elevated temperature. From the boiling point data, it can be seen that as reaction temperature increases the amount of distillable products increases. At a reaction temperature of 450°C, 64% of the reaction products boil below 1000°F. However, an optimum temperature of 425°C was chosen for ROSE pitch based on asphaltene conversion and also at 450°C, there is evidence that THQ degrades via ring-opening, which would render the solvent useless for recycle. The results show that increasing hydrogen pressure does not have a great effect on cracking of the pitch to distillable. There is a significant difference in conversion of asphaltenes with increasing hydrogen pressure, and variation in solvent composition. This backs up the idea that we are dealing with two distinct reactions and mechanisms. Asphaltene conversion needs hydrogen to saturate the aromatic rings before they can be cracked. Cracking of side chains is more of a purely thermal process which is not as sensitive to increase in hydrogen pressure, but is sensitive to hydrogen donation ability of donors.

The initial H/C value of ROSE pitch is 1.27. At 375°C, H/C increases to 1.46. As reaction temperature increases to 400-425°C, there is the onset of major thermal cracking, which gives a further increase in H/C to 1.54. At 450°C, the increase in thermal cracking, is counterbalanced by a decrease in aromatic ring hydrogenation (thermodynamically limited). Also, there is probably major hydrocarbon gas production (methane, ethane) at 450°C, which decreases the H/C ratio of the products. When molecular hydrogen is used in the reaction system, H/C ratio increases to 1.62 (thermodynamics more favorable for hydrogenation of rings).

It has been postulated before that when considering the upgrading of resids, two distinct reactions have to be accounted for. Firstly, the behavior of the heavy asphaltene fraction, and second, the cracking of the lower molecular weight compounds. To explore this idea, the ROSE pitch was separated into hexane-soluble (oil) and insoluble fractions (asphaltene) and reacted separately. The products were analyzed by elemental composition and SIMDIST. The data are shown in Table 1. By upgrading the ROSE pitch without the asphaltene fraction, it is possible to achieve a product which has a high H/C (1.70). We now know that we are achieving good products from the hexane-soluble fraction of ROSE pitch, but the question remains, what are we doing to the asphaltene molecules. At 425°C, 1000psi hydrogen, and 120 minutes reaction time, only 8% of the asphaltene fraction is converted to <800°F material, compared to 19% conversion from the oil fraction. 34% asphaltene conversion to <1000°F material is achieved under the same conditions compared to 36% oil conversion to <1000°F. This data is somewhat misleading, because a close look at the chromatograms obtained through SIMDIST, shows a different product distribution. Asphaltene molecules are converted to primarily 'pre-asphaltenes' shown by a hump in the chromatogram. The oil fraction is converted primarily to lower boiling compounds, e.g., alkanes.

Product evaluation of solvent donor experiments in stirred-tank reactor

Figure 3 shows how the <1000°F component concentration and contaminant removal varies with hydrogen consumption (measured by hydrogen donation from the solvent). Extrapolation shows that a hydrogen consumption of 4000-4400 scf/bbl of pitch will be required to obtain products of commercial interest, that is, products exhibiting <1000°F contents of 80-90 wt%.

During the upgrading of ROSE pitch with THQ at 425°C and 1000psi hydrogen, 38% of the sulfur was removed as hydrogen sulfide. This gives a final sulfur wt% of 3.7 (feed=6.0%). Of this 3.7 wt%, 8.8, 5.7, 40.7, and 44.6% of the unconverted sulfur was retained in the <460°F, 460-484°F, 484-1000°F, and >1000°F respectively. Calculation gives a product boiling less than 1000°F having a sulfur concentration of 2.1wt%. Therefore, the lighter products would still have to be further treated to remove the sulfur to acceptable levels.

Figure 4 show the boiling point distribution of upgraded ROSE pitch at 425°C for various reaction times. At 425°C, conversion of pitch was essentially completed after 97 minutes. The stop in conversion is probably due to the equilibrium conversion of THQ to quinoline, i.e., hydrogen transfer stops once THQ and quinoline have reached equilibrium conversion. Once all the available hydrogen is used, retrogressive reactions will set in, leading to coke formation. It may be possible to increase conversion at 425°C, if hydrogen availability is increased. This could be achieved by increasing the solvent to resid ratio or increasing the hydrogen pressure. If successful, hydrogen consumption may exceed 4000 scf/bbl, which could give a <1000°F component concentration approaching 90%. This should also lead to a greater removal of contaminants.

Hydrogen transfer from various solvents to pyrene

To determine the hydrogen transfer ability of various polar solvents, pyrene was used as a model reactant. Table 2 shows the pyrene/solvent conversion data for these compounds (dihydropyrene is the only major pyrene hydrogenation product under these conditions). It can be seen that in terms of pyrene conversion, THQ and indoline are the best H-donors. However, in terms of hydrogen-transfer efficiency (solvent conversion compared with pyrene conversion), THQ is the better candidate. This prompted a closer look at H-transfer from THQ to pyrene.

Figure 5 shows how pyrene and THQ conversion, and H-transfer efficiency vary with hydrogen pressure. At low pressure (0-500 psi), H-transfer is 50% efficient. There could be different explanations for this value. Thermodynamics (equilibrium conversion) could limit the hydrogenation of pyrene. Another reason for achieving only 50% efficiency can be expained if the docking reaction between THQ and pyrene is looked at more closely. Two of the hydrogens will be donated from THQ to pyrene to produce dihydropyrene. As they are transferred, THQ will become unstable and will have to release the remaining two hydrogens to produce the stable molecule, quinoline. However, they will probably not be able to transfer to pyrene because of steric constraints (only one pyrene molecule can dock with THQ at a time). Therefore, the hydrogen will be released from THQ as molecular hydrogen.

As pressure increases to 1000 and 1500psi, efficiency increases past 100% and approaches 130% at 1500psi. This means that gas phase hydrogen is being utilized in the hydrogenation of pyrene. Quinoline produced by the dehydrogenation of THQ is being hydrogenated by the gas-phase hydrogen back to THQ. This H-shuttling mechanism can explain the >100% efficiency.

Figure 6 shows how pyrene conversion and THQ conversion varies with reactant ratio at 425°C, 120 minutes reaction time and inert atmosphere. The figure shows that increasing the solvent ratio to 20:1 increases the conversion of pyrene with respect to THQ. At 425°C, pyrene hydrogenation is thermodynamically limited to a maximum conversion of 36% under these conditions (20:1 molar ratio). At 2:1 molar ratio, the reaction is limited by the availability of transferable hydrogen, which limits conversion to 24%. The thermodynamic limitation can be overcome by dropping the temperature to 400°C, but this will have an effect on the kinetics of the transfer of hydrogen from THQ to pyrene. Experimentation has shown that it takes 120 minutes more reaction time at 400°C to reach the same conversion level seen at 425°C. It will be necessary to make a trade-off between reaction temperature, reaction time and the solvent/resid ratio. This will depend on how good the final product needs to be, and the economics of the process.

CONCLUSIONS

This study has shown that polar H-donors such as THQ and indoline are good solvents for upgrading petroleum resids. Model compounds studies using pyrene have shown that THQ is a better donor in terms of amount of conversion of the solvent with respect to the model compound. This will be an important aspect of future research as any process involving H-donors will have to consider the recycle of the solvent, i.e., rehydrogenation. THQ also acts as a H-shuttler between the gas phase and the reactant.

It was found from research undertaken using a large batch reactor, that a hydrogen consumption level of 4400 scf/bbl will be required to get a 90% conversion of the resid to <1000°F boiling material. This will also increase heteroatom removal but further hydrogenation will have to be done on the product to get the sulfur levels to less than 1%.

Studies undertaken in smaller microautoclaves have shown that an increase in H/C ratio of 25% is possible (1.62 is maximum obtained using THQ and 1000psi hydrogen pressure). From the SIMDIST data, asphaltene conversion data, and elemental analysis, a potential trade-off between cracking and hydrogenation of both the heavy asphaltene molecules and the lighter boiling material is envisioned. Because this system is non-catalytic, it will not be possible to get high cracking and high hydrogenation levels. The final process should be determined based on the required final product, e.g., does the product only need to be good enough for feeding to the FCC?

ACKNOWLEDGEMENTS

This work was supported by a grant from USX foundation. Thanks to Rolf Schroeder for many useful discussions ands the research staff at Marathon Oil Technology Center, Denver, for running batch reactions and product analysis.

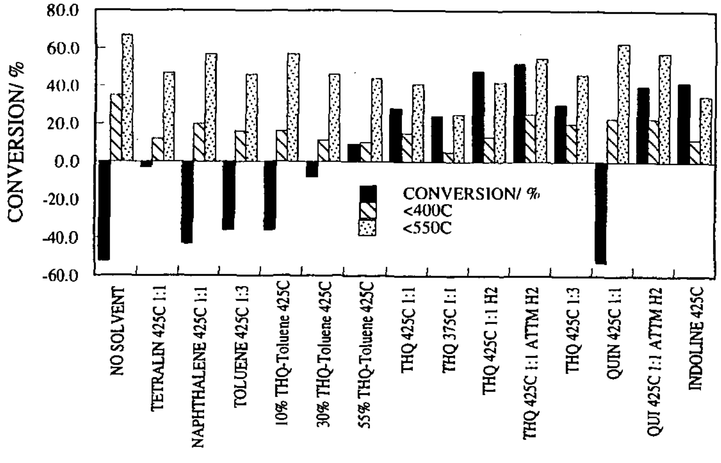

Figure 1. Effect of various solvents and reaction conditions on upgrading vacuum residue: 1 hour reaction time

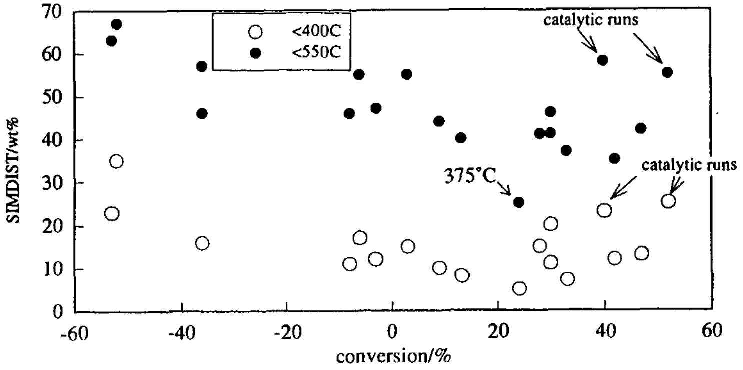

Figure 2. Vacuum resid conversion of asphaltene vs. SIMDIST results:various reaction conditions

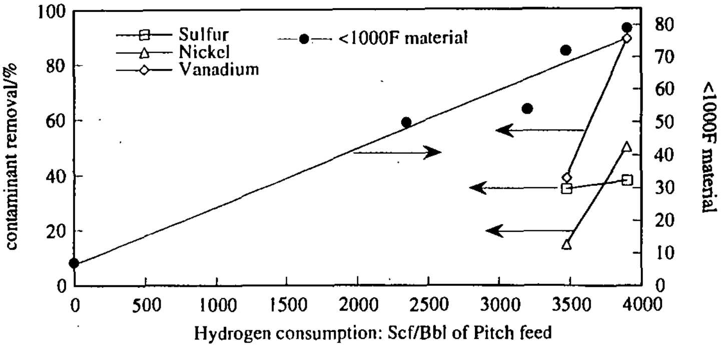

Figure 3. Conversion of ROSE pitch to <1000°F material and removal of contaminants vs. H-consumption: THQ and indoline

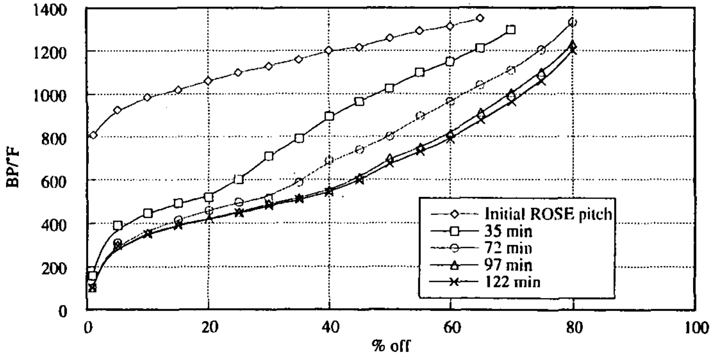

Figure 4. Boiling point distribution for products from THQ hydrogen donation to ROSE pitch: effect of donation time at 425°C, 2:1 solv/resid, 1000psi H2

Table 1. Effect of temperature, hydrogen pressure and reaction time on conversion of ROSE pitch and THQ, and H/C ratio of products.

Feedstock	Temperature/ °C	H_2 Pressure/ psi	time/ min	<800°F %	<1000° F %	Asphaltene Conv./%	THQ Conv. /%	H/C
ROSE pitch	-	-	-	2	9	-	-	1.27
ROSE pitch	375	0	60	7	18	12	-	1.46
ROSE pitch	400	0	60	9	23	17	-	1.54
ROSE pitch	425	0	60	18	38	33	-	1.51
ROSE pitch	450	0	60	40	64	24	-	1.55
ROSE pitch	425	500	120	32	55	32	53	1.55
ROSE pitch	425	1000	120	32	55	36	33	1.62
ROSE pitch	425	1500	120	29	50	40	36	-
ROSE pitch (oil)	-	-	-	5	8	-	-	1.33
ROSE Pitch (asphaltene)	-	-	-	0	2	-	-	1.09
ROSE pitch (oil)	425	1000	120	24	44	-	-	1.70
ROSE pitch (asphaltene)	425	1000	120	8	36	-	-	1.40

Table 2. Effect of various donor/non donor solvents on pyrene conversion : 425°C, 1000 psi hydrogen pressure

Model Compound	Solvent	mol/mol	Time/ min.	pyrene conversion/%	solvent conversion/%
pyrene	acridine	2	60	8.5	83
pyrene	acridine	2	120	13.7	95
pyrene	pyrolidine	2	120	13.1	-
pyrene	tetrahydrocarbazole	2	120	16.3	18
pyrene	indoline	2	60	47	48
pyrene	indoline	2	120	47	78
pyrene	toluene	2	120	7.4	-
pyrene	THQ	2	60	32	12
pyrene	THQ	2	120	32	14
pyrene	octahydroacridine	2	60	17	2
pyrene	octahydroacridine	2	120	22	12

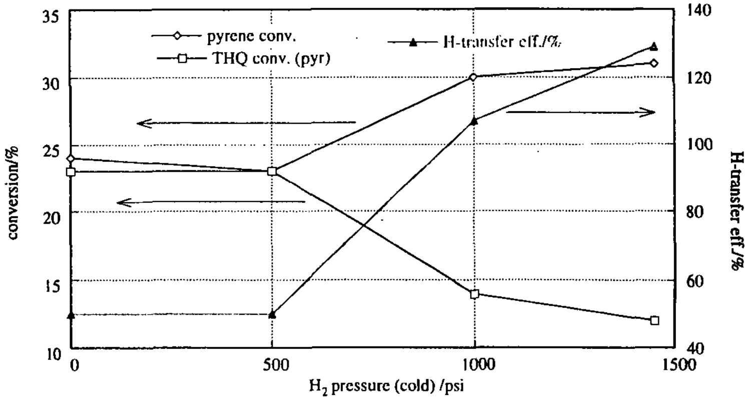

Figure 5. Pyrene/THQ conversion and H-transfer efficiency vs. H_2 pressure: 425°C, 120min

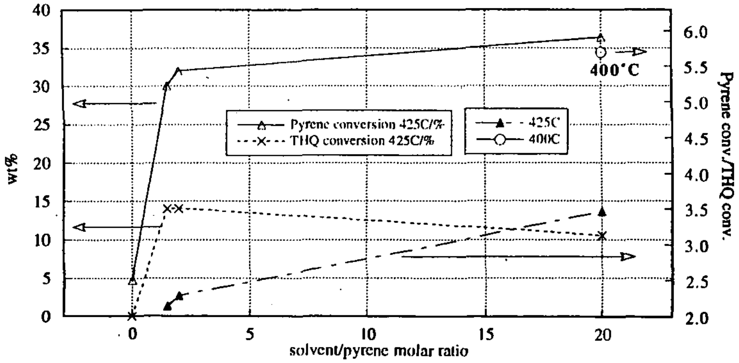

Figure 6. Pyrene and THQ conversion vs. reactant ratio : 425°C, 120 minutes, 1000psi H2

THIOPHENE HYDRODESULFURIZATION OVER COBALT OXIDE LOADED SMECTITE CLAY MINERALS

Eiji Iwamatsu1)*, Syed A. Ali1), Mohammad E. Biswas1), Shakeel Ahmed1)
Halim Hamid1), Yuzo Sanada1) and Toshikazu Yoneda2)

1) Research Institute, King Fahd University of Petroleum & Minerals,
Dhahran 31261, Saudi Arabia
2) Petroleum Energy Center, Japan

* Corresponding author: Tel & Fax +966-3-860-3847, E-mail iwamatsu@kfupm.edu.sa

Key words: hydrodesulfurization, cobalt, clay

ABSTRACT

Co oxide loaded smectite clay minerals catalysts showed high hydrodesulfurization (HDS) activity of thiophene used as a model compound. Among these catalysts, HDS activity of Co oxide loaded porous saponite was higher than $CoMo/Al_2O_3$ which is known to be a highly active catalyst for HDS. Further, HDS activity was increased by the calcination up to 600°C before Co oxide loading. MgO content was decreased and CoO content was increased with increasing calcination temperature up to 600°C before Co oxide loading. These catalysts were characterized by means of XRD and XPS. The correlation between the characteristics of catalysts and their activities were discussed. It can be concluded that (1) there are two types of Co oxide species : between the clay layers due to ion exchange with Na : and at the edge of the clay layer due to ion exchange with Mg, and (2) the latter type is highly active for thiophene HDS reaction.

INTRODUCTION

Generally, HDS catalyst applied in industry are derives from oxides of an element of Group VIB (Mo or W) and Group VIII (Co or Ni) supported on Al_2O_3. Catalytic activity is supposed to be connected with the presence of Group VIB elements while Group VIII elements are believed to act as promoters. However, it has been reported recently that only one metal, such as Co or Ni, oxide loaded on some supports shows higher HDS activity than $CoMo/Al_2O_3$ catalysts. Duchet et al. has reported the high HDS activity of carbon-supported Co sulfide1). In another report, Kloprogge et al. prepared Ni sulfide supported on Al oxide pillared montmorillonite catalysts with a high thiophene HDS activity2). Further, Sychev et al. has reported that sulfided Cr oxide pillared montmorillonite showed high activity for thiophene HDS and the consecutive hydrogenation of butenes3). In the above references, montmorillonite is a well known clay used as catalyst support. However, other smectite clay minerals (saponite, hectorite, stevensite and so on) have not been used as a support of HDS catalyst in spite of their similar feature. Therefore, in this study, Co oxide loaded smectite clays were prepared and HDS activity was evaluated. Moreover, the active sites of Co oxide loaded porous saponite, which showed the highest HDS activity, was also discussed.

EXPERIMENTAL

Smectite clay minerals were supplied by Kunimine Kogyo Co. Ltd. Co oxide was loaded on various clay minerals by means of ion exchange. Ion exchange method is as follows. Co nitrate solution ($Co(NO_3)_2 \cdot 6H_2O$ 29.0 g and distilled water 500 ml) was aged at 80 °C for 2 h. Then 10 g of clay was added to the solution and stirred at 80 °C for 1.5 h. After that, the solution was filtered. The residue thus obtained was washed with water and ethanol, and dried at 120 °C for 12 h and calcined at 400 °C for 12 h.

Hydrodesulfurization experiments were carried out in a pulse flow reactor. Prior to the activity test, the catalyst (0.1 g) was sulfided at 400 °C by using a mixed gas of 5 % H_2S in H_2 (60 ml/min., 2 kg/cm^2) for 2 h. Then, the temperature and the gas flow rate were changed to the reaction condition (H_2 60 ml/min., 2 kg/cm^2). Thiophene (0.3 μl) was injected and its conversion was measured by an on-line gas chromatograph, after the pulse reaction results had been stabilized.

RESULTS AND DISCUSSION

Table 1 shows thiophene HDS activity of Co oxide loaded smectite catalysts. As shown in this table, the smectite-supported catalysts showed higher activity than the Al_2O_3-supported catalyst (Co/Al_2O_3). Further, Co oxide loaded porous saponite showed the highest thiophene conversion in the Co oxide loaded other smectite series and its activity was higher than that of $CoMo/Al_2O_3$ which is known to be highly active catalyst for HDS reaction. Then, the modification of porous saponite was carried out in order to improve the activity, further. In this experiment, the precalcination at various temperatures up to 700 °C in the air for 24 h before Co oxide loading was carried out. Table 2 shows the results. As shown in this table, thiophene HDS activity was increased with increasing precalcination temperature up to 600 °C. It is noted that the HDS performance is remarkable as low as 225 °C.

Table 3 shows properties of Co oxide loaded porous saponite catalysts. As shown in this table, the amount of MgO was decreased and that of CoO was increased with increasing precalcination temperature up to 600 °C. Therefore, it is supposed that the ion exchange of Na with Co takes place at first, then, ion exchange of Mg with Co takes place. It seems that the increase of Co oxide amount loaded on porous saponite by precalcination up to 600 °C is one of the reasons for HDS activity improvement. Phase transition from saponite to enstatite between 600 and 700 °C was observed by means of XRD. The drastic change of specific surface area by the precalcination at 700 °C may be due to this phase transition. It seems that the decrease of thiophene HDS activity at 700 °C is caused by the decrease of CoO amount due to this phase transition which was observed by the substancial reduction in specific surface area and XRD.

Table 1. HDS activity of Co-smectite catalysts

Support	Loaded metal as oxide (wt%)	Thiophene conversion (%)		
		300°C	350°C	400°C
Montmorillonite	3.1	25.7	50.7	69.6
Saponite	5.0	73.1	78.5	86.2
Porous saponite	7.7	92.7	96.0	97.9
Hectorite	7.8	67.0	80.0	88.5
Stevensite	8.6	57.5	71.9	81.1
Al_2O_3	4.0	7.4	14.7	22.0
-	100[a)]	7.2	11.5	17.2
Al_2O_3	Co 4wt% + Mo 15wt%	85.0	97.0	98.3

a) CoO was used as catalyst

Table 2. HDS activity of Co-porous saponite catalysts

Sample	Precalcination Temperature (°C)	CoO (wt.%)	Thiophene conversion (%)			
			225	250	275	300°C
Porous saponite*	-	-	0.0	0.0	0.0	0.0
Co-porous saponite	-	7.7	28.2	73.5	81.8	92.7
	200	7.9	36.9	79.7	83.0	92.0
	300	8.6	33.5	85.5	90.7	94.6
	400	10.5	47.4	90.3	91.4	94.1
	500	13.5	56.4	92.2	92.8	95.1
	600	18.0	69.6	92.5	93.0	94.4
	700	9.3	10.7	25.1	40.0	52.1

* as received

Table 3 Properties of Co-porous saponite catalysts

Support	Precalcination Temperature (°C)	Composition (wt.%)					Surface Area (m^2/g)
		SiO_2	MgO	Al_2O_3	Na_2O	CoO	
Porous saponite*	-	49.2	29.2	4.5	3.0	-	514
Co-porous saponite	-	50.5	27.3	4.7	0.04	7.7	510
	200	46.9	24.9	4.5	0.05	7.9	415
	300	47.5	24.6	4.5	0.05	8.6	467
	400	46.9	22.9	4.5	0.05	10.5	402
	500	48.2	21.6	4.5	0.11	13.5	378
	600	44.9	16.9	4.3	0.08	18.0	342
	700	50.7	27.4	4.7	0.75	9.3	121

* as received

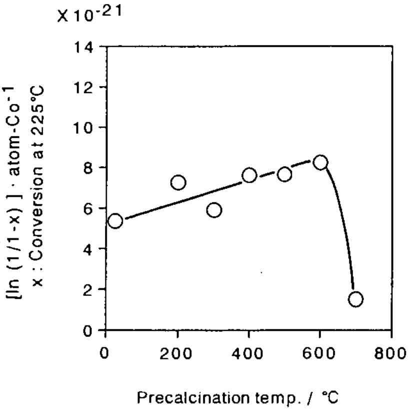

Fig. 1 [ln(1/1-x)] · atom-Co^{-1} as a function of precalcination temperature of porous saponite

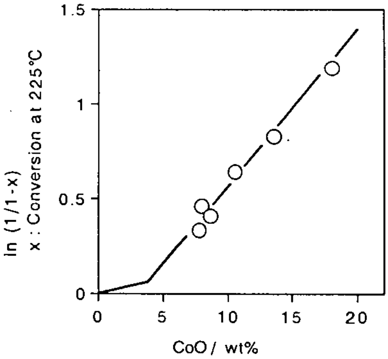

Fig. 2 ln(1/1-x) as a function of CoO content over porous saponite

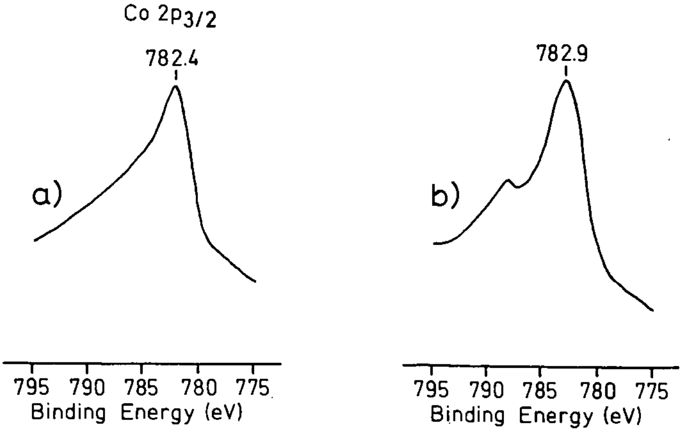

Fig. 3 XPS spectra of Co-poropus saponite
a) Co-porous saponite (non calcined before Co oxide loading)
b) Co-porous saponite (calcined at 600°C before Co oxide loading)

On the basis of the assumption that thiophene HDS is first-order reaction, the relation between $[\ln(1/1\text{-}x)]\cdot\text{atom-Co}^{-1}$ and precalcination temperature of Co oxide loaded porous saponite was investigated. The HDS activity at 225 °C was used as x, because of the low conversion values. Fig.1 shows the results. The vertical axis means the activity index per Co atom. This value was increased with increasing precalcination temperature up to 600 °C. Therefore, it seems that the increase of activity with increasing precalcination temperature is not due to the increase of the equivalent Co species.

Assuming that ion exchange of Na with Co takes place at first, then, ion exchange of Mg with Co takes place, as mentioned before, the amount of CoO just after the ion exchange of all Na with Co was 3.9 wt% in case of Co oxide loaded porous saponite. Hence, good relation between the activity and CoO amount was obtained by using this point (3.9 wt%) as an inflection point (Fig.2). The slope after this inflection point was larger than before 3.9 wt.%. Therefore, it seems that Co species which is exchanged with Mg is more active than that which is exchanged with Na.

Fig.3 shows XPS spectra of Co oxide loaded porous saponite. XPS spectra pattern of Co oxide loaded porous saponite, which was non-calcined before Co oxide loading, was similar with Co_3O_4 type, and that of Co oxide loaded porous saponite, which was precalcined at 600 °C before Co oxide loading was similar with CoO type4,5). Therefore, Co species exchanged with Na, which were located between the clay layers, seem to be mainly Co_3O_4 type. On the other hand, Co species exchanged with Mg, inside the clay layer, seem to be mainly CoO type. It seems that the part of Mg which exist at the edge of the clay is easier to exchange with Co than with Mg located inside the bulk. Consequently, this CoO type species at the edge of the clay seems to show higher HDS activity than Co_3O_4 type species between the clay layers.

CONCLUSIONS

Co oxide loaded smectite catalysts showed high HDS activity of thiophene. Among these catalysts, HDS activity of Co oxide loaded porous saponite was higher than $CoMo/Al_2O_3$ which is known to be a highly active catalyst for HDS. Further, HDS activity is increased by the calcination before cobalt oxide loading. MgO content was decreased and CoO content was increased with increasing calcination temperature before Co oxide loading. It can be concluded that (1) there are two types of Co oxide species : between the clay layers due to ion exchange with Na : and at the edge of the clay layer due to ion exchange with Mg, and (2) the latter type is highly active for thiophene HDS reaction.

ACKNOWLEDGEMENTS

The authors wish to acknowledge the support of Petroleum Energy Center, Japan, with the subsidy of the Ministry of International Trade and Industry Japan, and the Research Institute of the King Fahd University of Petroleum and Minerals, for this work under KFUPM/RI Project No.21151.

REFERENCES

1. J. C. Duchet, E. M. van Oers, V. H. J. de Beer and R. Prins, J. Catal., **80**, 386 (1983).
2. J. T. Kloprogge, W. J. J. Welters, E. Booy, V. H. J. de Beer, R. A. van Santen, J. W. Geus and J. B. H. Jansen, Appl. Catal., **97**, 77 (1993).
3. M. Sychev, V. H. J. de Beer, R. A. van Santen, R. Prihod o a nd V. Goncharuk, Stud. Surf. Sci. Catal., **84**, 267 (1994).
4. R. L. Chin and D. M. Hercules, J. Phys. Chem., **86**, 3079 (1982).
5. Y. Okamoto, T. Imanaka and S. Teranishi, J. Catal., **65**, 448 (1980).

DEEP HYDRODESULFURIZATION OF GASOILS - MECHANISM OF ALKYLDIBENZOTHIOPHENES TRANSFORMATION ON BIFUNCTIONAL CATALYSTS

G. PEROT, P. MICHAUD and J.L. LEMBERTON, Laboratoire de Catalyse en Chimie Organique, UMR 6503, UFR Sciences, 40 avenue du Recteur Pineau, 86022 Poitiers Cedex, France, email : Guy.perot@cri.univ-poitiers.fr

Keywords: hydrodesulfurization, dibenzothiophene, 4,6-dimethyldibenzothiophene, nickel-molybdenum sulfides, bifunctional catalysts

INTRODUCTION

In order to decrease the pollution by diesel engines, the authorized maximum sulfur content in fuels has been severely lowered in certain countries. However, total hydrodesulfurization of gasoils is very difficult to reach with the catalysts used at present in the industrial units, probably because of the presence of hydrodesulfurization resistant molecules, such as 4,6-dimethyldibenzothiophene (1,2). Indeed, while dibenzothiophene is easy to decompose, this is not the case for 4,6-dimethyldibenzothiophene. Most of the other dialkyldibenzothiophenes are as reactive as dibenzothiophene, some of them being even more reactive (3-5). Consequently, one possibility of improving the reactivity of 4,6-dimethyldibenzothiophene is to transform it into a more reactive molecule, for example through isomerization (6,7). This reaction can be performed using acid catalysts (8,9).

In the present work we compare the transformation of dibenzothiophene and of 4,6-dimethyldibenzothiophene on catalysts such as a sulfided commercial NiMo on alumina catalyst, a physical mixture of this catalyst with silica-alumina, and on a NiMo on alumina catalyst containing Y-zeolite.

EXPERIMENTAL

The hydrodesulfurization of dibenzothiophene (DBT) and of 4,6-dimethyldibenzothiophene (46DMDBT) was carried out in a flow reactor at 340°C under a 4 MPa total pressure. Decalin was used as a solvent to which dimethyldisulfide was added to generate H_2S. The partial pressures were: DBT or 46DMDBT = 0.01 MPa, decalin = 0.89 MPa, H_2 = 3.0 MPa, H_2S = 0.05 MPa.

The reference hydrotreating catalyst was a commercial NiMo/alumina containing 3 wt.% NiO and 14 wt.% MoO_3. The silica-alumina was a Ketjen K14 sample, containing 14 wt.% alumina. The NiMo-Y zeolite catalyst was supplied by the « Institut Français du Pétrole » (Rueil-Malmaison, France). It contained 5 wt.% Y zeolite mixed with NiMo on alumina (NiO + MoO_3 = 16.8%). All the catalysts were first sulfided *in situ* by a mixture of 5 vol.% dimethyldisulfide in n-heptane, under the same hydrogen partial pressure and total pressure as those used for the reaction. The H_2S partial pressure was 0.125 MPa and that of n-heptane 0.75 MPa. The sulfiding feed was injected at a starting temperature of 150°C, raised to 350°C at a 5°C.min^{-1} rate. After 14 hours, the temperature was lowered to 340°C, and the reaction mixture was substituted for the sulfiding feed.

The reactor effluents were condensed, and liquid samples were periodically collected and analyzed by gas-liquid chromatography (Varian 3400) on a 50-m DB17 capillary column (J&W Scientific). Unknown products were identified by GC-MS (Finnigan INCOS 500). The HDS conversions of the reactants were determined by using an external standard (1-methylnaphthalene).

4,6-Dimethyldibenzothiophene was synthesized (10) - and kindly supplied - by the « Institut de Recherche sur la Catalyse » (Villeurbanne, France). The other products were purchased from Aldrich.

RESULTS AND DISCUSSION

Transformation of dibenzothiophene and 4,6-dimethyldibenzothiophene over the sulfided NiMo on alumina catalyst.

The sulfided NiMo on alumina catalyst has a very stable activity for the conversion of DBT and of 46DMDBT. Figure 1 shows the total activity of the NiMo catalyst for the conversion of the two molecules. We can see that DBT, under our experimental conditions, is almost 5 times more reactive than 46DMDBT.

The DBT reaction products are biphenyl, tetrahydrodibenzothiophene, cyclohexylbenzene, and dicyclohexyl. If one considers the distribution of these products as a function of contact time, it is clear that biphenyl and tetrahydrodibenzothiophene are the only primary reaction products. In agreement with previous work (11,12), further experiments showed that, under our experimental conditions, biphenyl did not transform into cyclohexylbenzene, which means that cyclohexylbenzene is produced only from tetrahydrodibenzothiophene. Consequently, it can be concluded that the transformation of DBT occurs through two parallel reactions : direct desulfurization (DDS) yielding biphenyl, and desulfurization after hydrogenation (HYD), yielding first tetrahydrodibenzothiophene, then cyclohexylbenzene. We can estimate that the DDS reaction occurs faster than the HYD reaction (by a factor of 4 in this case), in agreement with the literature (13-15).

The 46DMDBT reaction products are similar to the DBT products, except for the methyl groups. The reaction scheme is the same as in the case of DBT, but the product distribution differs significantly from the one observed in the case of DBT. Figure 1 shows that the HYD reaction (yielding 4,6-dimethyltetrahydrodibenzothiophene and 3-(3'-methylcyclohexyl)-toluene) is 5 times faster than the DDS reaction (yielding 3,3'-dimethylbiphenyl), which is the contrary of what was observed with DBT. The HYD reaction occurs at similar rates for both molecules, whereas the DDS reaction of DBT is faster by a factor of 25 than the DDS reaction of 46DMDBT. Consequently, we can conclude that it is owing to a very slow DDS reaction that 46DMDBT, when compared to DBT, transforms with difficulty (5, 16).

Transformation of dibenzothiophene and 4,6-dimethyldibenzothiophene on silica-alumina.

Long contact times were needed to observe the transformation of DBT and 46DMDBT on pure silica-alumina. In both cases, a very high conversion was obtained initially, but this conversion decreased very rapidly during the first 4 hours, then slower to reach approximately a zero value after 15 hours. Surprisingly, even at high conversion, none of the reaction products obtained with the NiMo on alumina catalyst was detectable by chromatographic analysis. In fact, the reactant transforms into products impossible to distinguish from those resulting from the decalin isomerization and cracking which also occur under the operating conditions.

Transformation of dibenzothiophene and 4,6-dimethyldibenzothiophene on bifunctional (acid + sulfide) catalysts.

The transformations of DBT and 46DMDBT were carried out either on a (1:5) physical mixture of NiMo on alumina with silica-alumina, or on the NiMo-Y zeolite catalyst. Both catalysts exhibited a slow 2-hour-deactivation period with 46DMDBT (the activity decreased by a factor 1.5), and were fairly stable with DBT.

Figure 2 compares the activities of all the catalysts calculated per kg of the sulfide component alone. The presence of an acid component had no effect in the case of DBT conversion, but increased the 46DMDBT reactivity by a factor of 2-2.5, which has already been observed by other authors (6,7). Moreover, two new products were formed from 46DMDBT : the first one was identified by GC-MS as an isomer of 46DMDBT, we suppose it to be 3,6-dimethyldibenzothiophene (36DMDBT) according to the chromatographic analyses reported in the literature (7); the second one, identified by GC-MS as an isomer of dimethylbiphenyl, is most likely 3,4'-dimethylbiphenyl (7). However, we observed that the amounts of DBT and 46DMDBT which were consumed were not balanced by the amounts of the hydrodesulfurization reaction products. In the case of DBT, smaller amounts of cyclohexylbenzene were detected with the bifunctional catalysts than with the pure sulfide catalyst. In the case of 46DMDBT, no 3-(3'-methylcyclohexyl)-toluene was detected. Because of the presence of the acid component, the missing compounds were converted into products which, owing to chromatographic interactions with the solvent reaction products, could not be detected.

To be able to observe the lacking reaction products, the transformations of DBT and of 46DMDBT were carried out on the NiMo-Y zeolite catalyst substituting cyclohexane for decalin as a solvent. Under these conditions, methylcyclohexane and toluene could be detected, and the amounts of consumed reactants were well-balanced by the amounts of the products formed. Figure 3 shows that 3,6-dimethyldibenzothiophene, 3,3'-dimethylbiphenyl and 4,6-dimethyltetrahydrodibenzothiophene are obviously primary reaction products, whereas 3,4'-dimethylbiphenyl, methylcyclohexane and toluene are secondary products. This allows us to propose a reaction scheme for the transformation of 46DMDBT on a bifunctional catalyst (scheme 1). In this scheme, the two reactions identified in the case of the pure sulfide catalyst can be found, the direct desulfurization (DDS) yielding 3,3'-dimethylbiphenyl, and the hydrogenation (HYD) yielding the methylcyclohexyltoluenes. The presence of an acid component induces the appearance of another reaction (ISOM). This acid-catalyzed reaction allows 46DMDBT to transform into 36DMDBT which in turn transforms, mainly through direct desulfurization, into 3,4'-dimethylbiphenyl (no 3,6-dimethyltetrahydrodibenzothiophene was found in the 4,6DMDBT reaction products). No methylcyclohexyltoluenes could be detected in the presence of an acid component, as reported by Landau et al. (6), but the presence of toluene and methylcyclohexane suggests that the methylcyclohexyltoluenes transformed through hydrocracking, as is commonly observed with bifunctional catalysts (18). Moreover, Figure 3 shows that there is more toluene than methylcyclohexane at high 46DMDBT conversions. We must suppose that 3,3'-dimethylbiphenyl or

3,4'- dimethylbiphenyl transform into toluene, as proposed by Lecrenay and Mochida (19). This reaction can occur through a mechanism which is derived from the reverse of the mechanism proposed by Gates, Katzer and Schuit (20) for the transformation of benzene into biphenyl. Owing to the existence of the ISOM reaction (scheme 1), the DDS reaction rate is higher than the HYD reaction rate, and thus produces an excess in toluene.

CONCLUSION

As expected, our results indicate that, owing to a very significant deactivation, the use of a purely acid catalyst is of no interest. However, a « bifunctional » catalyst, such as a sulfided NiMo on alumina plus an acidic function (silica-alumina or Y zeolite) is reasonably stable compared to the pure acid catalyst. The combination of an acid component with a hydrogenating component changes the deactivation process, which is well-known in hydrocracking reactions on bifunctional catalysts. However, the initial decrease in activity of these catalysts observed during 46DMDBT transformation suggests that part of the active sites deactivate. If this deactivation could be avoided, it is clear that the gain in activity resulting from the addition of the acid component could be even greater.

The reactivity of 46DMDBT is higher, at least by a factor 2, on the stabilized bifunctional catalysts than on the pure sulfided catalyst, whereas there is no effect of the acid component on the reactivity of DBT. The increase in 46DMDBT reactivity is linked to the formation of an isomer, most likely 36DMDBT. This is in agreement with the conclusion that alkyl groups in the 4 and 6 positions in DBT inhibit the DDS reaction more significantly than alkyl groups in other positions. In the case of DBT, the isomerization reaction is of course impossible, and it is quite normal to have no effect of an added acid component on the DBT transformation rate.

ACKNOWLEDGEMENT

This work was carried out within the framework of a contract entitled « Hydrodésulfuration des gazoles ». It was supported by CNRS-Ecotech, Elf, IFP, Total and Procatalyse. The authors are particularly grateful to V. Lamure-Meille, C. Traversa and E. Schulz who contributed to this work by preparing 4,6-dimethyldibenzothiophene (10).

LITERATURE CITED

(1) Ma X., Sakanishi K. and Mochida I., Ind. Eng. Chem. Res., 33, 218 (1994).
(2) Kabe T., Ishihara A.and Tajima H., Ind. Eng. Chem. Res., 31, 1577 (1992).
(3) Kilanowski D.R., Teeuwen H., De Beer V.H.J., Gates B.C., Schuit G.C.A. and Kwart H., J. Catal., 55, 129 (1978).
(4) Houalla M., Broderick D.H., Sapre A.V., Nag N.K., De Beer V.H.J., Gates B.C.and Kwart H., J. Catal., 61, 523 (1980).
(5) Meille V., Schulz E., Lemaire M. and Vrinat M., J. Catal., 170, 29 (1997).
(6) Landau M.V., Berger D. and Herskowitz M., J. Catal., 158, 236 (1996).
(7) Isoda T., Nagao S., Korai Y. and Mochida I., Am. Chem. Soc. Prepr. Div. Petrol. Chem., 41, 559 (1996); 41, 563 (1996).
(8) Ward J.W. and Hansford R.C., J. Catal., 13, 154 (1969).
(9) Guisnet M. and Gnep N.S., in : *Zeolites : Science and Technology*, NATO ASI Series, eds. Ribeiro F.R., Rodriguez A.E., Rollmann L.D. and Naccache C., (Martinus Nijhoff Publishers, The Hague/Boston/Lancaster, 1984) p. 571.
(10) Meille V., Schulz E., Lemaire M., Faure R. and Vrinat M., Tetrahedron, 52, 3953 (1996).
(11) Nagai N., Sato T.and Aiba A., J. Catal., 97, 52 (1986).
(12) Rollmann L.D., J. Catal., 46, 243 (1977).
(13) Singhal G.H., Espino R.L., Sobel J.E. and Huff G.A., J. Catal., 67, 457 (1981).
(14) Houalla M., Nag N.K., Sapre A.V., Broderick D.H. and Gates B.C., AIChE J., 24, 1015 (1978).
(15) Nag N.K., Appl. Catal., 10, 53 (1984).
(16) Kabe T., Ishihara A.and Zhang Q., Appl. Catal. A : Gen., 97, L1 (1993).
(17) Prater C.D. and Lago R.M., Adv. Catal., 8, 293 (1956).
(18) Lecrenay E. and Mochida I., in : *Hydrotreatment and Hydrocracking of Oil Fractions*, Studies in Surface Science and Catalysis, Vol. 106, eds. Froment G.F., Delmon B. and Grange P., (Elsevier, Amsterdam/Lausanne/New York/Oxford/Shannon/Tokyo, 1997) p. 333.
(19) Gates B.C., Katzer J.R. and Schuit G.C.A., in : *Chemistry of Catalytic Processes*, Chemical Engineering Series, eds. Carberry J.J., Fair J.R., Peters M.S., Schowalter W.R.and Wei J. (Mc Graw-Hill Book Company, New-York, 1979) p. 17.

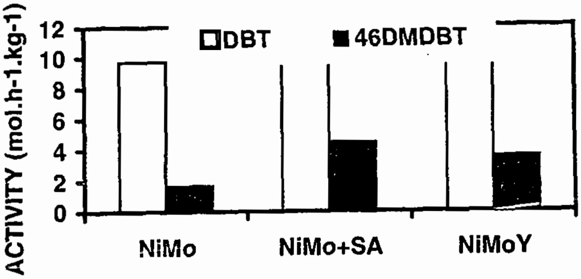

Figure 1. Activities of the sulfided NiMo on alumina catalyst for the transformation of dibenzothiophene (DBT) and 4,6-dimethyldibenzothiophene (46DMDBT). DDS = direct desulfurization reaction, HYD = hydrogenation reaction.

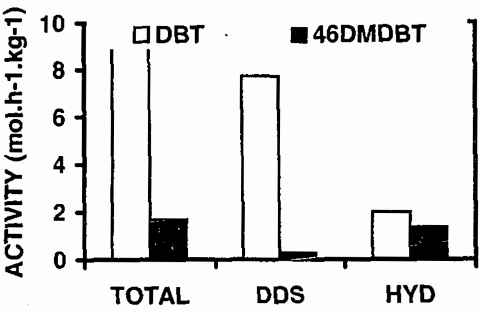

Figure 2. Activities of the sulfide functions of the catalysts for the transformation of dibenzothiophene (DBT) and 4,6-dimethyl dibenzothiophene (46DMDBT), NiMo = pure NiMo on alumina; NiMo + SA = NiMo on alumina mixed with silica-alumina; NiMoY = bifunctional NiMo - Y zeolite catalyst.

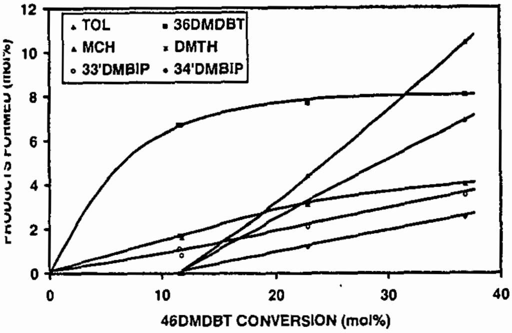

Figure 3. Hydrodesulfurization of 4,6-dimethyldibenzothiophene on sulfided NiMo on alumina - Y zeolite catalyst. TOL = toluene, 36DMDBT = 3,6-dimethyldibenzothiophene, MCH = methylcyclohexane, DMTH = 4,6-dimethyltetrahydrodibenzothiophene, 33'DMBiP = 3,3'-dimethylbiphenyl, 34'DMBiP = 3,4'-dimethylbiphenyl

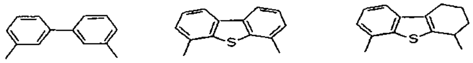

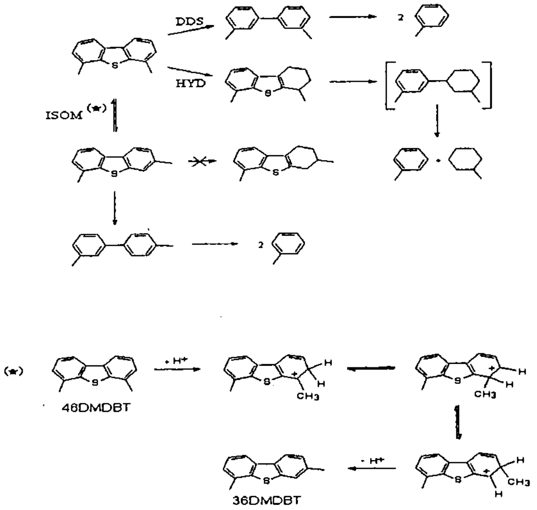
DDS
2
HYD
S
S
ISOM (*)
S
S
2
(*)
+ H+
S
46DMDBT
H
H
CH3
S
H
H
CH3
- H+
S
36DMDBT
H
CH3
H

Scheme 1. Transformation of 4,6-dimethyldibenzothiophene on sulfided NiMo on alumina - Y zeolite catalyst.

TRANSITION METAL TETRACHLOROALUMINATE CATALYSTS FOR PROBE REACTIONS SIMULATING PETROLEUM RESIDS UPGRADING

Masahide Sasaki, Chunshan Song and Mark A. Plummer[#]
Fuel Science Program & Laboratory for Hydrocarbon Process Chemistry
Pennsylvania State University, 209 Acad. Proj. Bldg.
Univ. Park, PA 16802
# Petroleum Technology Center, Marathon Oil Company, Littleton, CO 80160
Keywords: Transition Metal Tetrachloroaluminate, Acidity, Bond Cleavage

INTRODUCTION

In current commercial practice for catalytic upgrading of heavy oil and resids, there are two approaches. One is hydrocracking to obtain light and middle distillates, and the other is hydrotreating followed by FCC to produce gasoline components. While commercial hydroprocessing uses metal sulfide catalysts, an alternative approach would be to convert resids into lower-molecular-weight hydrocarbons with Lewis acidic catalysts. The present work deals with petroleum resid upgrading using Lewis acidic dual-functional salts as catalysts, which contain transition metal halides(1,2). Dual-function here refers to cracking via acid-catalyzed C-C bond cleavage for molecular weight reduction, and hydrogenation of reactive intermediates (from bond cleavage) and polyaromatics for production of stable molecules of low molecular weight. Plummer(3) suggested that sodium and hydrogen tetrachloroaluminates ($NaAlCl_4$ and $HAlCl_4$) was effective as catalyst for molecular weight reduction of resids. The $NaAlCl_4$ was the major molecular weight reduction and synthesis component, and $HAlCl_4$ added a hydrogenation function. Historically, such catalysts have been used in synthesis-type reactions such as isomerization, alkylation and polymerization(4,5).

The present work examines the potential of transition metal tetrachloroaluminates as resid upgrading catalysts. This is a fundamental applied research using model compounds as probe molecules. The MClx in the alkali metal or transition metal tetrachloroaluminate MClx-$(AlCl_3)$x includes three kinds of alkali metal chlorides, LiCl, NaCl and KCl, and six transition metal chlorides, VCl_3, $CoCl_2$, $NiCl_2$, $ZnCl_2$, $MoCl_3$. We selected four compounds as models, including 4-(1-naphthlymethyl) bibenzyl (NMBB), eicosane (n-C_{20}), dibenzothiophene and pyrene. Batch tests with model compounds were carried out at 425 °C for 20 min in autoclave under hydrogen pressure. The catalytic performance was evaluated in the reaction of model compounds with respect to bond cleavage reaction of C-C bond, hydrogenation, methylation and ring opening of aromatics.

EXPERIMENTAL

Catalyst Precursor and Compound

Three kinds of alkali metal chlorides, LiCl, NaCl and KCl, and six transition metal chlorides, VCl_3, $CoCl_2$, $NiCl_2$, $ZnCl_2$, $MoCl_3$ and $PdCl_2$, were used for preparing the MClx-$(AlCl_3)_x$ catalysts. Ammonium tetrathiomolybdate (ATTM) also was used as catalyst precursor.

4-(1-naphthylmethyl)bibenzyl (NMBB), eicosane (n-C_{20}), dibenzotiophene and pyrene were used as a model compound. The structure of NMBB is

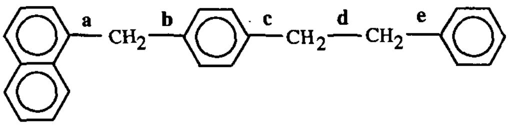

An intriguing feature of the NMBB structure is the presence of five different C_{ar}-C_{al} or C_{al}-C_{al} bonds. Following the system established by earlier workers, these bonds are denoted as a through e in the structure shown above. (Some authors refer to this compound as naphthylbibenzylmethane and use the abbreviation NBBM; the system of labeling the bonds remains the same.) ATTM and these model compounds were used without further purification.

Catalyst Preparation

Before catalyst preparation, the precursors were dried at 210 °C for 6 h in vacuum. Catalyst were prepared by using a quartz tube insert, which was placed in a vertical microautoclave reactor with a capacity of 25 mL. Precursor loading amount depends on its valence number, x, for example, $CoCl_2$-$(AlCl_3)_2$ was $CoCl_2/AlCl_3=0.5$. The reactor was heated at 400 °C for 20 min, including heat-up time for about 6 min, under nitrogen pressure (300 psig-cold). The combination of LiCl, NaCl, KCl and $ZnCl_2$ with $AlCl_3$ were melt at 400 °C, which indicated these catalysts made molten salt. Other combinations did not become molten salts even at 400 °C. However, strong interactions between MCl_x and $AlCl_3$ may occur even if the combination MCl_x-$(AlCl_3)_x$ is not in molten state at the reaction temperature.

Model Compound Reaction

A horizontal microautoclave reactor with a capacity of 25 mL was loaded with the reactant and 10 mol% of catalyst based on molar number of reactant. The amounts of reactants were as follows; NMBB: 0.78 mmol; eicosane : 1.8 mmol; DBT : 2.0 mmol; pyrene: 2.0 mmol. After loading reactant and catalyst, the reactor was sealed and purged three times with hydrogen, then pressurized with 800 psig-H_2 at room temperature. A preheated fluidized sand bath was used as a heating source, and the reactor was vertically agitated to provide mixing (about 240 strokes / min). Most of the reactions were carried out at 425 °C for 20 min including heat-up time for about 6 min. After the reaction the reactor was quenched in a cold water bath. Gaseous products were collected into a sample bag. The solid and liquid products were washed out with about 20 mL CH_2Cl_2, then filtered to separate to solid and liquid products. The solid material was dried at 50 °C for 6 h in vacuum. The CH_2Cl_2 insoluble product was defined as coke.

Analysis

Gaseous products were analyzed by GC-FID using a Parkin Elmer AutoSystem GC for C_1 to C_6 hydrocarbon gases.

Liquid products were identified by GC-MS using a Hewlett-Packard 5890 II GC coupled with a HP 5971 A mass-selective detector operating at electron impact mode (EI, 70 eV). The column used for GC-MS was a J&W DB-17 column; 30 m x 0.25 mm, coated with 50 % phenyl - 50 % methylpolysiloxane with a coating film thickness of 0.25 μm. For quantification, a Perkin Elmer 8500 GC with flame ionization detector and the same type of DB-17 column used. Both GC and GC-MS were programmed from 80 to 280 °C at a heating rate of 6 °C/min, and a initial holding time of 0 min and a final holding time of 2 min (or 22 min for NMBB as a reactant). The response factors for all the reactant and 8 of the products were determined using pure compounds(6,7).

RESULTS AND DISCUSSION

NMBB conversion over MClx-($AlCl_3$)x catalyst

Table 1 shows the results of non-catalytic and catalytic runs of NMBB at 425 °C for 20 min. Complete conversion of NMBB was achieved with significant coke formation with $CoCl_2$, $NiCl_2$, $ZnCl_2$ and $PdCl_2$ containing catalyst. For coke formation, the yield with the fourth row in periodic table metal containing catalysts were much higher than that with the fifth raw ones. It was with $MoCl_3$ containing catalyst that there was no coke formation.

For liquid products distribution, the main products in liquid were naphthalene, methylnaphthalene, bibenzyl and methylbibenzyl. Using transition metal MCl_x-$(AlCl_3)_x$ enhanced hydrogenation activity (yield of tetralin), especially $NiCl_2$, $ZnCl_2$ and $PdCl_2$. Table 1 also gave the results of ATTM as a catalyst precursor, which produces MoS_2 in situ. For the reaction with ATTM, there was no dimethylated products in liquid, for example DiMe-naphthalene and DiMe-bibenzyl. It means that methylation activity of molybdenum sulfide catalyst is much lower than that of MCl_x-$(AlCl_3)_x$ catalysts. However, molybdenum sulfide catalyst showed much higher hydrogenation activity (yield of tetralin).

Computer-aided reaction pathway analysis(8) indicated that bond cleavage in catalytic reaction of NMBB may occur favorably in bond **a** (between naphthyl and methylene) with Mo sulfide catalyst, in bond **b** (between the two methylene carbon in bibenzyl part) with Lewis acidic Mo chloride catalyst, and bond **d** (between naphthyltolyl and methylene) in noncatalytic thermal reaction. These results suggested that the main cracking products for catalytic reaction can be represented by Me-bibenzyl and bibenzyl. Therefore, we introduced the molar ratio Me-bibenzyl / bibenzyl as an index of bond cleavage of NMBB, as summarized in Table 2. For thermal cracking of NMBB, the yields of these compounds were very low, because bond cleavage reaction mainly occurred at **d**. In this case, the main cracking products were naphthyltolymethane and toluene. For catalytic reaction with MCl_x-$(AlCl_3)_x$, a/b values for transition metals were lower than those with alkali metal, but in all cases, a/b values were less than 1. It means bond cleavage reaction at **b** position was significant for MCl_x-$(AlCl_3)_x$ catalyst. On the other hand, a/b value with ATTM is much higher than the others (over 1). This higher value indicated that bond cleavage reaction mainly occurred at **a** position. These experimental data of bond cleavage reaction are consistent with the results of computational analysis.

In addition, we also determined the ratio of i-C_4 / n-C_4 as an index, which is a relative measure of the acidity of the catalysts. Figure 1 shows the relation between a/b value and i-C_4/n-C_4 ratio. From this figure, the selectivity of bond cleavage (a/b) decrease with increasing i-C_4/n-C_4 ratio. This result suggests that the selectivity of bond cleavage of NMBB depends on catalyst acidity for MCl_x-$(AlCl_3)_x$ catalysts.

Table 2 also specified the result with Na tetrachloroaluminate catalyst at 400 °C. There was no remarkable difference in conversion between reaction at 400 °C and that at 425 °C, conversion value was 91.5 and 91.7 wt%, respectively. At 400 °C, the degree of bond cleavage reaction at **a** position was almost same as that at **b** position(selectivity: 1.12). On the other hand, bond cleavage reaction at **b** was dominant reaction at 425 °C(selectivity: 0.48). These results indicated that bond cleavage reaction of NMBB with binary catalyst is sensitive to reaction temperature. On the other hand, it should be noted that demethylation reaction and some hydrocracking reaction also occurred, as can be seen from the C_1-C_4 products shown in Table 1.

Eicosane conversion over MClx-($AlCl_3$)x catalyst

Table 3 shows the results of non-catalytic and catalytic runs of eicosane (n-C_{20}) at 425 °C for 20 min. Using transition metal in MCl_x-$(AlCl_3)_x$[MClx=VCl_3, $CoCl_2$, $NiCl_2$, $ZnCl_2$, $PdCl_2$] caused great enhancement in long-chain paraffin hydrocracking. In these cases, C_3 and C_4 hydrocarbons were main products. Complete conversion of eicosane was achieved without any coke formation with $NiCl_2$, $ZnCl_2$ and $PdCl_2$. $MoCl_3$-$(AlCl_3)_3$ catalyst was not very active for eicosane hydrocracking among the transition metal-containing catalysts.

On the other hand, alkali metal-based MCl_x-$(AlCl_3)_x$ [MClx = LiCl, NaCl, KCl] catalysts were not as effective as transition metal-containing ones. The order of conversion was : LiCl > NaCl > KCl.

Table 4 shows a selected group distribution of liquid products. Here the liquid products are divided into two groups for convenience, one is C_9 to C_{11} and the other is C_{12} to C_{19}. The value of A/(A+B) (the fifth column) indicates the degree of hydrocracking of eicosane molecule. In all cases, the values of transition metal are higher than that of alkali metal, which means transition metal catalyst has higher hydrocracking activity for eicosane molecule. In addition, this value is closely related to total conversion.

Table 1 NMBB Conversion at 425 °C for 20 min.

Exp. #	393	336	340	344	348	352	374	360	364	368	420
MClx-(AlCl3)x	None	LiCl	NaCl	KCl	VCl3	CoCl2	NiCl2	ZnCl2	MoCl3	PdCl2	ATTM
Conv. (wt%)	17.1	82.8	64.3	36.2	81.0	100.0	100.0	100.0	72.9	100.0	96.8
Gas yield (wt%)	6.1	0.0	2.2	0.0	2.4	1.5	12.4	10.5	3.4	13.5	2.8
Liquid yield (wt%)	5.8	48.8	45.1	13.1	54.2	62.6	52.3	48.1	43.8	52.0	77.7
Coke yield (wt%)	0.0	7.3	2.9	0.0	8.9	15.1	20.0	20.3	0.0	10.3	0.0
Liquid products (mol%)											
toluene	2.4	5.1	4.3	1.2	4.3	6.5	4.5	6.4	2.9	6.5	1.4
p-, m-xylene	0.6	2.9	2.7	0.4	3.2	5.0	5.5	8.1	1.9	9.7	6.9
o-xylene	1.1	0.3	0.2		0.3	0.5	0.5	0.6	0.2	0.7	
1,3,5-trimethylbenzene		0.4	0.3		0.5	0.9	1.1	1.6	0.2	2.0	0.9
1,2,4-trimethylbenzene					0.1	0.1	0.2	0.3		0.3	
1,2,3-trimethylbenzene						0.2	0.2	0.3		0.4	
tetralin	0.7	2.0	0.7		1.8	2.3	7.6	13.7	0.8	20.6	34.4
Me-tetralin*		0.5			0.4	0.6	2.0	3.3		4.7	3.2
naphthalene	1.0	41.0	44.5	19.0	45.7	46.4	32.3	20.7	47.7	11.3	37.3
1-Me-naphthalene		3.6	3.9	0.7	4.8	4.2	3.3	2.3	3.7	2.1	4.0
2-Me-naphthalene		7.0	4.9		6.4	8.0	5.8	4.0	4.8	3.5	0.6
1,2-DiMe-naphthalene		0.1				0.2		0.2		0.3	
1,3-DiMe-naphthalene		0.5			0.3	0.4	0.2	0.2		0.2	
1,4-DiMe-naphthalene		0.3	0.2		0.2	0.4	0.3	0.2	0.1	0.2	
1,5-DiMe-naphthalene		0.6	0.4		0.5	0.8	0.6	0.5	0.3	0.6	
1,6-DiMe-naphthalene		0.3				0.1		0.2		0.2	
2,6-DiMe-naphthalene					0.4	0.4					
2,7-DiMe-naphthalene						0.4	0.1	0.6		0.5	
bibenzyl	0.2	36.0	29.0	4.7	36.1	43.9	40.5	34.0	25.7	36.2	12.5
4Me-bibenzyl	1.6	5.9	12.6	3.0	14.9	11.7	7.4	2.7	13.0	3.1	54.8
Me-bibenzyl		3.5	1.3		2.7	4.3	4.2	3.5	1.2	4.2	0.7
DiMe-bibenzyl*					0.4	1.1	0.5	0.5		1.5	
1-benzlynaphthalene	0.5			0.2							
naphthyltolylmethane	2.3			1.1							
4H-NMBB	0.3	0.0									
NMBB isomer		1.9	6.9	38.0	5.0				6.1		
NMBB	82.9	15.3	28.8	25.8	16.8				21.0		3.2
Gaseous Products (mol%)											
CH4	35.9	0.0	13.8	0.0	6.1	5.0	15.0	22.9	14.4		8.0
C2H6	3.1	0.0	2.8	0.0	3.3	2.4	14.5	18.3	1.8		2.7
C3H8	14.3	0.0	1.5	0.0	5.8	3.8	22.5	20.9	1.8		1.7
iso-C4H10	0.0	0.0	2.2	0.0	2.0	1.3	18.1	18.3	3.1		1.5
n-C4H10	1.3	0.0	0.5	0.0	0.8	0.4	5.8	2.0	1.0		1.5
i-C4 / n-C4	0.0		3.8		2.8	2.9	5.9	9.1	2.9		1.0

* including isomers

Table 2 Selectivity bond cleavage of binary catalyst system at 425 °C for 20 min.

Exp #	Catalyst	Cleavage at (a),	Me-Bibenzyl	Cleavage at (b),	Bibenzyl	Selectivity	i-C4 / n-C4
	MClx-(AlCl3)x	(mmol)(1)	(mol %)(2)	(mmol)	(mol %)(2)	(a)/(b)	
393	None	0.012	1.6	0.004	0.5	3.21	0.00
336	LiCl	0.073	9.3	0.282	36.0	0.26	n/a
340	NaCl	0.109	13.9	0.228	29.0	0.48	3.84
313*	NaCl	0.128	16.3	0.114	14.6	1.12	n/a
344	KCl	0.024	3.0	0.037	4.7	0.64	n/a
348	VCl3	0.138	17.6	0.284	36.1	0.49	2.78
352	CoCl2	0.127	16.1	0.346	43.9	0.37	2.92
374	NiCl2	0.092	11.6	0.320	40.5	0.29	5.86
360	ZnCl2	0.048	6.2	0.267	34.0	0.18	9.05
364	MoCl3	0.111	14.2	0.201	25.7	0.55	2.88
368	PdCl2	0.057	7.2	0.284	36.2	0.20	n/a
425	ATTM	0.456	55.5	0.098	12.5	4.65	1.00

(1): 4Me-Bibenzyl + iosmer

(2): Based on feed molar number of NMBB

*: Reaction temperature 400°C

n/a : not available

Table 3 Eicosane Conversion at 425 °C for 20 min.

Exp. #	392	333	337	341	345	349	371	357	361	365
MCl_x-$(AlCl_3)_x$	None	LiCl	NaCl	KCl	VCl_3	$CoCl_2$	$NiCl_2$	$ZnCl_2$	$MoCl_3$	$PdCl_2$
Conv. (wt%)	21.8	36.0	26.9	23.0	88.7	83.2	100.0	100.0	37.2	100.0
Gas yield (wt%)	7.7	15.7	4.7	3.6	59.0	47.9	85.4	71.6	22.6	81.5
Liquid yield (wt%)	7.8	7.1	5.9	8.8	2.9	2.6	0.8	2.1	5.2	1.2
Coke yield (wt%)	0.0	0.0	0.0	0.0	4.9	6.0	0.0	0.0	0.0	0.0
Liquid products (mol%)										
n-nonane	1.0	2.4	0.7	4.5	1.9	0.5	0.6	3.7	0.8	0.5
C_9H_{18}	0.7			0.2		0.2			0.6	
C_9H_{18} or C_9H_{20} isomer		0.1	1.4	0.5	0.4	0.6			1.7	
n-decane	0.9	0.5	1.2	1.1	0.7	0.3	0.7	0.2	0.9	0.8
$C_{10}H_{20}$	0.7		0.1	0.1		0.1			0.1	
$C_{10}H_{20}$ or $C_{10}H_{22}$ isomer	0.3	0.2	0.2	0.9	0.6	0.7	0.0	0.5	0.9	0.7
n-undecane	0.9	0.5	1.2	1.1	0.3	0.2	0.2	0.1	0.8	0.0
$C_{11}H_{22}$	0.6			0.1					0.2	
$C_{11}H_{22}$ or $C_{11}H_{24}$ isomer		0.2	0.3	0.4	0.8	0.9	0.1		0.3	0.4
$C_{12}H_{24}$	0.6		0.1	0.1	0.1	0.1		0.0	0.0	
$C_{12}H_{24}$ or $C_{12}H_{26}$ isomer				0.4	0.3	0.4			0.1	
n-tridecane	0.8	0.5	1.0	1.0	0.2	0.2			0.7	
$C_{13}H_{26}$	0.5		0.1	0.1						
$C_{13}H_{26}$ or $C_{13}H_{28}$ isomer				0.4		0.0				
n-tetradecane	0.8	5.6	0.9	1.0	0.1	0.4			0.6	
$C_{14}H_{28}$	0.5			0.1						
$C_{14}H_{28}$ or $C_{14}H_{30}$ isomer				0.2						
n-pentadecane	0.7	0.4	0.9	0.9	0.1	0.1			0.6	
$C_{15}H_{30}$	0.4			0.1						
$C_{15}H_{30}$ or $C_{15}H_{32}$ isomer				0.1						
n-hexadecane	0.7	0.4	0.7	0.8	0.1	0.1			0.5	
$C_{16}H_{32}$	0.4			0.1						
$C_{16}H_{32}$ or $C_{16}H_{34}$ isomer				0.1						
n-heptadecane	0.6	0.4	0.7	0.8	0.1	0.1			0.5	
$C_{17}H_{34}$	0.3									
$C_{17}H_{34}$ or $C_{17}H_{36}$ isomer				0.1						
n-octadecane	0.2	0.1	0.1	0.1					0.1	
$C_{18}H_{36}$	0.3									
$C_{18}H_{36}$ or $C_{18}H_{38}$ isomer				0.1						
n-nonadecane	0.1									
$C_{19}H_{38}$	0.1									
$C_{19}H_{38}$ or $C_{19}H_{40}$ isomer									0.0	
n-eicosane	78.3	64.0	73.1	77.0	11.3	16.8			62.8	
Gaseous Products (mol%)										
CH_4	3.3	5.0	2.9	2.0	27.3	16.7	17.4	26.4	6.1	19.9
C_2H_6	12.0	6.4	10.2	8.1	19.9	13.6	18.5	20.4	11.1	28.4
C_3H_8	12.9	29.9	10.4	7.4	140.3	99.3	148.0	170.4	37.2	180.2
iso-C_4H_{10}		42.6	1.2	1.2	123.8	112.7	161.8	160.6	46.4	157.0
n-C_4H_{10}	7.0	2.1	1.6	1.7	31.3	25.7	34.0	31.7	13.2	39.4
i-C4 / n-C4	0.0	20.7	0.7	0.4	4.0	4.4	4.1	5.1	3.5	4.0

Table 4 Degree of Hydrocracking of eicosane with MCl_x-$(AlCl_3)_x$ Catalysts

Exp.#	MCl_x-$(AlCl_3)_x$	A: C9-C11(mmol)	B: C12-C19(mmol)	A/(A+B)	i-C4 / n-C4	Conv.(wt%)
392	None	0.1016	0.1162	0.466	0.00	21.8
333	LiCl	0.0706	0.1314	0.350	20.65	36.0
337	NaCl	0.0964	0.0790	0.550	0.72	26.9
341	KCl	0.1693	0.1035	0.621	0.41	23.0
345	VCl_3	0.0918	0.0082	0.918	3.96	88.7
349	$CoCl_2$	0.0696	0.0159	0.814	4.39	83.2
371	$NiCl_2$	0.0289	0.0000	1.000	4.11	100.0
357	$ZnCl_2$	0.0804	0.0000	1.000	5.07	100.0
361	$MoCl_3$	0.1124	0.0528	0.680	3.52	37.2
365	$PdCl_2$	0.0427	0.0000	1.000	3.99	100.0

* With transition metal catalyst, more cracking occures, giving A / (A+B) ratio of close to or equal to 1.0.

DBT conversion over MClx-($AlCl_3$)x catalyst

The results of DBT reaction with MCl_x-$(AlCl_3)_x$ catalyst are summarized in Table 5. It was observed that transition metal-based catalysts gave higher conversion compared with alkali metal-based ones. From the liquid products distribution, $MoCl_3$ containing catalyst afforded higher biphenyl yield compared with others. This result suggests that Mo containing catalyst has high hydrodesulfurization activity and selectivity. In addition there was no coke formation with Mo containing catalyst. Other transition metal catalyst showed good methylation activity of DBT molecule and significant coke formation. On the contrary, alkali metal-containing catalysts showed much less activity for DBT conversion. Their order of activity (DBT conversion) was LiCl > NaCl > KCl, which is the same as that observed for eicosane conversion.

Pyrene conversion over MClx-($AlCl_3$)x catalyst

Table 6 shows the results of pyrene reaction with MCl_x-$(AlCl_3)_x$ catalyst. Hydrogenation and ring opening and subsequent dealkylation were more remarkable with VCl_3-$(AlCl_3)_3$, $NiCl_2$-$(AlCl_3)_2$ and $ZnCl_2$-$(AlCl_3)_2$. The yield of C_2H_6 appears to be the most important dealkylation product. $MoCl_3$ containing catalyst showed high hydrogenation activity (higher yield of hydrogenated pyrene) and selectivity, and there was no coke formation. Other transition metal containing catalysts resulted in significant amount of coke formation. The alkali metal containing catalysts displayed an order of activity (LiCl > NaCl > KCl) which is consistent with those observed in other reactions.

CONCLUSION

From the results of model compounds reactions, transition metal containing catalysts showed higher activity in most cases, especially with eicosane and DBT as reactants. The selectivity of bond cleavage of NMBB molecule appears to be related to i-C4 / n-C4 ratio which is a relative measure of the acidity of the catalysts. In addition, this selectivity was sensitive to reaction temperature. $MoCl_3$-$(AlCl_3)_3$ catalyst has a specific character for model compound reaction compared with other transition metal containing catalysts, for example, higher activity and selectivity of desulfurization of DBT and higher activity of hydrogenation of pyrene. The most important feature with $MoCl_3$-$(AlCl_3)_3$ is no coke formation in all cases. In the present paper there was no remarkable difference than can be attributed to the molten state of the catalyst, such as that between molten $ZnCl_2$-$(AlCl_3)_2$, and a mixture of MCl_x-$(AlCl_3)_x$ catalyst that do not become molten salt at the reaction temperature. The activity of alkali metal tetrachloroaluminate catalysts was found to decrease in the order of LiCl > NaCl > KCl in all the reactions examined.

ACKNOWLEDGMENT

The authors wish to thank Marathon Oil Company for supporting this work. We also thank Prof. Harold H. Schobert for technical support and helpful discussions.

LITERATURED CITED

(1) Song, C., Nomura, M. and Ono, T., PREPRINTS, Am. Chem. Soc., Div. Fuel Chem., 36, 586 (1991)

(2) Song, C., Nomura, M. and Miyake, M., Fuel, 65, 922 (1986)

(3) Plummer, M. A., Fuel Process. Technol., 11, 313 (1985)

(4) Lien, A.P., D'Ouville, E.L., Evering, B. L., and Crubb, H. M., Ind. Eng. Chem., 44, 351 (1952)

(5) Alul, H.R.and McEwan, G.J., J. Org. Chem., 37, 4157 (1972)

(6) Schmidt, E., Song, C. and Schobert, H.H., Energy & Fuels, 10, 597 (1996)

(7) Cooke, W. S., Schmidt, E., Song, C. and Schobert, H.H., Energy & Fuels, 10, 591 (1996)

(8) Song, C., Ma, X., Schmidt, E., Yoneyama, Y. and Schobert, H. H., PREPRINTS, Am. Chem. Soc., Div. Petrol. Chem., 42, 674 (1997)

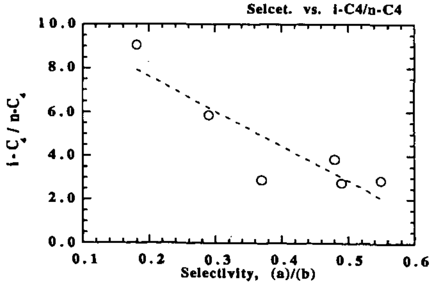

Figure 1 Relation between i-C_4 / n-C_4 ratio and selectivity of bond cleavage

Table 5 DBT Conversion at 425 °C for 20 min.

Exp. #	334	337	341	346	350	372	358	362	366
MClx-(AlCl3)x	LiCl	NaCl	KCl	VCl3	CoCl2	NiCl2	ZnCl2	MoCl3	PdCl2
Conv. (wt%)	23.8	15.4	10.2	79.5	46.5	82.0	76.2	83.5	87.6
Gas yield (wt%)	0.0	1.3	0.0	13.8	7.0	12.8	13.8	25.0	22.5
Liquid yield (wt%)	3.6	2.0	1.2	9.3	10.4	14.3	11.0	33.1	18.4
Coke yield (wt%)	0.0	0.0	0.0	25.9	3.6	26.4	36.8	0.0	3.9
Liquid products (mol%)									
toluene	0.0	0.3		0.9	0.3	0.8	1.0	0.6	3.6
p-, m-xylene	0.1			1.0	0.3	1.0	0.7	0.8	3.0
o-xylene	0.5	0.1		0.1		0.1	0.1	0.1	0.6
1,3,5-trimethylbenzene				0.2		0.2	0.1		0.7
1,2,4-trimethylbenzene	0.7								
1,2,3-trimethylbenzene									
biphenyl	1.7	1.5	1.0	1.1	1.5	1.3	1.7	29.8	1.4
2-Me-biphenyl						0.1	0.1		0.1
3-Me-biphenyl				0.2	0.1	0.3	0.3	0.3	0.3
4-Me-biphenyl				0.1	0.1	0.2	0.1	0.2	0.2
4H-DBT*	1.3	0.6	0.3	0.8	2.2	1.0	1.4	1.8	1.8
Me-DBT*	0.1			3.5	3.6	5.1	3.6		3.4
DiMe-DBT*				1.5	1.7	3.2	1.8		2.6
DBT	76.2	84.6	89.8	20.5	53.5	18.0	23.8	16.5	12.4
Gaseous Products (mol%)									
CH4	0.0	0.7	0.0	5.2	1.9	2.5	5.3	12.6	3.5
C2H6	0.0	0.6	0.0	5.9	1.5	3.3	4.4	9.5	5.6
C3H8	0.0	0.4	0.0	18.3	7.0	8.3	18.2	25.9	21.1
iso-C4H10	0.0	0.9	0.0	17.5	10.8	12.1	19.2	27.0	25.8
n-C4H10	0.0	0.3	0.0	4.2	1.1	3.4	4.7	4.2	7.2
i-C4 / n-C4		3.3		4.2	10.0	3.0	4.1	6.4	3.6

* including isomers

Table 6 Pyrene Conversion at 425 °C for 20 min.

Exp. #	335	339	343	347	351	373	359	363	367
MClx-(AlCl3)x	LiCl	NaCl	KCl	VCl3	CoCl2	NiCl2	ZnCl2	MoCl3	PdCl2
Conv. (wt%)	73.5	69.3	9.0	85.7	69.5	86.7	93.9	44.4	89.7
Gas yield (wt%)	0.0	0.0	0.0	2.8	0.2	3.4	2.2	4.8	7.2
Liquid yield (wt%)	19.6	18.6	6.5	15.0	17.3	12.6	9.4	17.9	12.4
Coke yield (wt%)	31.6	19.9	0.0	50.4	33.2	53.6	64.9	0.0	49.1
Liquid products (mol%)									
toluene	0.2	0.2		0.1	0.1	0.2	0.1	0.1	0.1
p-, m-xylene	0.2	0.1		0.2	0.2	0.2	0.2	0.1	0.2
o-xylene	0.1	0.1			0.0	0.1			
2H-fluorene	0.7	0.5		0.7	0.4	0.9	0.9		1.1
2H-Me-fluorene	0.2	0.1		0.1	0.1	0.2	0.2	0.1	0.2
4H-pyrene*	2.2	2.5	0.2	1.7	1.7	0.9	0.6	2.1	0.8
6H-pyrene*	1.9	2.2	0.2	1.5	1.2	0.8	0.5	1.5	0.8
2H-pyrene*	8.3	9.1	5.3	5.0	8.1	3.9	1.9	13.2	3.1
Me-pyrene*	1.1	0.7		1.0	1.2	1.2	1.1	0.1	2.0
DiMe-pyrene*	3.3	1.8		2.9	3.1	2.9	2.3	0.3	2.1
pyrene	25.6	30.6	91.0	14.3	30.5	13.3	6.1	55.6	10.3
Gaseous Products (mol%)									
CH4	0.0	0.0	0.0	3.1	0.3	3.3	3.6	2.9	7.3
C2H6	0.0	0.0	0.0	9.4	0.9	9.8	8.8	3.6	19.9
C3H8	0.0	0.0	0.0	2.0	0.2	2.4	1.7	1.5	4.7
iso-C4H10	0.0	0.0	0.0	0.7	0.1	1.2	0.3	2.8	2.0
n-C4H10	0.0	0.0	0.0	0.3	0.1	0.7	0.2	1.0	1.6
i-C4 / n-C4				2.1	2.0	4.3	1.5	3.0	1.2

* including isomers

NEW DEVELOPMENTS IN DEEP HYDROCONVERSION OF HEAVY OIL RESIDUES WITH DISPERSED CATALAYSTS: THE EFFICIENCY OF HYDROGEN DONORS ADDITION IN HYDROCRACKING OF LIAOHE VACUUM RESIDUE WITH DISPERSED CATALYSTS.

Shi Bin ,Li PeiPei, Que GuoHe

Department of Chemical Engineering, University of Petroleum
Dong Ying, Shan Dong 257062, P.R.China

Introduction

Among other future challenges, refineries must cope with heavy feed stocks of lower quality, i.e, with higher viscosity, Conradson Carbon, heteroatom content and metal content. Furthermore, to satisfy market demand for light petroleum cuts, improved treatment of the "bottom of the barrel" is needed. To achieve deep conversion of heavy residues into distillates, it is necessary to develop new hydrocracking processes because of theirs applicability. Among these hydrocracking processes, "slurry-bed" hydrocracking seems to be a promising process to converse poor-quality petroleum residues into distillates. During reaction time, inhibition of excessive coke yield is critical in high conversion of heavy poor-quality feed stocks in order to keep the reaction units smoothly operating. According to literature and patents[1], the dispersed catalysts in reaction system could be an important inhibitor of coking.

It is well known that hydrogen donor solvents have been employed into coal hydroliquefaction [2-4] and some processes of oil residues such as hydrogen-donor visbreaking (HDV)[5-6] . However, they have never been used with the combination of dispersed catalysts in heavy petroleum residue upgrading. Hydrogen donors exhibit hydrogen-donating properties and inhibit coke formation [5-9]. Thus the donor could reduce coke yield, which was added into hydroconversion system of heavy oil residue with dispersed catalysts.

Experimental

The heavy oil chosen was Liaohe vacuum residue. Its main characteristics are C%,86.9%,H%,11.0%,N%,1.08%,S%,0.43%,Ni,123ppm,V,2.9ppm,Fe,38ppm,Ca,96,density,0.9976,CCR,19.0.

The oil-soluble metal compounds tested were molybdenum-dithiocarboxylate (MoDTC), FeNaphthenate (Fenaph), NiNaphthelate (Ninaph), CoNaphthelate (Conaph). Runs were conducted batch-wise in an 100cm^3 stainless steel autoclave pressured with H_2(7.0 or 5.0Mpa cold) . About 30g feed and the catalyst precursor and Tetralin(5 or 10wt% to feed) were introduced. Element sulfur(0.1000g)was added into the autoclave to keep the catalysts totally sulfurized. The run temperature were attained in 40 mins by heating stove and efficient stirring ensured dispersion of the oil-soluble metal compounds. After run completion, gases were vented off and a solid fraction was seperated from the liquid effluent by centrifugation in toluene. The fractions(150-350^{0}C ,350-450^{0}C) were distillated after toluene was recovered. Naphthalene and Tetralin in 150-350^{0}C fraction were analyzed for donating yield by GC. Conversion of the feed into distillates were calculated by the difference between the weight of the residue feed and of coke and reacted resid.

Results

The inhibition for coking of the catalysts is known for us and take an important role in achieving deep conversion of residues[1].The four oil-soluble catalysts tested were all effective for hydrocracking of Liaohe VR . The catalytic activities of base metals were in order of :Mo>Co>Ni>Fe(see Table 1). RN of Mo was 3.51 and of Fe was 8.63 .This means that MoDTC provide the smallest coke yield in the four metals tested when achieving the same conversion. After combined with 10%wt tetralin, the coking yields were considerably decreased at the same conversion, and more VGO yields were achieved comparing with non-addition of tetralin, and hydrocracking conversion could hardly be affected . In this case, the order of inhibiting coke still was Mo>Co>Ni>Fe, all of the RN became smaller, but Mo combined with tetralin was more outstanding for reducing coke yields and RN .(see Fig.1—4 and Table 1). Only Mo combined with tetralin could remain higher activity for inhibiting coking during the most reaction time.

Literature and patents[1] show that most of the "slurry-bed" hydrocracking processes employed disposable catalysts under high hydrogen pressure (up to 20Mpa). It is necessary to reduce the amounts of used catalysts in order to decrease the cost of catalysts at the same time the reactors maintain smooth operation. However , excessively coking would generate if insufficient coke inhibitors such as active catalysts existed in the reaction system. But combined with small amounts of tetralin, little amounts of catalysts play the same part in decreasing coke yields. Table 2 show that 60ppm Mo combined with 10%wt tetralin could decrease coke yields from 3.54% to 0.98%wt, on the other hand ,500ppm Mo alone give 1.45%wt. 30ppm Mo combined with 10%wt tetralin provide smaller coke yields than 100ppm Mo alone .

To take advantage of hydrogen donor, it is necessary to combine with reasonable amount of dispersed catalysts. The disposed catalysts will be saved and the expense of operation will be decreased.

Conclusion

It was found that hydrogen donor has efficient inhibition of the coke production. Dispersed catalysts combined with hydrogen donors would be a way to upgrade heavy petroleum residues. More active catalysts with the addition of donors could yield less coke. The amounts of employed catalysts could be reduced and high hydroconversion would be achieved at non-excessive coke formation by way of this method.

Literature cited

(1)Del Bianco,A. et al, Chemtech, 11,35-42,1995.
(2)Furlong,L.E. et al Chem. Eng. Prog. 72.(8).1976.
(3)Er.V.J.Kuhlmann. et al Fuel.64.1552-1557
(4)Isao. Mochida. et al. Advances in Catalysis. Vol(40).39-85.1994.
(5)Fisher,I.P, et al. Oil Gas J.(22).111.1982.
(6)Baskshi, et al. Oil Gas J.(13).84.1987.
(7)U.S Patent 4615 791,1986.
(8)U.S Patent 4814 065,1989.
(9)Del Bianco, et al. Fuel (72).81-85.1993.

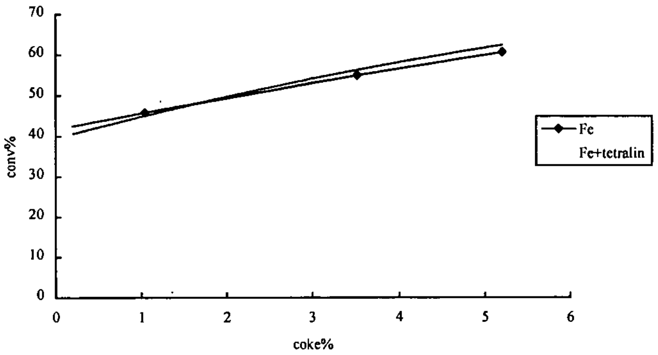

Figure 1.Comparison between Fenaph and Fenaph+Tetralin residue hydrocracking.

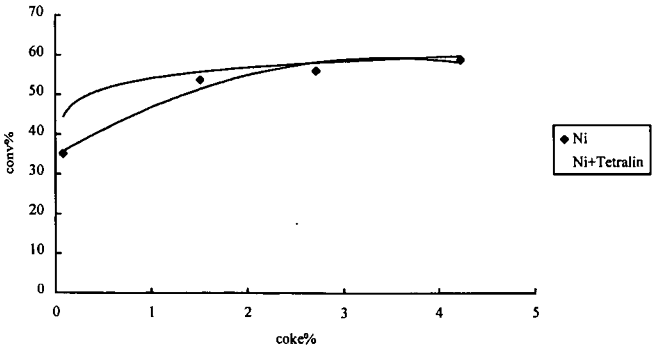

Figure 2. Comparison between Ninaph and Ninaph+Tetralin residue hydrocracking.

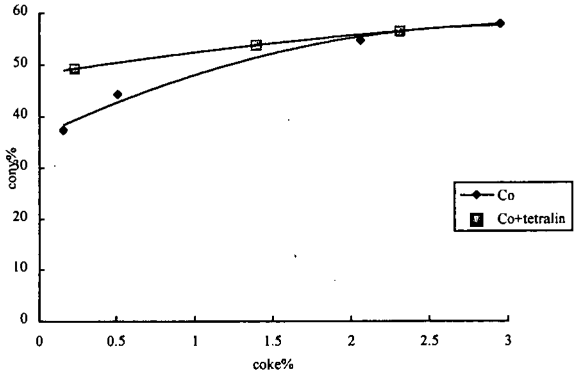

Figure3.Comparison between Conaph and Conaph+Tetralin residue hydrocracking.

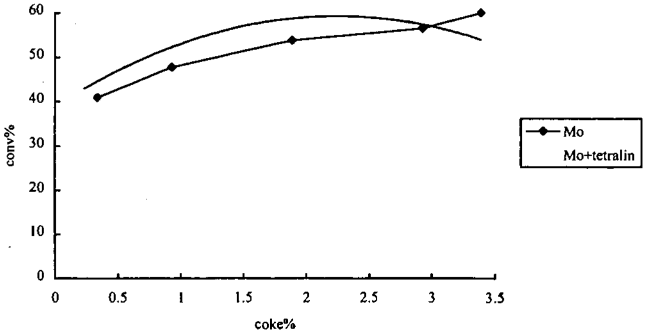

Figure 4 Comparison between MoDTC and MoDTC+Tetralin residue hydrocracking.
(all experimental conditions of the four figures are 430°C,7.00Mpa,200ppmmetal ,10.00%Tetralin)

Table 1 Hydroconversion of LHVR in the presence of Mo,Co,Ni,Fe and 10.00wt%Tetralin
(at 430oC,60 mins ,200ppm base metal and 7.0Mpa,cold)

	product yields ,wt%				conv. of resids. wt%	$^{\&}$RN
	<350°C	350~450°C	>450°C	coke		
MoDTC	31.12	22.71	47.37	1.89	53.83	3.51
	25.14	27.29	47.57	0.71	52.43	1.35
Ninaph	34.13	21.50	44.37	2.72	55.63	4.89
	30.90	23.90	45.20	1.89	54.80	3.45
Conaph	30.96	24.00	45.04	2.06	54.96	3.75
	27.65	26.15	46.20	1.39	53.80	2.58
Fenaph	37.78	22.60	39.62	5.21	60.38	8.63
	33.98	24.61	41.42	4.06	58.58	6.93

footnotes:1. $^{\&}$RN =(coke %/conv.of resids %*100) 2. is 200ppm metal+10.00wt%tetralin.

Table 2 Hydroconversion of LHVR in the presence of MoDTC and Tetralin
(at 430^0C , 60mins and 7.0Mpa H_2 at cold)

	0%tetralin		5.00%tetralin		10.00%tetralin	
MoDTC	coke wt%	conv wt%	coke wt%	conv wt%	coke wt%	conv wt%
30ppm	4.45	58.80	2.95	56.30	2.25	54.76
60ppm	3.54	56.90	2.71	55.79	0.98	53.81
100ppm	2.89	54.65	1.11	53.49	0.74	52.98
200ppm	1.89	53.83	0.94	52.85	0.71	52.43
500ppm	1.45	50.90	1.05	49.54	0.75	48.42.

footnote: conv% =(feed-coke-reacted resids)%wt

THE REDUCTION OF NITROGEN- AND SULFUR-CONTAINING HETEROAROMATIC COMPOUNDS IN A BIPHASIC MEDIUM USING A GROUP VIII HYDROSOLUBLE ORGANOMETALLIC COMPLEX

Páez, D. E.;[a] Andriollo, A.;[a] López-Linares, F.;[a] Galiasso, R. E.:[a] Revete, J. A.;[a] Sánchez-Delgado, R.;[b] and Fuentes, A.[b]

a. PDVSA-INTEVEP, Process Department, Apdo. 76343, Caracas 1070A, Venezuela. Fax (582) 908-7415.
b. IVIC, Centro de Química, Apdo. 21827, Caracas 1020A, Venezuela.

Keywords: Heteroaromatic, Biphasic, Organometallic.

ABSTRACT

Two-phase hydrogenation of heteroaromatic compounds such as quinoline (Q) and benzothiophene (BT) were performed using as catalytic precursor a mixture of ruthenium trichloride and an excess of the water-soluble ligand m-sulfonatophenildiphenylphosphine, in its sodium salt form (TPPMS). The products obtained from the hydrogenation were 1.2,3,4-tetrahydroquinoline (THQ) and dihydrobenzothiophene (DHBT), respectively.

The initial rate of hydrogenation for benzothiophene is enhanced in the presence of quinoline. Other organic nitrogen bases such as aniline, acridine, tetrahydroquinoline, piperidine and triethylamine were also important as promoters in the hydrogenation of benzothiophene. Understanding novel upgrading processes in fuels is the quest for this investigation.

1. INTRODUCTION:

Sulfur and nitrogen-containing aromatics are major contaminants in petroleum derived fuels (e.g., Naphtha, Diesel, etc.). Thiophene (Th), benzothiophene (BT) and derivatives are the most abundant sulfur aromatics in fuel. Quinoline (Q) and other related species represent the main nitrogen-containing aromatics [1]. New legislation represent a threat to these highly refractory compounds because they have to be reduced severely to comply with quality product standards. Degradation of these compounds is carried out via hydrotreating like HDS and HDN; however, limitations in heteroaromatic reduction severely affect upgrading [2].

Industrial HDS and HDN are generally carried out together with many other reactions such as aromatic saturation, olefin hydrogenation, hydrocracking, etc. [1]. Some of these side-reactions are desirable (e.g. regioselective aromatic saturation) because it permits a rational transformation of other undesirable products (polyaromatics). The ability to understand and eventually control hydrotreating reactions may lead to highly selective ways of either removing contaminants for continuing downstream processes or improving the quality of the hydrocarbon itself (e.g. transformations of two-rings fused aromatics into alkyl monoaromatics, helping octane and avoiding smoke in fuel combustion).
To understand the actual mechanistic details in hydrotreating, one could study the selective hydrogenation or hydrogenolysis of heteroaromatic compounds in a homogeneous medium [2]. It will be interesting to investigate whether the rupture of the C-S and C-N bonds (hydrogenolysis) occurred prior or subsequent to the hydrogenation of the heterocyclic rings on solid catalysts. While this information is unknown, it is believed that is much easier to remove sulfur and nitrogen once the aromatic rings have been reduced via hydrogenation [2]. Selective hydrogenation could shed light on novel upgrading in hydrotreating.

A way to go is the use of transition metal complexes, because they may be characterized by spectroscopic techniques that are much easier to comprehend and handle [2]. Several late transition metal complexes are known to catalyze the regioselective homogeneous hydrogenation of BT and that of Q, and the mechanisms of such reactions have been investigated in detail [3, 4]. Nevertheless, separation problems commonly encountered in homogeneous processes make this approach unattractive for application in petroleum-derived fuels [5,6]. To overcome this problem, the selective hydrogenation step could be done using liquid biphasic catalysis [7]. In this case, the catalytic active species is immobilized in one of the two liquid phases (e.g., water), with the reactants and products maintained in the other (Naphtha); thus allowing a continuous flow process design and better understanding of the different steps involved [8].

2. EXPERIMENTAL:

All manipulations were carried out using standard Schlenck technique, under dry argon or nitrogen. Solvents were purified by conventional procedures. Catalytic runs were performed in an autoclave (PARR, 300 ml, SS-316) with internal stirring and temperature controller. The hydrogenation conditions were 130°C, 69 bar, 613 rpm, S/C, 50:1. Products were analyzed via GC and GC-MS against authentic samples, when available. TPPMS was prepared following published procedure [9].

3. RESULTS AND DISCUSSION:

3.1 Hydrogenation of BT

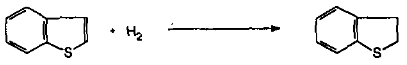

Eq. 1

When a water solution of ruthenium trichloride hydrated and excess TPPMS was placed in a reactor together with a decaline solution of BT, under hydrogenation reaction conditions, the catalytic transformation of BT to DHBT was observed soon after the first hour of reaction (Eq. 1). Two experiments were carried out to establish the responsibility of ruthenium in the catalysis:

(i) Addition of elemental mercury to the reaction mixture did not affect the catalysis [10].
(ii) A thermally decomposed aqueous solution containing $RuCl_3$ and TPPMS yielded a Ru metal suspension which was found to be inactive toward BT hydrogenation under the same reaction conditions.

The initial turnover rate for the conversion of BT to DHBT was 2.9 mol (mol Ru)$^{-1}$h^{-1}. For comparison, the homogeneous hydrogenation of BT using $RuCl_2(PPh_3)_3$ and $RuHCl(CO)(PPh_3)_3$ as the catalyst precursors proceeded with initial turnover frequencies of 6.1 and 2.2 mol (mol Ru)$^{-1}$h^{-1}, respectively, under more stringent conditions (170°C, 110 bar H_2) [3a].

As expected for a reaction at an interface, the stirring rate has a strong influence on the rate of hydrogenation, which went from 30% conversion to 70% conversion, after 18 h, on going from 200 rpm to 600 rpm under the conditions described above [11]. The catalytic solutions were recycled up to four times under strictly anaerobic conditions and used to hydrogenate fresh BT in decaline, without any apparent loss of activity. In contrast, a solution exposed to air after the first hydrogenation run was completely inactive for further hydrogenation.

When the biphasic hydrogenation of BT is carried out in the presence of a nitrogen base (1:1 molar ratio with respect to TPPMS), the initial turnover rate is enhanced. Fig. 1 shows typical reaction profiles in the presence of bases such as quinoline (Q) and aniline (An) in comparison with a non base promoted (NB) reaction. From the lineal part of the curves, maximum turnover frequencies can be estimated at 10.2 and 10.4 mol (mol Ru)$^{-1}$h^{-1} for Q and An, respectively. The basicity of aniline (p_kb 9.3) resembles that of Q (p_Kb 9.1). This may be a good reason for the apparent behavior. However, Q plays also a role as phase transfer and emulsion stabilization agent.

Other nitrogen bases such as acridine (Ac, p_kb 8.4), piperidine (Pp, p_kb 2.9) and triethylamine (Tea, p_kb 2.9) can also enhanced the rates of BT hydrogenation to the various degrees presented in Fig. 2. The base neutralizes the HCl that is formed in the heterolytic cleavage de H_2 during formation of the catalyst precursor [3e].

3.2 Hydrogenation of Q

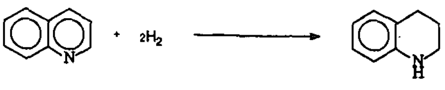

Eq. 2

Quinoline acts as a co-catalyst in the hydrogenation of BT and it is also hydrogenated to THQ (Eq. 2). Under the same reaction conditions, the hydrogenation of Q is faster than that of BT. The initial turnover rate for this reaction was 78 mol (mol Ru)$^{-1}$h^{-1}, compared with 2.9 mol (mol Ru)$^{-1}$h^{-1} for BT (27 times less active). Organic bases do not influence the initial rate. However, increasing hydrogen pressure has a positive influence in the hydrogenation. In fact, most of the studies on the biphasic hydrogenation of Q were carried out at 35 bars in order to determine more accurately the initial turnover rate (35 mol (mol Ru)$^{-1}$h^{-1}).

3.3 Catalytic species in aqueous solutions

In the absence of the base, $RuCl_3 \cdot 3H_2O$ reacts with excess TPPMS in water or methanol to yield $[RuCl_2(TPPMS)_2]_2$, which in turn reacts with hydrogen to produce the hydride $[RuHCl(TPPMS)_2]_2$. The latter complex is broken, for instance by cinnamaldehyde leading to an active catalyst for the regioselective hydrogenation of the carbonyl (C=O) bond of CA [12]. In agreement with this, the major Ru-containing products isolated from the aqueous phases after BT hydrogenation in presence of Q or An were characterized by ^1H and $^{31}P\{1H\}$ NMR spectroscopy as the complexes $RuHCl(TPPMS)_2L_2$ (L= THQ, **1** and An, **2**;).

Complexes **1** and **2** were independently synthesized by reaction of $[RuHCl(TPPMS)_2]_2$ with an excess of THQ or An in water, and characterized by NMR and FAB/MS [13].

A fresh sample of **1** was used in the hydrogenation of Q (35 bars, 135°C, 3 h) given the profile observed in Fig. 4 (P1). The water solution was carefully worked up under anaerobic conditions and the brown solid obtained was characterized by NMR, after the catalysis (signals were identical to the fresh catalyst). The complex was redissolved in water and reused in the catalysis of a fresh decaline solution of Q, given the profile P2. This work is a clear indication of the recycle capacity of the complex; which must have a structural relationship with the catalytic active species formed when ruthenium halide reacts with excess TPPMS in the presence of an organic base.

Since both complexes **1** and **2** are coordinately saturated, they are probably not the ones directly involved in the catalysis, but a stabilized form of the actual catalyst, which could conceivably be the corresponding 16-electron species "$RuHCl(TPPMS)_2L$". Further mechanistic studies are in progress and will be reported elsewhere.

4. CONCLUSIONS:

The regioselective hydrogenation of BT and Q was achieved using a biphasic (water/decaline) catalytic system comprised by ruthenium trichloride and excess *meta*-sulfonatophenyldiphenylphosphine (TPPMS). The hydrogenation of BT is influenced by the addition of organic nitrogen bases as co-catalysts; the order of hydrogenation being: An ≈ Q > Ac > THQ > Pp > Tea. Species of the type $HRuCl(TPPMS)_2L_2$ (L = An, THQ) have been isolated from the aqueous solutions after the hydrogenation. These species were also obtained using preparative procedures and characterized by NMR and FAB/MS. The tensoactivity of the TPPMS ligand and the phase transfer character of the base are important in the transformation of BT under biphasic conditions. Novel upgrading process of petroleum fuel is the main quest of the work presented.

REFERENCES:

[1] *(a)* C. J. Thompson, in: *Organic Sulfur Chemistry*, Eds. R. Kh. Friedlina, A. E. Skovora, p201 (Pergamon, New York, 1981); *(b)* B. C. Gates, J. R. Katzer and G. C. A. Schuit, *Chemistry of Catalytic Processes* (McGraw-Hill, New York, 1979); (*c*). A. N. Startsev, *Catal. Rev. -Sci. Eng.*, 37 (1995) 353; *(d)* P. T. Vasudevan and J. L. G. Fierro, *Catal. Rev. -Sci. Eng.*, 38 (1996) 161; *(e)* H. TopsØe; B. S. Clausen and F. E. Masoth, *Hydrotreatting Catalysis-Science and Technology*, in: Catalysis, Science and Technology, Ed. M. Boudart, Vol. 11 (Springer-Verlag, Berlin, 1996).

[2] (*a*) R. J. Angelici, *Acc. Chem. Res.*, 21(1988) 387; (*b*) R. J. Angelici, *Coord. Chem. Rev.*, 105(1990) 61, (*c*) R. A. Sánchez-Delgado, *J. Mol. Catal.*, 86 (1994) 287; (*d*) R. J. Angelici, *Bull. Soc. Chim. Belg.*, 104 (1995) 265; (*e*) T. B. Rauchfuss, Prog. Inorg. Chem.,39 (1991) 259; (*f*) C. Bianchini and A. Meli, in: *Applied Homogeneous Catalysis with transition metal Compounds*, Eds. B. Cornils and W. A. Herrmann, Vol. 2, p 909 (VCH, Weinheim, 1996); (*g*) Bianchini, C.; Herrera, V.; Jimenez, M. V.; Meli, A.; Sánchez-Delgado, R. and Vizza, F.; *J. Am. Chem. Soc.*, 117 (1995) 8567; (h) Bianchini, C. and Meli, A., *J. Chem. Soc., Dalton Trans.*, (1996) 801.

[3] (*a*) R. A. Sánchez-Delgado and E. Gonzalez, *Polyhedron*, 8 (1989) 1431; (*b*) R. A. Sánchez-Delgado, V. Herrera, L. Rincón, A. Andriollo and G. Martín, *Organometallics*, 13 (1994) 553; (*c*) V. Herrera, A. Fuentes, M. Rosales, R. A. Sánchez-Delgado, C. Bianchini, A. Meli and F. Vizza, *Organometallics* (in press).

[4] (*a*) R. H. Fish, J. L. Tan and A. D. Thormodsen, *J. Org. Chem.*, 49 (1984) 4500; (*b*) R. H. Fish, J. L. Tan and A. D. Thormodsen, *Organometallics*, 4 (1985) 1743; (*c*) R. H. Fish, E. Baralt and S. J. Smith, *organometallics*, 4 (1991) 54; (*d*) E. Baralt, S. J. Smith, I. Hurwitz, I. T. Horváth and R. H. Fish, *J. Am. Chem. Soc.*, 104 (1992) 5187; (*e*) R. H. Fish, in *Aspects of Homogeneous Catalysis*, R. Ugo (Ed.), Vol. 7, P 65 (Kluver; Dordrecht, 1990).

[5] G. W. Parshall and S. D. Ittel, *Homogeneous Catalysis* (John Wiley & Sons, New York, 1992).

[6] B. Cornils and W. A. Herrmann, in: *Applied Homogeneous Catalysis with Transition Metal Complexes*, eds. B. Cornils and W. A. Herrmann, Vol. 2, p 576 (VCH, Weinheim, 1996).

[7] Y. Dror and J. Manasen, *J. Mol. Catal.*, 2 (1977) 219.

[8] (*a*) D. E. Páez, A. Andriollo, R. A. Sánchez-Delgado, N. Valencia, F. López-Linares and R. Galiasso, *U. S. Pat. Appl.* 08/657.960 (June 4, 1996); (*b*) Bianchini, C.; Meli, A.; Patinec, V.; Sernau, V. and Vizza, F.; *J. Am. Chem. Soc.*, 119 (1997) 4945.

[9] S. Ahrland, J. Chatt, N. R. Davies, and A. A. Williams, *J. Chem. Soc.*, 88 (1958),276.

[10] (a) Lin, Y. and Finke, R. G., *Inorg. Chem.*, 33 (1994) 4891; (b) R. Crabtree and D. R. Anton, *Organometallics*, 2 (1983) 855.

[11] D. E. Páez, A. Andriollo, J. Carrasquel, J. Mariño, F. A. López-Linares, I. Rojas and N. Valencia, *J. Mol. Catal.*, 116 (1997) 157.

[12] R. A. Sánchez-Delgado, M. Medina, F. López-Linares and A. Fuentes, *J. Mol. Catal.* A: Chem., 116 (1997) 167.

[13] Data for complex 1: ^1H NMR (CD_3OD), THQ: 5.62 (t, J= 5.7 Hz, H_2), 4.38 (t, J= 6.6 Hz, H_3), 5.14 (t, J0 5.7 Hz, H_4), 8.30 (s, H_5), 8.33 (s, H_6), 8.51 (s, H_7), 8.55 (s, $H_{5,8}$), -10.30 (t, J_{H-P} = 36 Hz, Ru-H), 8.11 - 7.10 (M, tppms). $^{31}P\{^1H\}$ NMR system δA 60.38; δM 57.57 (J_{P-P} = 35 Hz).

Data for complex 2: ^1H NMR (CD_3OD), 8.37 (m, aniline), 5.43 (t, J = 6 Hz, NH_2), -10.18 (t, J_{H-P} = 37 Hz, Ru-H), 8.11-7.10 (m, TPPMS). $^{31}P\{^1H\}$ NMR: 57.9 (s). FAB-MS (m-nitrobenzyl alcohol) (Z/e): 1122 $[RuHCl(TPPMS)_2(An)_2]$ + H; 996 $[RuHCl(TPPMS)_2(An)]$+H; 941 $[RuHCl(TPPMS)_2]$+H; 902 $[Ru(TPPMS)_2]$+H; 880 $[Ru(TPPMS)_2Na]$+H; 400 $[TPPMS\text{-}Na\ 2H_2O]$.

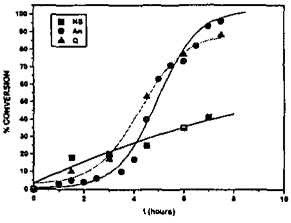

Fig. 1 Profile for the biphasic hydrogenation of BT. NB, No base added, An, aniline and Q, quinoline.

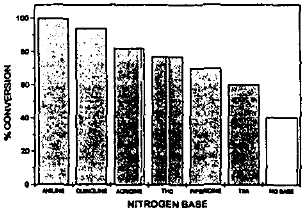

Fig. 2 Influence of basicity in the biphasic hydrogenation of BT with $RuCl_3$ and TPPMS.

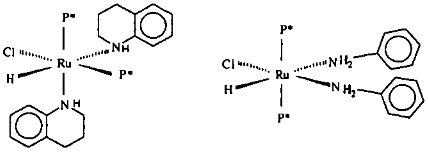

1

2

$P^{*} = TPPMS = (C_6H_5)_2P(m\text{-}C_6H_4SO_3Na)$

Fig. 3. Structures of aqueous organometallic species characterized during the reaction of $RuCl_3$, excess TPPMS and THQ or An.

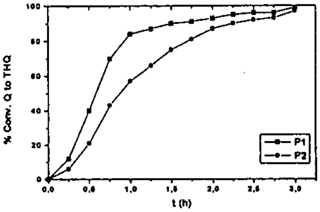

Fig. 4. Profiles for the biphasic hydrogenation of Q using the same catalyst, but two fresh solutions of Q in decaline.